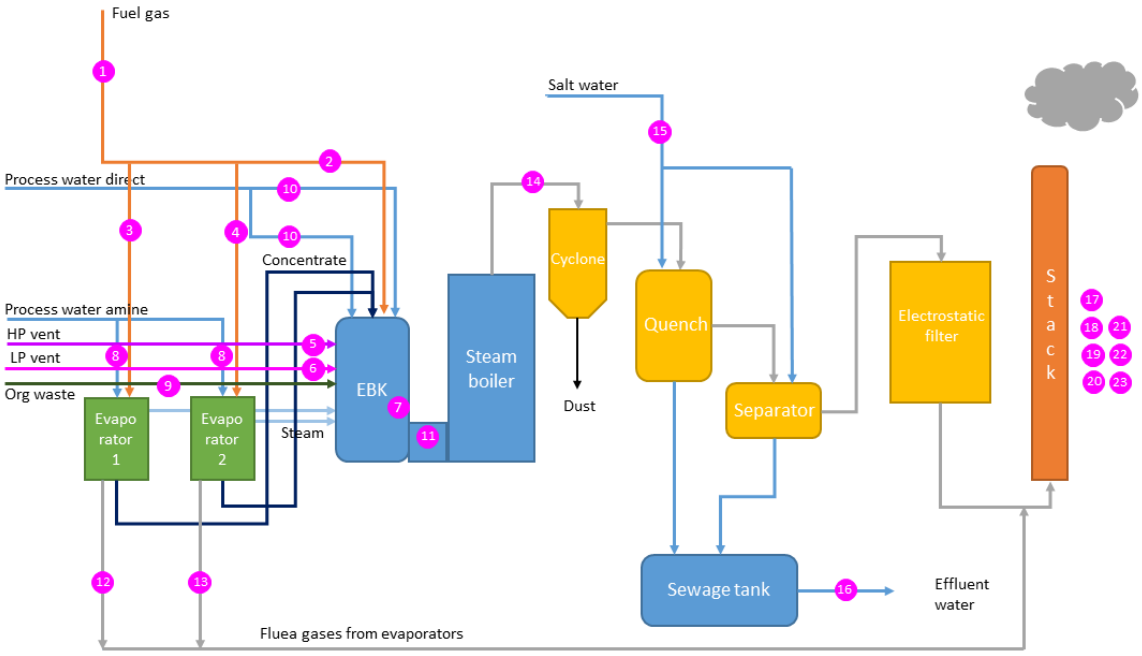
CHALMERS
UNIVERSITY OF TECHNOLOGY



Evaluation of waste water incineration

A case study at AkzoNobel in Stenungsund

Master's thesis in Innovative and Sustainable Chemical Engineering

MARIA HALLBÄCK

Department of Energy and Environment
CHALMERS UNIVERSITY OF TECHNOLOGY
Gothenburg, Sweden 2017

Master's thesis 2017

Evaluation of waste water incineration

A case study
at AkzoNobel in Stenungsund

MARIA HALLBÄCK



CHALMERS
UNIVERSITY OF TECHNOLOGY

Department of Energy and Environment
Division of Energy Technology
Combustion and Carbon Capture Technologies
Chalmers University of Technology
Gothenburg, Sweden 2017

Evaluation of waste water incineration
A case study at AkzoNobel in Stenungsund
MARIA HALLBÄCK

© MARIA HALLBÄCK, 2017.

Supervisors: Rikard Edland, Division of Energy Technology - Combustion and Carbon Capture Technologies
Christian Gustafsson - Sulfur and Ethylene derivatives, AkzoNobel
Charlotte Bergek - Sulfur and Ethylene derivatives, AkzoNobel
Examiner: Fredrik Normann, Division of Energy Technology - Combustion and Carbon Capture Technologies

Master's Thesis 2017
Department of Energy and Environment
Division of Energy Technology
Combustion and Carbon Capture Technologies
Chalmers University of Technology
SE-412 96 Gothenburg
Telephone +46 31 772 1000

Cover: Schematic picture of the incineration process with measurement points indicated in purple.

Typeset in LaTeX

Evaluation of waste water incineration
A case study at AkzoNobel in Stenungsund
MARIA HALLBÄCK
Department of Energy and Environment
Chalmers University of Technology

Abstract

Waste incineration is an important part of many processes. Waste water incineration is however, not a common practice. This thesis has evaluated the performance of waste water incineration through a case study at AkzoNobel in Stenungsund. The primary aim of the process is the destruction of ammonia present in the waste water and ventilation gas feed streams. Secondary focus is to reduce the formation of NO_x in the process. The waste water incineration process consists of two evaporators, one furnace, one dust cyclone, a separation step containing one quench and one separation unit, and lastly one electrostatic filter before the flue gases are emitted to the atmosphere via a flue gas fan and a stack.

The evaluation was performed in three parts. The first part included mapping mass balances of the incinerator and the important units. The balances were based on real time data from the process. In the second part a chemical reaction modelling software was used to make a sensitivity analysis for the operating parameters with respect to the NO_x formation. The third part consisted of experimental tests varying a set of parameters that were run over a period of around six days.

The result of the mapping shows that the mass balance may be completed. The modeling results indicates that the most important parameters are temperature, amount of excess air and amount of water fed to the furnace. The Experimental test results are consistent with both literature and modeling outcome.

The conclusion from this thesis work is that high temperature and high oxygen levels yields a low ammonia slip but increase the amount of NO formed. On the other hand, low temperatures and low oxygen levels gives low levels of NO but increase the amount of un-reacted ammonia in the stack. The flow of direct water also has a large effect on the performance of the furnace. The most important uncertainties are the ventilation gas composition and the amount of ammonia washed away in the quench step.

Keywords: waste management, incineration, combustion, waste water, mass balances, process modeling.

Acknowledgements

I would like to express my gratitude towards my examiner Fredrik Normann and especially my supervisor Rikard Edland at Chalmers for being extremely helpful regarding theoretical questions and availability for discussions during this study.

I would also very much like to thank my supervisors Christian Gustafsson and Charlotte Bergek at AkzoNobel who have kindly answered all my questions and provided me with the information and data that I needed during the thesis. Also included in this warm thank you are all the wonderful people at AkzoNobel who where not my supervisors but have taken their time to help me anyway and made me feel very welcome at the site.

Thank you all very much!

Maria Hallbäck, Gothenburg, May 2017

Contents

List of Figures **xi**

List of Tables **xv**

1 Introduction **1**
1.1 Waste water incineration . . . 1
1.2 Project Description and Aim . . . 1
1.3 Limitations . . . 2

2 Background **3**
2.1 Effects of incineration . . . 3
2.2 Legislation and Best Available Technology . . . 4
2.3 Emissions . . . 4
2.3.1 NH_3 emissions . . . 4
2.3.2 Sources of NO_x . . . 5
2.3.2.1 Thermal NO . . . 5
2.3.2.2 Prompt NO . . . 5
2.3.2.3 Fuel NO . . . 6
2.3.3 NO interaction with NH_3 . . . 6
2.3.4 Sources of SO_x . . . 8
2.3.4.1 SO_x reduction methods . . . 8
2.3.5 Products from incomplete combustion . . . 9
2.3.6 Particulate matter and slag . . . 9

3 Process description **11**
3.1 Process data . . . 14
3.2 Feed streams . . . 14
3.2.1 Operating conditions . . . 15
3.2.2 Fuel gas . . . 18
3.2.3 Waste water . . . 18
3.2.4 Ventilation gases . . . 19
3.3 Process units . . . 20
3.3.1 Evaporators . . . 20
3.3.2 Destruction furnace (EBK) . . . 21
3.3.3 Post-combustion units . . . 23
3.3.3.1 Quench system . . . 23
3.3.3.2 Stack . . . 27

3.4 Measuring instrumentation . . . 27
3.5 Control systems . . . 28

4 Methodology **29**
4.1 Balances and calculations . . . 29
4.1.1 Combustion process balances . . . 29
4.1.2 Post-combustion steps . . . 32
4.1.2.1 Quench . . . 32
4.1.2.2 Stack/total . . . 32
4.1.3 Real time data overview . . . 32
4.2 Modeling . . . 33
4.2.1 Chemkin setup . . . 33
4.3 Experimental . . . 36
4.3.1 Assumptions, set points, experimental setup . . . 36

5 Results and discussion **39**
5.1 Validation of calculations and balances . . . 39
5.1.1 Stack/total . . . 39
5.1.1.1 Volume flows . . . 39
5.1.1.2 Gas fractions . . . 40
5.2 Correlations . . . 42
5.3 Chemkin results . . . 52
5.3.1 NH_3 . . . 52
5.3.2 NO . . . 54
5.3.3 N_2O . . . 56
5.4 Experimental . . . 58
5.4.1 Direct water (P) . . . 58
5.4.1.1 Ammonia slip and NO reduction, (P) . . . 59
5.4.2 Temperature (T) . . . 61
5.4.2.1 Ammonia slip and NO reduction, (T) . . . 62
5.4.3 Excess air (L) . . . 64
5.4.3.1 Ammonia slip and NO reduction, (L) . . . 65
5.4.4 Amine water from evaporators, (A) . . . 67
5.4.4.1 Ammonia slip and NO reduction (A) . . . 68

6 Conclusion **71**

Bibliography **73**

A Appendix 1 **I**
A.1 Calculation results and operationg conditions . . . I
A.1.1 January 2017 . . . I
A.1.1.1 Evaporators . . . I
A.1.1.2 EBK . . . II
A.1.2 February 2017 . . . V
A.1.3 March 2017 . . . IX
A.1.4 April 2017 . . . XIII

List of Figures

2.1 Main reaction pattern for the conversion of fuel-N to NO and N_2 (Redrawn from (Van der Lans et al., 1997)). 6

3.1 Schematic picture of the waste water incineration process (WINC). . 12
3.2 Total direct water flow in January 2017. 16
3.3 Total amine water flow in January 2017. 16
3.4 Flue gas temperatures in January 2017. 17
3.5 Oxygen levels after EBK in January 2017. 17
3.6 Fuel gas composition in January 2017. 18
3.7 Simplified evaporator design. 20
3.8 Schematic view of the EBK design. 22
3.9 General design of the quench and separation step. 24
3.10 Volume flow of flue gases before and after the quench. 25
3.11 Water fraction in flue gases before and after the quench. 26

5.1 Volume flow of flue gases in the stack January 2017. 40
5.2 O_2 fraction from balance calculations compared to measured O_2 fraction in the stack January 2017. 41
5.3 Water fraction from balance calculations compared to measured water fraction in the stack January 2017. 42
5.4 Lower heating value plotted against the molar flow of fuel for the EBK in January to April 2017. 44
5.5 Molar flow of NH_3 plotted against total molar flow of waste water in January to April 2017. 45
5.6 Molar flow of NH_3 plotted against molar flow of amine waste water in January to April 2017. 46
5.7 Molar flow of NH_3 plotted against molar flow of direct waste water in January to April 2017. 47
5.8 Molar flow of NH_3 plotted against molar flow of CO in January to April 2017. 48
5.9 Molar flow of CO plotted against total molar flow of waste water in January to April 2017. 49
5.10 Molar flow of NH_3 plotted against molar flow of NO in January to April 2017. 50
5.11 Molar flow of NO plotted against total molar flow of waste water in January to April 2017. 51

5.12 Molar flow of NO plotted against the oxygen level after the EBK in January to April 2017. 52
5.13 NH3 molar flow at end point over the given temperature interval for all four test parameters. 53
5.14 NO molar flow at end point over the given temperature interval for all four test parameters. 55
5.15 N_2O molar flow at end point over the given temperature interval for all four test parameters. 57
5.16 All test parameters during the direct water testing period. 58
5.17 Total heat from fuel in the EBK during direct water test run. 59
5.18 The test parameters plotted against NO and NH_3 to investigate their influence on the ammonia slip and NO reduction during the direct water test run. 60
5.19 All test parameters during the temperature testing period. 61
5.20 Total heat from fuel in the EBK during the temperature test run. . . 62
5.21 The test parameters plotted against NO and NH_3 to investigate their influence on the ammonia slip and NO reduction during the temperature test run. 63
5.22 All test parameters during the excess air testing period. 64
5.23 Total heat from fuel in the EBK during the excess air test run. . . . 65
5.24 The test parameters plotted against NO and NH_3 to investigate their influence on the ammonia slip and NO reduction during the excess air test period. 66
5.25 All test parameters during the amine water testing period. 67
5.26 Total heat from fuel in the EBK during the amine water test run. . . 68
5.27 The test parameters plotted against NO and NH_3 to investigate their influence on the ammonia slip and NO reduction during the amine water test period. 69

A.1 The calculated value for lambda plotted against the measured oxygen fraction after the evaporators in January 2017. I
A.2 Fuel gas, flue gas and air flows for evaporator 1 and 2 in January 2017. II
A.3 Lambda for the EBK plotted against oxygen levels in the steam boiler for January 2017. III
A.4 Volume flows of fuel gas, air and flue gas for the EBK during January 2017. IV
A.5 Fuel gas composition in February 2017. V
A.6 Lambda EBK February 2017. VI
A.7 Volume flows EBK February 2017. VI
A.8 Test parameters during February. VII
A.9 Calculation results from February. VIII
A.10 Fuel gas composition in March 2017. IX
A.11 Lambda EBK March 2017. X
A.12 Volume flows EBK March 2017. X
A.13 Test parameters during March. XI
A.14 Calculation results from March. XII

A.15 Fuel gas composition in April 2017. XIII
A.16 Lambda EBK April 2017. XIV
A.17 Volume flows EBK April 2017. XIV
A.18 Test parameters during April. XV
A.19 Calculation results from April. XVI

List of Tables

3.1 Table of measuring points with placement in the process, parameter measured and unit. 13
3.2 Average percentage of the feed streams in mol%, January to April, excluding 31st of March because of EBK shut down. 15
3.3 HP and LP vent gas composition. 19
3.4 Table for all in streams and out streams in evaporators. 21
3.5 Technical data for both evaporators. 21
3.6 Table for all inlet streams and outlet streams to the EBK. 23
3.7 Technical data for the quench system, quench and separator. 27

4.1 Model parameters and values for evaporators and EBK. 33
4.2 Base line parameter values. 34
4.3 Air staging distance, inlet C2 and length of staging. 35
4.4 Direct process water parameters, inlet C6. 35
4.5 Excess air parameters, inlet C2. 35
4.6 Amine water parameters, inlet C5. 35
4.7 Process water direct from south side. 36
4.8 Temperature parameter set up. 37
4.9 Excess air parameters. 37
4.10 Amine water from evaporators. 37

Nomenclature

Symbols

λ	Lambda, theoretical excess air	

Constants

R	Ideal gas constant	[J/mol K]

Subscripts

EBK	Efterbrännkammare, destruction furnace
$HP - vent$	High Pressure ventilation gas
$LP - vent$	Low Pressure ventilation gas
$WINC$	Waste Incinerator

1
Introduction

1.1 Waste water incineration

A secure and efficient disposal of waste is crucial in many parts of today's society. One such part that creates waste streams needing efficient disposal is the operation industrial production plants of any kind. To manage the waste streams in the industry a number of different methods have been developed during the years, the traditional and most common ones being landfill or incineration. The waste management in production plants is however ever changing as new regulations and incentives for better reuse of energy and material as well as stricter rules for emissions and disposal of effluent streams are being implemented. Incineration as means of destroying waste material and in some part reusing energy is commonly applied, mostly when it comes to solid or gaseous dry to semi dry materials with high energy content. More unusual types of waste species to destroy by incineration are waste water streams. This type of waste incineration is performed at AkzoNobel in Stenungsund. Other methods of separation for removing the unwanted species from the waste water such as reverse osmosis filters have been investigated, but the most efficient and cost effective way of waste water management today has been found to be incineration according to the company. The amount of water in the waste stream however provides difficulties in designing a robust incineration system and the lack of similar processes means little comparison to other solutions can be made. The problems facing this combustion process is irregular operation, trouble keeping the load at the desired level, occasionally high emissions of unwanted species, e.g. un-reacted ammonia, dust and slag deposits in the equipment following after the furnace.

1.2 Project Description and Aim

The primary aim of the thesis is to evaluate the operation of waste water incineration to maximise running capacity while minimising the amount of emissions. The performance of the incineration process was evaluated using real time data from an actual process and modelling of the combustion and nitrogen chemistry.

The project aim was carried out in three parts. First a pre-study was performed, including literature search regarding chemical aspects of waste incineration and nitrogen oxide emissions as well as regulations for emission limits. This part also includes structuring and analysis of data. The second part models the process and

evaluate the sensitivity to the combustion parameters. For the third part an experimental design was set up and executed and the results were evaluated.

1.3 Limitations

The scope of the thesis is limited to the combustion process. Pre- and post treatment of the process water streams and flue gases will not be investigated. Data from 2017 has been considered in the analysis - analytic measuring equipment being less accurate in earlier years.

2
Background

This section presents a short introduction and background concerning the project at hand.

2.1 Effects of incineration

Incineration is as a waste treatment process that involves the combustion of organic substances contained in waste materials. Incineration of for example solid waste or other fuels for heat and power production have been used for a long time and the effects of these types of combustion emissions are well documented. The most commonly used fuel for combustion is fossil fuel or biomass, both of which creates various oxide emissions. The emissions from incineration processes causes problems since for example carbon dioxide, sulfur oxides and nitrogen oxides all have negative effects on both environment and human health at a local, regional and global scale (Thomas, 1997). Depending on the type of emission the consequences are ranging from acid rain to tropospheric ozone as well as contributing to the greenhouse effect (Bowman, 1992). Since these types of incineration processes have such well documented environmental effects they have been regulated for a long time, although smaller scale industrial combustion processes have been less affected. This is changing and over the past two decades increasingly stringent regulations for e.g. nitrogen oxides (NO_x) have been implemented, calling for the industry to make improvements in both the combustion process and treatment of flue gases (European Environment Agency, 2010). Industrial scale combustion processes, especially waste incineration and steel manufacturing processes, also experience problems with dust emissions and unwanted slag products that can inhibit the equipment, as well as cause incomplete combustion leading to emissions of potentially hazardous chemical compounds (Raask, 1985). Further regulations concerning emissions and mitigation stratergies is to be expected and it is of importance to improve the relevant processes so as to comply with future requirements.

The waste water incinerator studied in this thesis is located at a plant owned by AkzoNobel in Stenungsund, where production of chemicals including amine derivatives and surface coatings takes place. The incinerator furnace is used for the destruction of contaminated process water and organic waste from production and laboratory work. The waste contains a range of compounds containing nitrogen, most notably ammonia, and organic material. The different waste feeds as well as the provided fuel gas composition varies over a daily and a weekly basis. This leads to problems

concerning the stability of the process, affecting emissions of nitrogen oxides as well as incomplete combustion of the species that are to be destroyed, such as ammonia. In recent time the control system for the incinerator has not responded the way it is expected to, leading to a higher level of oxygen in the flue gases than desired, which leads to lower capacity of the process. The incinerator also produces slag products and very light fly ashes that are cause for concern in the flue gas treatment.

2.2 Legislation and Best Available Technology

The concept of Best Available Technology (BAT) stems from the idea that to reduce emissions and continuously improve the industry from an environmental point of view, all new facilities should implement the best available technology at the time being. This is regulated in the EU via so called BREF documents that contain reviews of the latest technology for different areas of the industry (European Commission - Environment, 2017). The process of waste water incineration at AkzoNobel falls under the legislation of waste incineration. The emission limits of NO_x for this type of process is regulated in an EU directive for medium size combustion plants, and varies from 150 to 250 mg/Nm^3 depending on the size of the plant (Parliament and the Council of the European Union, 2017). The incineration plant was built 2004 and the emission limits were then decided by two now outdated documents. The first one is the EU directive 2000/76/EG (directive for waste incineration) which is now replaced by the directive (EU) 2015/2193 on the limitation of emission of certain pollutants to the air from medium combustion plants and the second one is the NFS 2002:28, which is Naturvårdsverkets emission limit paper concerning waste incineration, now replaced by the (2013:253) regulation (Naturvårdsverket, 2017). For ammonia Sweden has a emission ceiling of 47 000 tonnes for 2020, while for 2010 it was at 57 000 tonnes (European Environment Agency, 2017).

2.3 Emissions

All types of combustion generates emissions of flue gases, defined as the products of combustion that are emitted to the ambient air. These flue gases usually contains compounds classified as pollutants and the following chapter will describe the ones that are relevant for this thesis.

2.3.1 NH_3 emissions

In Europe, the agricultural sector is the largest contributor responsible for ammonia emissions, around 90%. Ammonia release to water ways cause eutrophication and acid deposits, leading to large negative impacts on ecosystems and severe reduction in biodiversity and water quality. As a secondary particulate precursor, ammonia also contributes to the formation of particulate aerosols in the atmosphere. Particulate matter has adverse impact on human health and ammonia is therefore also unwanted as an airborne emission (European Environment Agency, 2017).

2.3.2 Sources of NO_x

The two types of NO_x emissions that are of importance in combustion processes are NO, NO_2. They are formed either from fixation of N_2 in the combustion air at high temperatures or from oxidation of nitrogen bound in the fuel. Almost all combustion processes lead to the formation of NO_x, and NO is the most common nitrogen emission in fossil fuel fired boilers (Van der Lans et al., 1997). NO is then subsequently oxidized to NO_2 or N_2O in the atmosphere (Kampa and Castanas, 2008). NO and NO_2 are contributors to acid rain and participate in the generation of photochemical smog, while N_2O is a strong green house gas that also contributes to the reduction of ozone in the atmosphere (Glarborg et al., 2003). The reaction mechanisms described below are most extensively studied using fossil fuel such as varieties of coal, peat and oil. Since NO is the most common precursor for other NO_x compounds after combustion and also the most commonly formed NO_x compound during combustion, the following sections will focus on the formation of NO. There are three mechanisms that form NO in combustion; thermal NO, prompt NO and fuel NO which are all explained in more detail below.

2.3.2.1 Thermal NO

Thermal NO formation occurs when local temperatures are above 1530°C (Van der Lans et al., 1997). The formation takes place by reaction of N_2 with O_2, and the high temperatures are required to break the strong nitrogen triple bond. The reaction was discovered by Zel'dovich (Zeldovich et al., 1947) and mechanism named after him is as follows:

$$N_2 + O^\bullet \rightleftharpoons NO + N^\bullet \tag{2.1}$$

$$N^\bullet + O_2 \rightleftharpoons NO + O^\bullet \tag{2.2}$$

In fuel rich flames the following reaction is also of importance:

$$N^\bullet + {}^\bullet OH \rightleftharpoons NO + H^\bullet \tag{2.3}$$

Most low NO_x burners avoid NO formation by operating at temperatures below 1530°C, either by recirculation of flue gases or air staging. The contribution of thermal NO to the total amount of NO is generally small for solid fuels, but can be significant at local peak temperature. For gaseous fuels, thermal NO is the most important formation mechanism.

2.3.2.2 Prompt NO

A more rapid generation of NO is called prompt NO. It is only found in hydrocarbon flames and is often negligible in solid fuels. The initial step is the reaction of hydrocarbon radicals to form the intermediate HCN. The most important reaction has been shown to be (Miller and Bowman, 1989):

$$CH^\bullet + N_2 \rightleftharpoons HCN + N^\bullet \tag{2.4}$$

or (Moskaleva and Lin, 2000):

$$CH^{\bullet} + N_2 \rightleftharpoons NCN + H^{\bullet} \tag{2.5}$$

The N_2O mechanism is another nitrogen oxide formation reaction, initiated by (Glarborg et al., 1986):

$$O^{\bullet} + N_2 + M \rightleftharpoons N_2O + M \tag{2.6}$$

Where M is a third body that can absorb the energy needed for the reaction. The reactive nitrogen compounds that are formed (NCN, HCN, N_2O) can then be further oxidized to NO or N_2 depending on the conditions in the furnace. The amount of NO formed by prompt NO reactions is only slightly dependent on temperature but displays a proportional relationship to the amount of N_2 and hydrocarbon radicals in the flame (Van der Lans et al., 1997).

2.3.2.3 Fuel NO

Chemically bound nitrogen in the fuel (fuel-N) can be oxidized during combustion and form NO, most common for combustion of solid fuels. During devolatilization some nitrogen are released with the volatiles. The release can be up to 100% of the total fuel-N depending on temperature. The rate of nitrogen release is proportional to total mass loss and depends on type of fuel and temperature. During the devolatilization the nitrogen is evolved directly as HCN or NH_3 or indirectly from tar. These two compounds are as explained above the main precursors for the formation of NO, see Figure 2.1 for the main reaction path (Van der Lans et al., 1997).

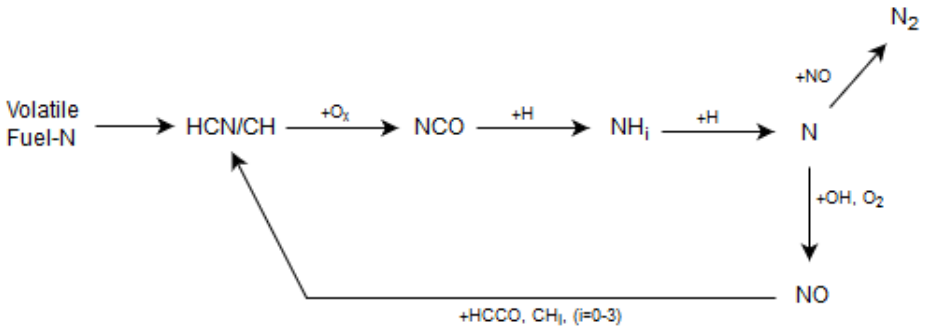


Figure 2.1: Main reaction pattern for the conversion of fuel-N to NO and N_2 (Redrawn from (Van der Lans et al., 1997)).

Temperature and residence time in the furnace also influences the amount of nitrogen pollutants that are formed (Miller and Bowman, 1989).

2.3.3 NO interaction with NH_3

One way of reducing NO emissions is by using selective homogeneous gas phase reduction with NH_3 or selective catalytic reduction with NH_3. Since the furnace at AkzoNobel has no catalytic reduction only the gas phase reduction is considered

here. If NH_3 is injected in to the flue gas the following reactions takes place (Lodder and Lefers, 1985):

$$4\,NH_3 + 4\,NO \longrightarrow 4\,N_2 + 6\,H_2O \tag{2.7}$$

$$4\,NH_3 + 5\,O_2 \longrightarrow 4\,NO + 6\,H_2O \tag{2.8}$$

The reduction efficiency is temperature dependent. The temperature interval for when the reduction takes place is between 830-1130°C. Reaction (2.7) is dominating in temperatures around 980°C and reaction (2.8) becomes more important above 1230°C. Both reactions are slow below 830°C (Lodder and Lefers, 1985).

The strong temperature dependence of the reduction of NO with ammonia described above is explained by the generation and consumption of radicals. The reaction in Equation (2.7) is initiated by the formation of NH_2 via the following reactions (Fan et al., 2014):

$$NH_3 + O^\bullet \rightleftarrows NH_2 + {}^\bullet OH \tag{2.9}$$

$$NH_3 + {}^\bullet OH \rightleftarrows NH_2 + H_2O^\bullet \tag{2.10}$$

Only when the NH_3 is converted to NH_2 the NO can be reduced to N_2 according to the following sequence:

$$NH_2 + NO \rightleftarrows N_2 + H_2O \tag{2.11}$$

$$NH_2 + NO \rightleftarrows NNH + {}^\bullet OH \tag{2.12}$$

$$NNH + NO \rightleftarrows N_2 + HNO \tag{2.13}$$

The $O^\bullet$ and ${}^\bullet OH$ radicals initially result from the thermal decomposition of O_2 and H_2O, and then mainly stem from the regeneration via reactions (2.12) and (2.13) followed by:

$$HNO + M \rightleftarrows NO + H^\bullet + M \tag{2.14}$$

$$H^\bullet + O_2 \rightleftarrows {}^\bullet OH + O^\bullet \tag{2.15}$$

The formation of these radicals is not fast enough to convert NH_3 to NH_2 at temperatures below 800°C, leading to a limitation in the NO reduction. With rising temperatures, the build up of $O^\bullet$ and ${}^\bullet OH$ radicals leads to a better NO reduction. Above optimum temperatures however the reduction efficiency of NO decreases due to acceleration of NO formation where NH_2 radicals are converted to NH and HNO by $O^\bullet$ and ${}^\bullet OH$, instead of reacting with NO directly (Fan et al., 2014).

The effect of these radicals indicate that the gas composition and the temperature will have a large impact on the NO reduction efficiency as well as the risk of ammonia slip. In the article by (Fan et al., 2014) they also found that the ammonia slip as good as disappears at temperatures above 900°C because of the change in rate constants of reaction for most importantly reaction (2.14). This forward rate constant increase in the order of 10^2 to 10^4 while the other reaction constants does not change significantly in magnitude, leading to an increase in the generation of the $O^\bullet$ and $^\bullet OH$ radicals that are crucial for the NH_3 to NH_2 conversion and therefore also important for the reduction of NO with NH_3. In the presence of water the following reaction will happen:

$$O^\bullet + H_2O \rightleftarrows {}^\bullet OH + {}^\bullet OH \tag{2.16}$$

Although the reaction consumes one $O^\bullet$ radical it also generates two $^\bullet OH$, meaning it could promote NO reduction at low temperatures.
The effect of oxygen is found to be that the best NO reduction effect is at low O_2 concentrations and high temperatures, while the minimum ammonia slip can be found at high temperatures, no matter the oxygen concentration as long as there is oxygen present. However, high oxygen concentrations at low temperatures provides the lowest ammonia slip (Fan et al., 2014).

2.3.4 Sources of SO_x

SO_x refers to two types of sulfur oxides, SO_2 and SO_3. Sulfur oxides are formed during the combustion of sulfur containing fuel, most commonly fossil fuels such as coal, oil and during the smelting of metal ores that contain sulfur. The oxidation of sulfur forms the sulfur oxides according to (Zandaryaa and Buekens, 2009):

$$S + O_2 \longrightarrow SO_2 \tag{2.17}$$

Sulfur dioxide is highly soluble in water and forms sulfuric acid (H_2SO_4). SO_2 is stable during combustion conditions (>1000°C). SO_3 is extremely reactive and corrosive as a compound. They are main precursors of atmospheric acidification and cause serious impacts on human health and the environment both directly and as a result of reactions with other substances in the air.

2.3.4.1 SO_x reduction methods

Reduction of sulfur oxide emission is usually achieved by switching to low-sulfur content or by cleaning high-sulfur content fuel. Fuel cleaning is usually cost effective but creates large amounts of solid wastes that need to be treated and disposed of properly. Flue gas treatment methods with limestone addition are also used. The flue gas treatment methods are either in regenerable or once-through systems, depending on if the catalyst used is recoverable or has to be disposed of after use (Zandaryaa and Buekens, 2009).

2.3.5 Products from incomplete combustion

Complete combustion of carbohydrates produces only water and carbon dioxide. Combustion with either oxygen deficiency, bad mixing or local low temperatures leads to incomplete combustion and the emission of intermediate compounds. These are most commonly carbon monoxide, hydrogen, volatile organic compounds (VOC), halogenated hydrocarbons (dioxins, furans) and/or soot (Thunman, 2016).

2.3.6 Particulate matter and slag

Another problem that might occur in a destruction furnace is the formation of dust and particulates, either formed by incomplete combustion of the fuel, most commonly with solid or liquid fuels, or formed by reactions in the combustion process. There is a limit to the maximum amount of dust allowed to be emitted via the stack and this is regulated by EU directives, see Chapter 1 section 2.2. The size of the particles is another aspect of the emissions. Most particles emitted from combustion processes are in the 0.1 to 10 μm diameter range. The larger particles are removed by for example filters or cyclones, but smaller particle may still be emitted. Particles smaller than 2.5 μm in diameter, called PM2.5 stay suspended in the atmosphere and may affect human health negatively, and it is of importance to minimize the emissions of this size as well (Thunman, 2016).

3
Process description

The incineration operation in Stenugsund consists of a series of process operations. The general layout of the process including measurement points relevant for this project can be seen in Figure 3.1. See Table 3.1 for measurement point explanation.

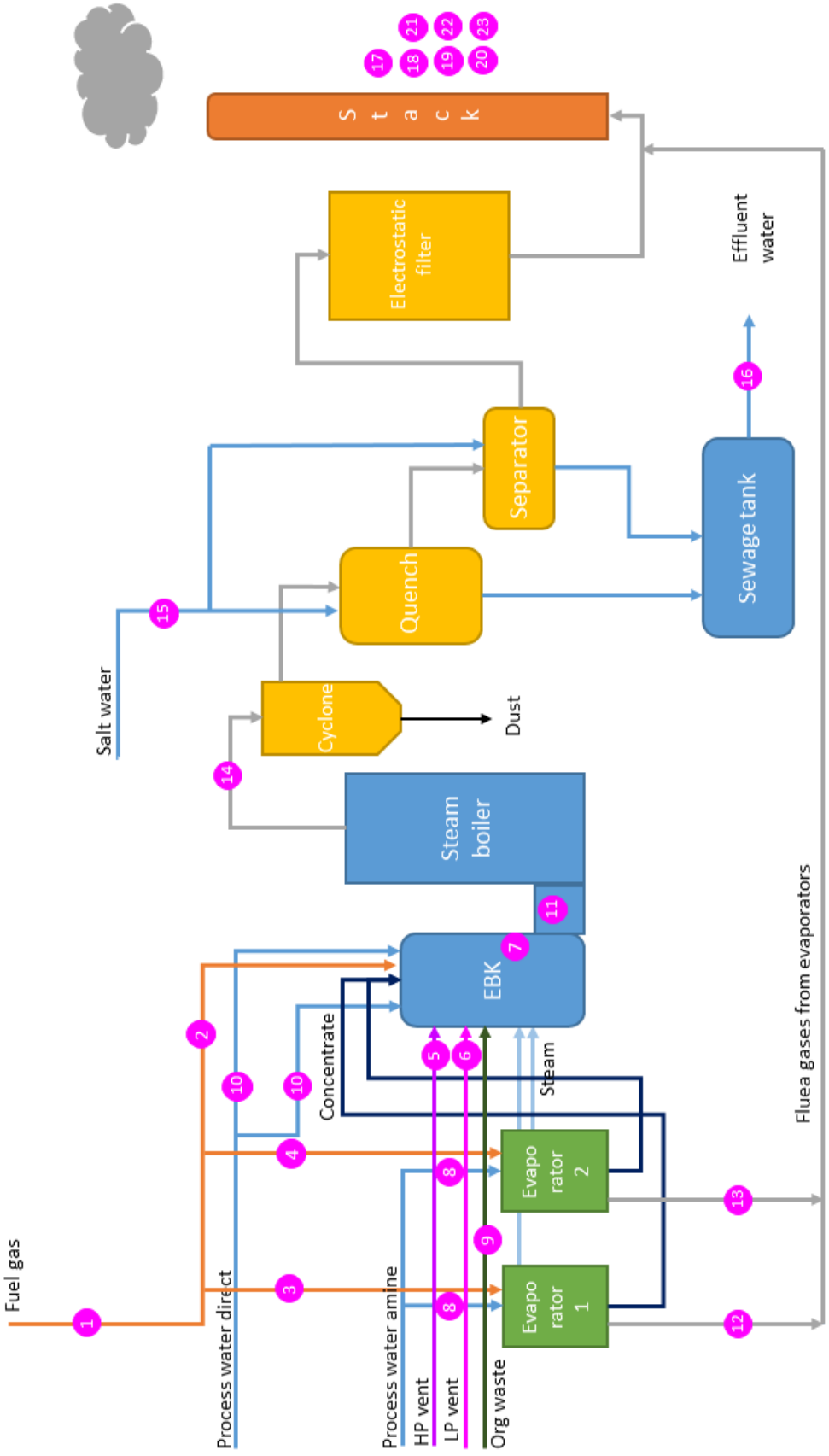


Figure 3.1: Schematic picture of the waste water incineration process (WINC).

Table 3.1: Table of measuring points with placement in the process, parameter measured and unit.

Name	Parameter	Unit	Placement
T_{fuel}	temperature of fuel gas	[°C]	1
$V_{fuelEBK}$	fuel gas flow to EBK	[m^3/h]	2
$P_{fuelEBK}$	pressure of fuel gas to EBK	[barg]	2
V_{fuel1}	fuel gas flow to evap 1	[m^3/h]	3
P_{fuel1}	pressure of fuel gas to evap 1	barg]	3
V_{fuel2}	fuel gas flow to evap 2	[m^3/h]	4
P_{fuel2}	pressure of fuel gas to evap 2	[barg]	4
V_{HPvent}	HP vent flow	[Nm^3/h]	5
V_{LPvent}	LP vent flow	[Nm^3/h]	6
$T_{wallEBK}$	temperature of the wall	[°C]	7
V_{wwamin}	waste water from amine plant	[l/h]	8
V_{org}	organic waste	[l/h]	9
m_{wws}	waste water from south side	[kg/h]	10
$T_{fluegasesEBK}$	temperature of flue gases	[°C]	11
X_{O_21}	oxygen fraction wet basis after evap 1	[vol%]	12
X_{O_22}	oxygen fraction wet basis after evap 2	[vol%]	13
X_{O_2EBK}	oxygen fraction wet basis after EBK	[vol%]	14
V_{sw}	salt water for quench	[m^3/h]	15
V_{aw}	sewage water from storage tank	[m^3/h]	16
T_{aw}	temp sewage water from storage tank	[°C]	16
X_{O_2stack}	oxygen fraction wet basis in stack	[vol%]	17
C_{NO}	NO concentration in stack	[mg/Nm^3]	18
C_{N_2O}	N_2O concentration in stack	[mg/Nm^3]	19
C_{NH_3}	NH_3 concentration in stack	[mg/Nm^3]	20
C_{CO}	CO concentration in stack	[mg/Nm^3]	21
C_{CO_2}	CO_2 concentration in stack	[mg/Nm^3]	22
$X_{H_2Ostack}$	water fraction in stack wet basis	[vol%]	23

In the waste incineration plant, short name WINC, the destruction of waste water, organics residues and ventilation gas from the whole site is achieved by incineration in a furnace. A gas fired furnace would yield a flame temperature ranging from 1100 to more than 1600°C based on the temperature of a natural gas flame (Keck et al., 2002). The temperature in the EBK furnace is probably lower than this considering the amount of water that is distributed in the furnace. Incineration temperature according to data sheets from AkzoNobel states that the incineration takes place at 950°C during a residence time of at least 2 seconds with excess air. The capacity of the plant is approximately 6 tonnes of process water per hour. The hot furnace exhaust gases are used to produce around 10 tonnes per hour of steam at 40 bar.

The process consists of the following process units:

- Two evaporators before the furnace
- Destruction furnace (Efterbrännkammare, EBK)
- Flue gas steam boiler
- Dust separation cyclone
- Quench
- Separator
- Electrostatic particulates filter
- Sewage tank
- Flue gas stack

There are effectively seven inlet streams, counting steam and concentrate as one waste stream, to the EBK in total, and eight to the WINC including the salt water for the quench. There are only two outlets, the stack and the effluent water. The units that are of importance for this thesis are explained in more detail in section 3.3.

3.1 Process data

The program Aspen Process Explorer is used on site to document the process. Through this program it is possible to access actual run time data with a resolution of maximum every minute. For this project data have been collected every ten minutes monthly for 2017. The data was then exported to Excel and recalculated to an hourly average over each month. For complete table of measuring points used in this project, see Table 3.1 and Figure 3.1.

3.2 Feed streams

The fuel used for both the destruction furnace and the evaporators is a "burner gas" provided from a nearby steam cracker plant, referred to as fuel gas. Ventilation gases from the AkzoNobel production site is also used. The ventilation gas streams are referred to as HP-vent (High Pressure ventilation gas) and LP-vent (Low Pressure ventilation gas). The waste process water that is the subject of destruction comes from two different sources. One stream (amine waste water) origins in the amine production side of the plant and is concentrated by evaporation of excess water, and thereafter introduced to the furnace. The other stream (direct water) comes from the surfactant production side and is not concentrated but introduced straight to the furnace, referred to as direct water. The design idea of the process was to reduce the necessary size of the EBK by managing the largest part of the excess water evaporation from both waste water streams by the use of evaporators, but this proved to be technically difficult since the south side stream contains a considerable amount of surfactants. This caused foaming problems in the evaporator which led to the current setup with only one stream passing the evaporators. There is also a third waste stream, containing organic waste. This stream is almost purely unusable

products from the amine plant. It is not a constant stream but is incinerated when needed.

Table 3.2 displays the average molar percentage that the feed streams contribute with to the EBK. January to March uses average values for HP- and LP-vent gas flows, April uses real time measurements.

Table 3.2: Average percentage of the feed streams in mol%, January to April, excluding 31st of March because of EBK shut down.

Feed stream	January average %	February average %	March average %	April average %
HP	1.24	1.28	1.26	0.95
LP	2.02	2.09	2.09	1.47
waste water amine	17.79	16.50	21.62	16.48
waste water direct	11.48	10.83	11.02	9.89
air	62.97	65.28	59.62	68.33
fuel gas	4.30	3.45	3.97	2.76
organic waste	0.21	0.56	0.396	0.10
tot	100	100	100	100

Note that April calculated over the period of maintenance shut down time, leading to lower values of everything but air.

3.2.1 Operating conditions

The operating conditions for some parameters during January 2017 are presented in Figure 3.2 to 3.5. Figure 3.2 shows the total mass flow of direct waste water from surfactants. The regular dips in the flow is explained by the de-sooting process of the steam boiler tubes. This process is performed once every 36 hours. When this process is started all direct water flow is temporarily on hold. It can also be observed that the WINC was shut down during the 19th of January, when all water flows where zero. For operating data from February to April, see Appendix A.

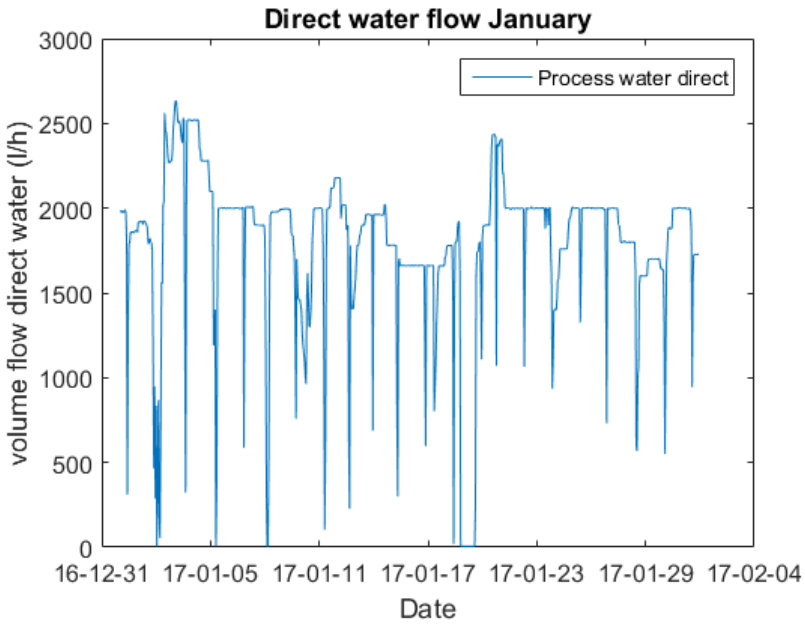


Figure 3.2: Total direct water flow in January 2017.

In Figure 3.3 the total mass flow of amine water from January 2017 is presented. The flow is less regular than the direct water flow and the dips during the de-sooting is less visible, though still observable. This is because the amine water flow is not directly controlled by flow, but by regulating the load on the evaporators.

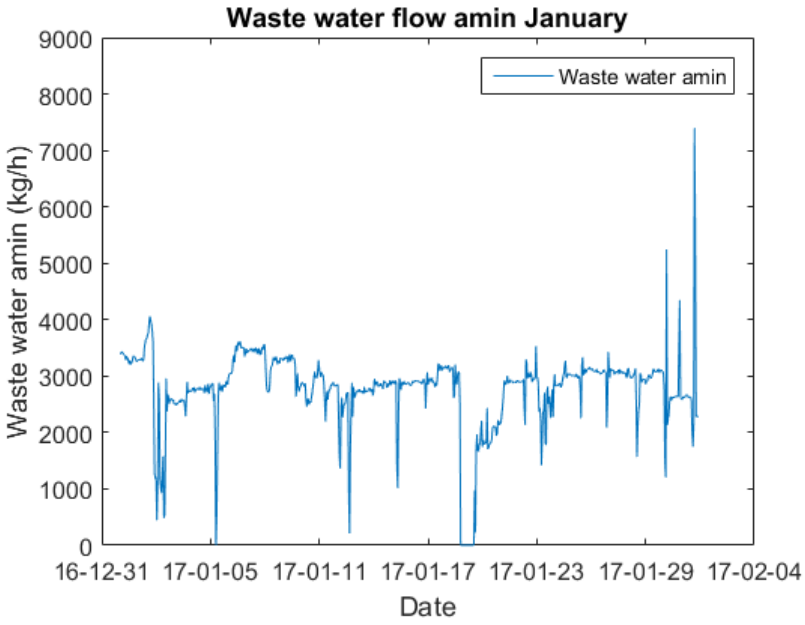


Figure 3.3: Total amine water flow in January 2017.

In Figure 3.4 the flue gas temperature after the EBK is displayed for January. It is also here visible that the WINC was shut down during 19th of January.

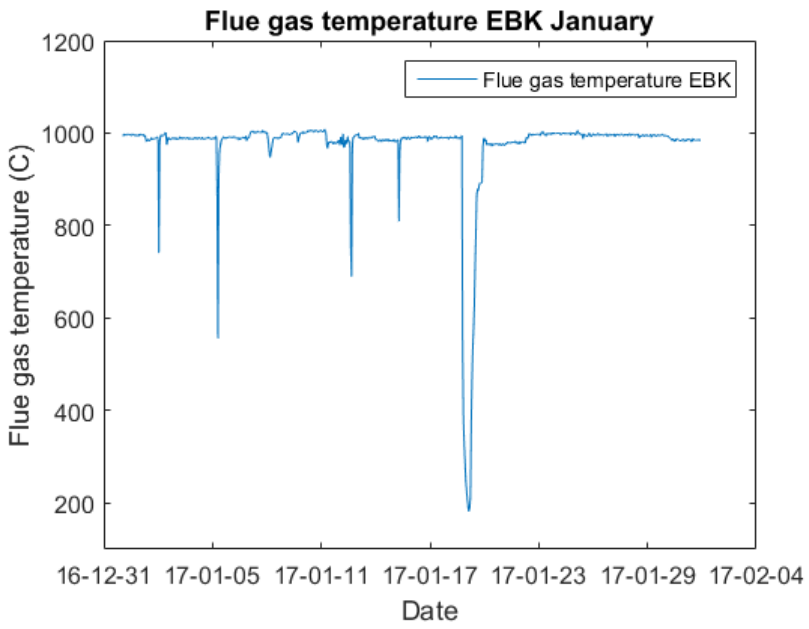


Figure 3.4: Flue gas temperatures in January 2017.

The last graph to represent the operating conditions of the process during January is the oxygen levels. They also peak and approach atmospheric levels during periods of de-sooting since the measuring instrumentation is a laser that is turned off during said periods.

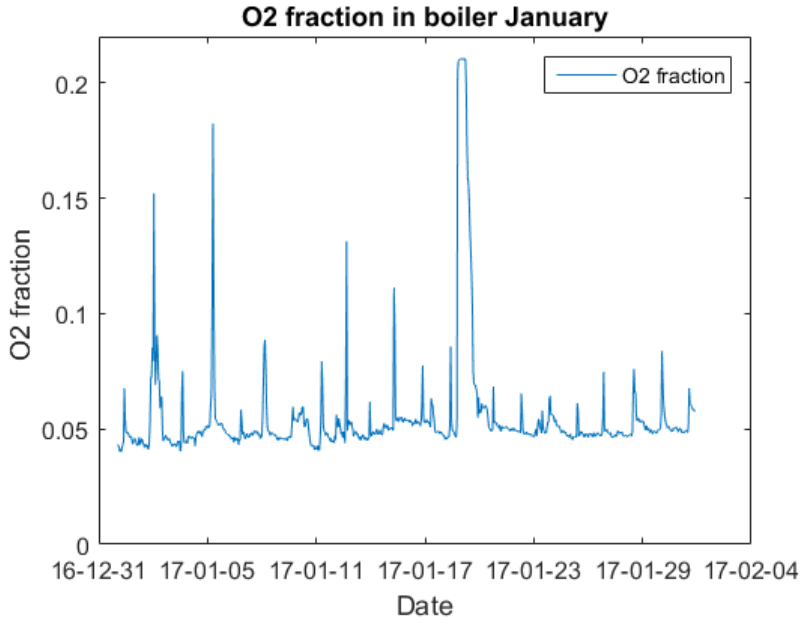


Figure 3.5: Oxygen levels after EBK in January 2017.

3.2.2 Fuel gas

The fuel gas composition varies daily, and the four largest components are hydrogen gas, methane, ethane and propane. The composition and the lower heating value (MJ/kg) of the gas is delivered retroactively at the end of each month from the cracker plant. At the AkzoNobel site the mass and volume flow is measured as well as pressure and temperature, and a density is calculated and converted to kg/Nm^3. This density is used to calculate the heating value in kWh/Nm^3. The heating value is then used to regulate the pressure of the fuel gas, i.e. the flow. The flow then divides into two channels, one for the EBK and one for the evaporators. The average volume split between the evaporators and the EBK ranges between 16-25% and 75-84% respectively.

The fuel gas compositions for January 2017 can be seen in Figure 3.6, together with the lower heating value. For fuel gas composition during February to April 2017, see Appendix A.

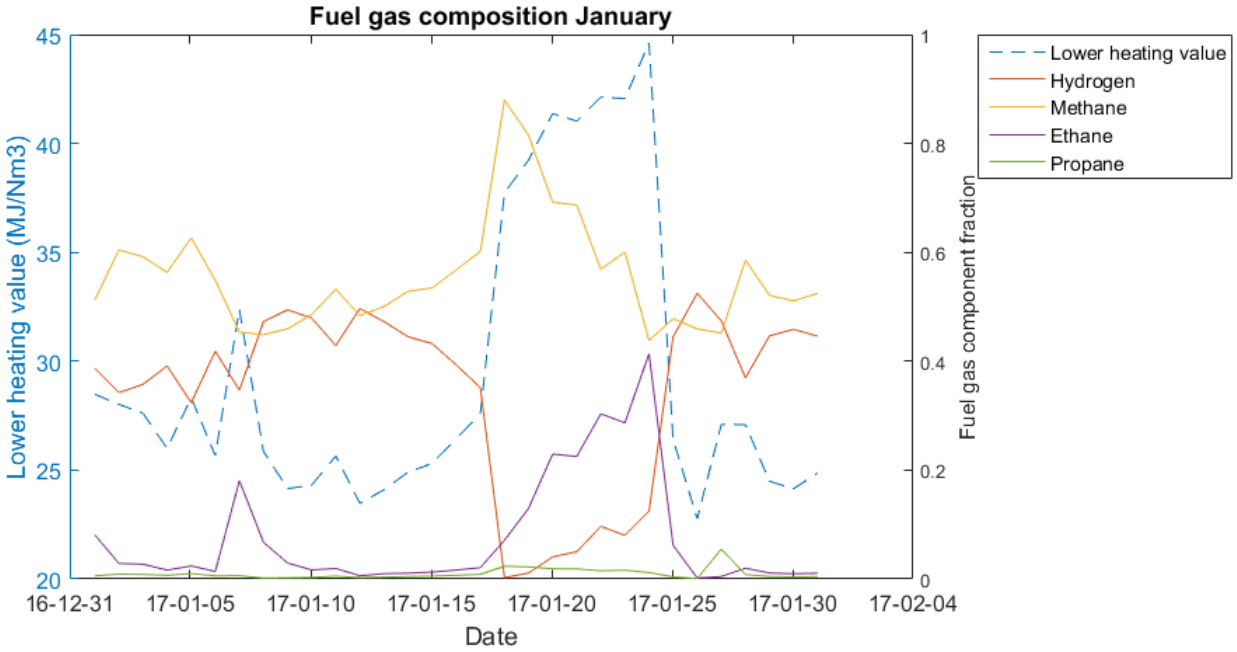


Figure 3.6: Fuel gas composition in January 2017.

It is clear that the heating value varies from between 25-45 MJ/Nm^3 and the heavier compounds ethane and propane have the largest influence of the heating value. The heating value of the fuel gas affects the fuel gas flow to all primary burners.

3.2.3 Waste water

The composition of the amine process waste water is not completely known. It is assumed in this thesis that the two main components in the waste water stream are H_2O and NH_3. Other amine compounds and salts are probably present, but ammonia is the largest contributing fraction besides water. The amount of NH_3 in

the waste water is determined by a three step analysis. A GC-analysis of the water indicates the amounts of the amines that are expected to be found in the water, and by titration and further calculation the amount of NH_3 in the water is determined. This analysis is done once every Tuesday, and the values are therefore not as frequently measured as other components. For this thesis the value is therefore assumed to be constant during the week. Mean value of the amount of NH_3 in the amine waste water stream over the year of 2016 is around 2.3% on mass basis and can be assumed to be around that value for 2017 as well. There is one outlier that has been removed from the average calculation where the ammonia mass percentage is at 28.6%. The maximum value below this is 3.8%. The minimum value over the year is 0.7%.

The waste water from the surfactant side of the plant is not regularly analysed, but contains mostly organic material in the form of surfactants. The amount of organic material is measured by COD analysis, Chemical Oxygen Demand, which is an indirect method of determining the amount of organic compounds in water. One such analysis is available but since it does not identify any compounds specifically it has been emitted from this report. The water does not contain any NH_3.

A third liquid waste stream is sometimes introduced, referred to as organic waste. This stream also varies in composition and most importantly in size, but the amounts are small compared to other feed streams so it is not assumed that this stream has a great impact on the combustion.

3.2.4 Ventilation gases

Ventilation gases are effluent gas removed from the amine production plant at different pressure levels. Both the high and low pressure ventilation gas composition varies with unknown frequency. Unfortunately only one analysis exist for each gas respectively and this result will therefore be used for calculations, see Table 3.3.

Table 3.3: HP and LP vent gas composition.

HP vent gas component	% of vol
H_2	57.0
CH_4	4.8
NH_3	38.2

LP vent gas component	% of vol
N_2	82.7
NH_3	15.4
O_2	1.9

The flow meters for the ventilation gases are also an uncertainty. They have been malfunctioning and can only be deemed reliable since after the WINC maintenance stop during week 14 in 2017. This means that a mean value for high and low pressure vent gases have to be used for calculations with data from January, February and March. The analysis of the ventilation gases compositions together with the malfunctioning flow meters are two of the biggest uncertainties in this thesis.

3.3 Process units

The following section will describe the most relevant process unit steps and their function in more detail.

3.3.1 Evaporators

The two evaporators are used to evaporate a large fraction of the amine process water. The evaporators are fed with fuel gas and air in the burner, and process water from the amine plant on the liquid side. The hot flue gases from combustion are led through a network of tubes to heat the surrounding water of which the concentrate is removed from the bottom and injected to the furnace. The steam generated in the evaporators is also introduced to the furnace because of light components in the waste water that also needs to be destroyed. The purpose of the evaporators is to reduce the energy need in the furnace, effectively reducing the size of the destruction furnace. See Figure 3.7 for schematic picture of the evaporators.

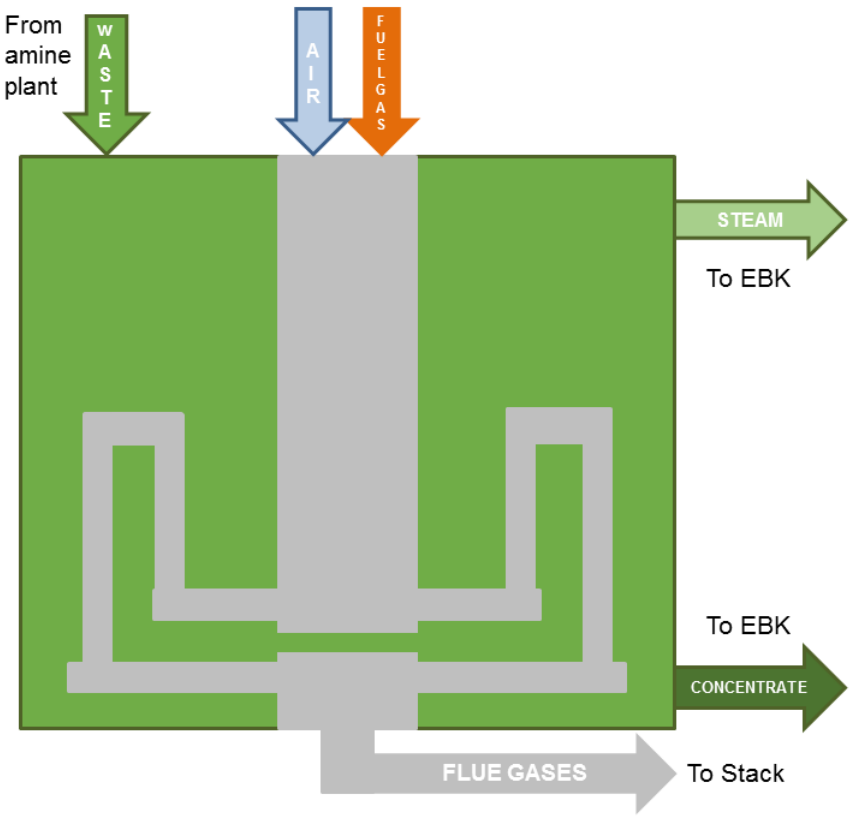


Figure 3.7: Simplified evaporator design.

The relationship between mass flow of the waste water feed stream to the evaporator and mass flow of the concentrate stream leaving the evaporator is a set value in the control system, usually around 5-20%, and the amount of fuel gas needed to

fulfill this requirement is then calculated . The air is then in direct proportion to this calculated relationship and the fan effect is set to a value that correlates to the volume flow of the fuel gas. See Table 3.4 for all inlet and outlet streams in the evaporator.

Table 3.4: Table for all in streams and out streams in evaporators.

Inlet streams (same for evap. 1 and 2)	Outlet streams (same for evap. 1 and 2)
Fuel gas	Flue gases to stack
Air	Concentrate for EBK
Waste water from amine plant	Steam for EBK

In Table 3.5 some technical data for the EBK provided by AkzoNobel is presented. Actual values may vary significantly.

Table 3.5: Technical data for both evaporators.

Effect of gas burners	2 500 kW
Concentrate flow to EBK	350 kg/h
Steam flow to EBK	3 000 kg/h
Flue gas flow to stack	3 000 Nm^3/h
Flue gas temperature	130-140°C
Total volume of tanks	30 m^3

3.3.2 Destruction furnace (EBK)

The destruction furnace is a down-fired combustion oven. It is 7.7 m high internally and 3.1 m in diameter. The waste water streams are injected by 4 lances placed in a square around the main burner. Two lances are used for the concentrate and two for the direct waste water. The organic waste is injected horizontally in to the flame further down in the furnace. Air is introduced to the feed streams before the lances for the direct water that have not gone through the evaporators to create a more evenly distributed and cloud shaped spray. This air flow is referred to as secondary air. The primary air is introduced to the main burner house resulting in a turbulent diffusion flame. The steam from the evaporators is introduced horizontally around 30 cm below the main burner at the top of the furnace. HP and LP vent gases are introduced at the same height and placement as the primary air. See Figure 3.6 for simplified design of the EBK.

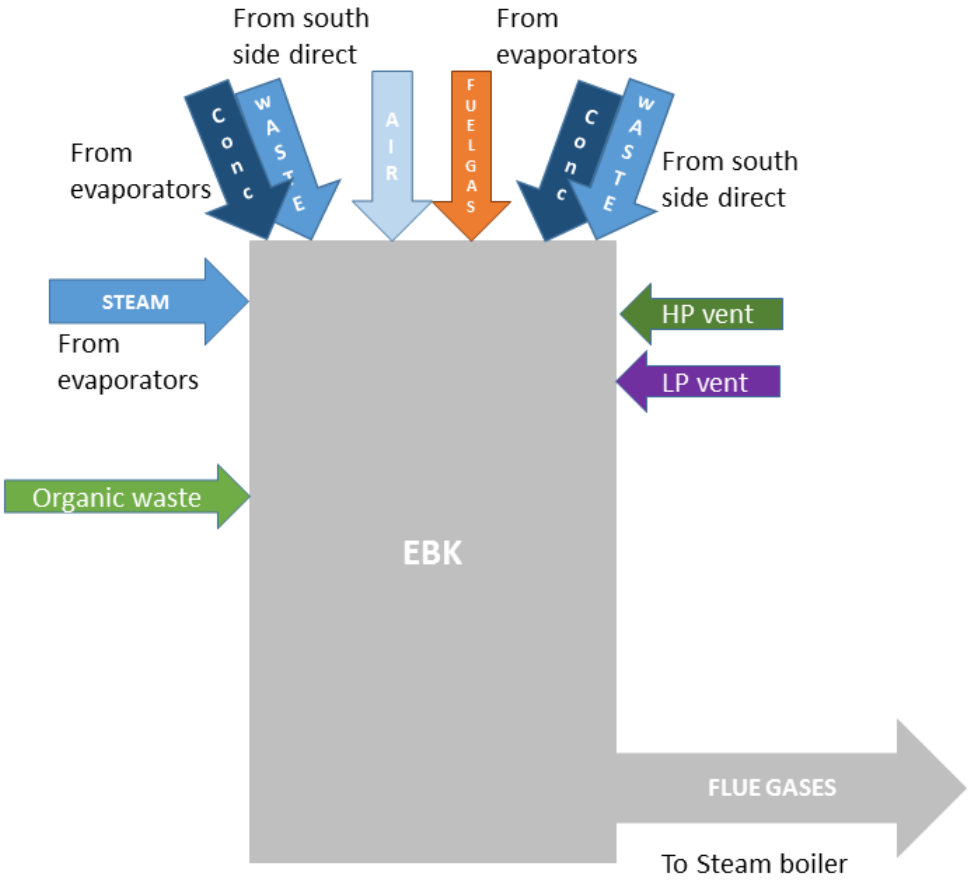


Figure 3.8: Schematic view of the EBK design.

The temperature is measured at two places. One is at the flue gas exit (point 11 in Figure 3.1) before the exhaust enters the steam boiler, generally around 950-1050°C, and the second is at the wall of the EBK (point 7, Figure 3.1), about 1.5 m above the flue gas exit, generally around 1000-1100°C. The temperature at the flue gas exit point controls the flow of fuel gas while the oxygen level after the EBK controls the flow of primary air to the furnace. The control system is explained further in section 3.5. The percentage of valve opening for HP and LP is a set value. See Table 3.6 for all EBK inlet and outlet stream definitions.

Table 3.6: Table for all inlet streams and outlet streams to the EBK.

EBK, inlet streams	EBK, outlet streams
Fuel gas EBK	Flue gases to steam boiler
HP vent gas	
LP vent gas	
Primary air (for fuel gas, HP and LP)	
Waste water ethylene oxide, 1	
Waste water ethylene oxide, 2	
Secondary air (for diffusion of process water)	
Waste water concentrate from evap 1	
Steam from evap 1	
Waste water concentrate from evap 2	
Steam from evap 2	
Tertiary air/cooling air	

3.3.3 Post-combustion units

The hot flue gases after the furnace are led to a steam boiler where 10 tonnes of steam at a pressure of 40 bar is produced every hour. After the steam boiler the flue gas after treatment consists of a dust cyclone, quench, separation and an electrostatic filter. Dust is separated by circulating the air in the cyclone, collecting dust and particles in a container below. In the quench sea water is sprayed over the flue gases to lower the temperature. This also condenses water from the flue gases and this water and the salt water used is then separated before the electrostatic filter, leaving the flue gases saturated. This is important since to much water in the gases would damage the filter. The electrostatic filter is then used to remove the last particles before the flue gases are emitted to the surrounding air via the stack. The stack is 50 m high and the composition of the gas is measured continuously around 5 meters above ground. The quench/separation of water and the stack are described in more detail below since they are important for the over all balance of the system.

3.3.3.1 Quench system

The object of the quench is to lower the temperatures and remove excess water from the hot flue gases from the EBK. See Figure 3.9 for schematic picture of quench and separation step.

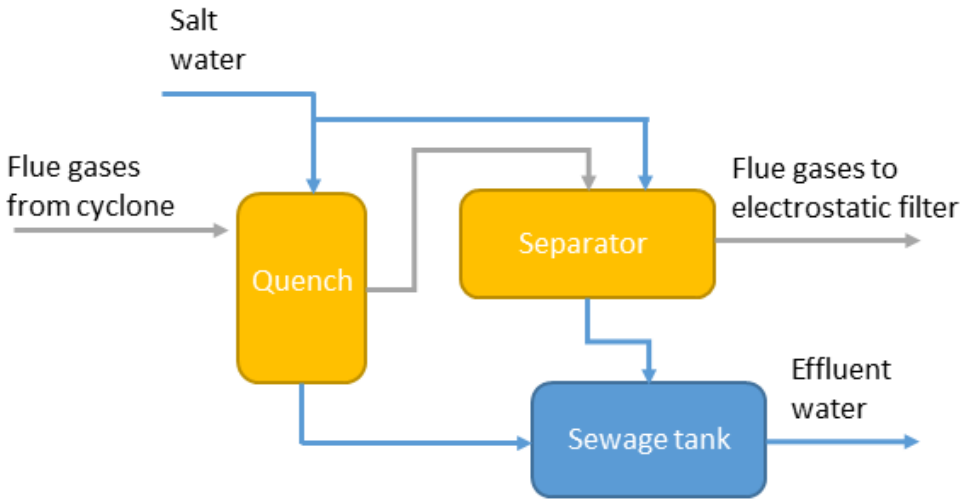


Figure 3.9: General design of the quench and separation step.

The flue gases enter the quench system after the steam boiler, and salt water is sprayed in a circular pattern from the top. The gases cool down from 300°C to around 57°C after the separation. They then enter a separator where extra water is sprayed over the gases to reach saturation point at this pressure, and the gases then enter the electrostatic filter. The liquid water that leaves the quench is deposited in a storage tank. This water is also used to flush the electrostatic filter and the tank also collects the excess water from the de-sooting process in the steam boiler. The water in the tank is led via a heat ex-changer before it is emitted to the ocean.

There is one flow meter for the salt water before it enters the quench and separator and one flow meter in the stream leaving the storage tank, making it possible to determine the amount of water leaving the flue gases in the quench and separator. The temperatures are however not equal but this can be overcome by use of nearby temperature meters for both salt water and effluent water. The amount of liquid water removed from the flue gases using this method is on average 6 m^3/h. The volume flow of flue gases before and after the quench are presented in Figure 3.10, where it is clear that the amount of water that condensates in the separation step corresponds to around 7 000 Nm^3 of flue gases per hour.

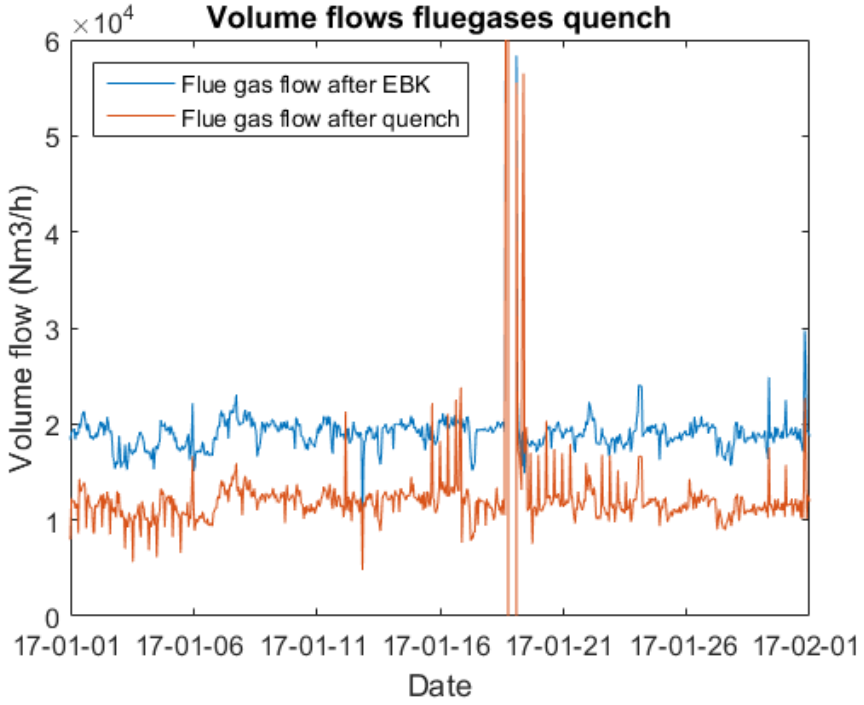


Figure 3.10: Volume flow of flue gases before and after the quench.

The more uneven flow in the flue gases after the quench is explained by the uneven level of the storage tank accommodating the water after the quench. Since this water is also used to flush the electrostatic filter it leads to uneven measurements at times. This is because the water flow from the storage tank to disposal then goes down when the water is instead used for the electrostatic filter and up when that water is returned to the tank.

In Figure 3.11 the water fraction before and after the quench is presented.

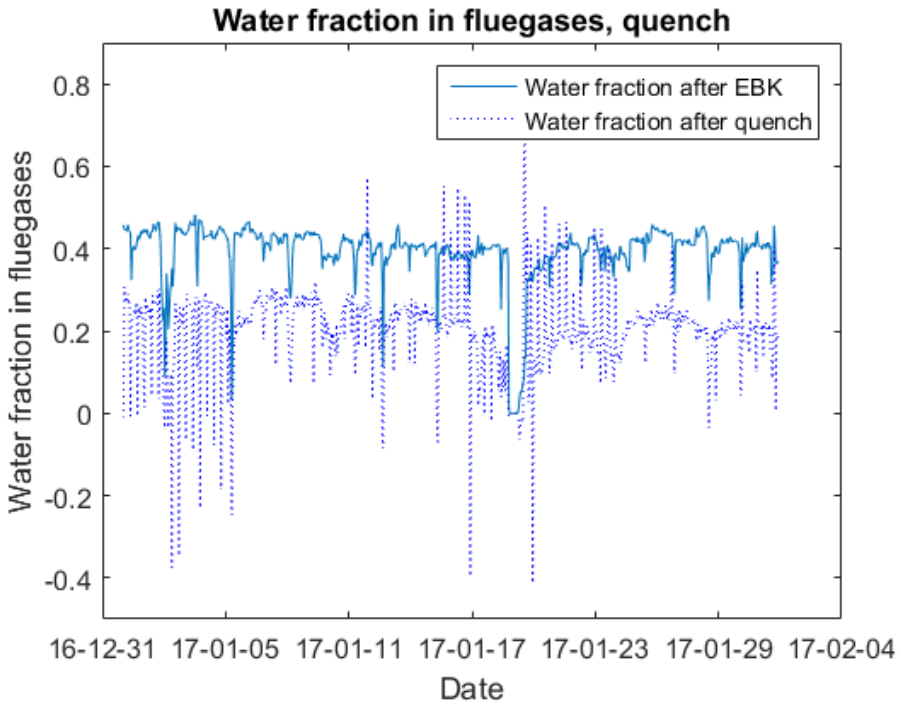


Figure 3.11: Water fraction in flue gases before and after the quench.

As can be seen in Figure 3.11 the water fraction after the EBK is around 40-41% and the water fraction after the quench around 20%. In Table 3.7 the data provided by the company states that these values should be 41.5 and 18.3%. The flow of water from the storage tank is however very dependent on the water temperature since the density of a liquid varies a lot with this parameter, and there is just one temperature meter that is not placed exactly where the flow meter is. Therefore this flow is an uncertainty. It is also visible here as well that the flow after the quench has many local maxumim and minimum values because of the flushing of the electrostatic filter.

The water from the tank is analysed once a week, measuring total amount of nitrogen in mg/L. These values range from 0 to a maximum of 31 mg/L during the period of January 2016 to February 2017. The maximum limit of nitrogen allowed to dispose of in the sea is 20 mg/L. This value is met or surpassed in total 12 days during said time period. There are no analyses made for ammonia specifically in the effluent water, but since ammonia is soluble in water it is probable that some or all of the nitrogen in the water comes from the ammonia washed out from the flue gases. This makes the quench and separation step one of the biggest uncertainties together with the vent gases in the material balance since it is the only other outlet part from the stack.

In Table 3.7 some technical data for the quench system is presented. This data is retrieved from the process documentation at AkzoNobel.

Table 3.7: Technical data for the quench system, quench and separator.

	Inlet	Outlet
Gas flow	max 21 000 Nm^3/h	15 000 m^3/h
Gas temperature	250-300°C	57°C
Water temperature	26°C	69°C
Gas components in flue gases(wet basis)		
H_2O	41.5 vol%	18.3 vol%
CO_2	7.8 vol%	10.9 vol%
O_2	4.3 vol%	6.0 vol%
N_2	46.4 vol%	64.9 %

3.3.3.2 Stack

The flue gases from the EBK are joined with the evaporator flue gases after the electrostatic filter and then let out through the chimney via flue gas fan. The stack is 50 m high. Around 5 m above the inlet to the stack there is instrumentation that performs continuous analysis of the flue gas composition. All measurements are made on wet basis in mg/Nm^3.

3.4 Measuring instrumentation

The on-line instrument for O_2 level analysis after the EBK are made in the steam boiler and is of laser type. It has two primary elements on each side of the flue gas channel and is therefore not in operation during de-sooting since the operation obstructs the straight visual line needed.

In the stack the flue gases are analysed with regards to inorganic components, organic components, oxygen level and dust level. For the organic and inorganic compound an FTIR is used. An FTIR - Fourier Transform Infra Red Spectrometer, detects gaseous compounds based on the absorption of infra red light. The FTIR in the stack uses a helium/neon laser and sample temperature of 180°C. The instrument is calibrated once every day.

The oxygen measurement instrumentation in the stack is a Zirconium type Oxitec. Zirconia oxygen analysers use the conductivity of ceramic zirconium walls to determine the oxygen level in a sample since they only allow oxygen ions to pass at high temperature levels. The sample gas pass one one side and reference gas on the other, oxygen passing the wall then creates a current that can be measured to determine amount of oxygen. (Toray Engineering Co, Ltd., 2017). It uses the same sample flow as the FTIR, hot wet sample, and the same instrumentation for oxygen level measurement is used after the evaporators.

The dust measurement is done by using a sensor that registers loaded particles and multiplies the signal to show up in the system.

3.5 Control systems

The conditions in the furnace are partly controlled by self-regulatory systems. The control parameters are the temperature of the flue gases after the EBK and the oxygen fraction of the flue gases, measured after the steam boiler.

The total air flow to the furnace is regulated by the oxygen level after the EBK. A value is set, usually around 3.5% oxygen on wet basis, and this value is used to calculate the required load on the air fan providing primary air to maintain this set value after the furnace. The load in the fan then regulates the pressure and effectively flow of primary air to the furnace.

For the temperature and fuel gas flow regulation a set value of the flue gas exit temperature is decided. By using the previously calculated heating value of the fuel gas feed stream the amount of gas necessary for maintaining the set temperature after the EBK is calculated. This then controls a set of pressure valves in the fuel gas and primary air supply, regulating the amounts entering the furnace and effectively the temperature until the set value is achieved. This regulation of air and fuel gas takes place after the primary air fan and opens and closes both streams equally, keeping the calculated excess oxygen relation the same as before.

4
Methodology

The following chapter describes the methods and relations used to evaluate the incineration process in the EBK and the evaporators and also the separation process in the quench.

4.1 Balances and calculations

The first stage of the thesis work consisted of data interpretation. The process in Stenungsund has been in use since 2005 and it is possible to study continuous operation data of the process from 2009. The aim of this step in the project was to organize and process the existing data to get an overview of composition and amount of all streams entering and leaving the process. The measurement data from the stack is measured in concentrations, mg/Nm^3, meaning it is not possible to distinguish if changes in these values are because of dilution or actual changes in the combustion process. It is therefore of interest to find the molar flow of the interesting compounds in the process. Since there is no equipment to measure any actual mass or volume flow after the EBK, evaporators or in the stack, it has been necessary to calculate this flow. This is done by means of material balances. The resulting molar flow data is then plotted against different parameters to look for trends and/or correlations between feed streams and furnace conditions as well as products that are formed and released in the stack.

To map what happens in the process it was necessary to single out the most important parts and balance in- and outlet streams. These are the evaporators and the EBK where the combustion takes place, and the quench system where water is separated from the flue gases. The balances have been constructed using stoichiometric relationships for complete combustion and real time data from the process analyser program. The time frame have been set to the months of January to April 2017. This limit is set because of malfunctioning instrumentation before that, the most important ones being the oxygen level meters after the evaporators and the HP and LP vent gas meters. The WINC was shut down for maintenance during week 14 and the oxygen level control system for the EBK and ventilation gas meters can be considered malfunctioning before that.

4.1.1 Combustion process balances

The combustion is assumed to be complete and stoichiometrically correct, producing only water and carbon dioxide.

The basic fuel for the combustion processes in both evaporators and the EBK is the fuel gas. The composition varies on a daily basis. The largest fraction contributions in the fuel gas usually comes from hydrogen, methane, ethane and propane and these daily fractions and substance properties will be used for combustion calculations.

The evaporators only burn fuel gas, but since the EBK has more than one combustible feed stream the same principle will be used for all inlet stream. The theoretical amount of oxygen needed for the combustion is denoted by z and corresponds to the exact amount needed to convert all fuel to carbon dioxide and water. The excess air ratio is denoted by λ (lambda). In air nitrogen is related to oxygen by the ratio 79% to 21%.

The general molar balance for the combustion process of only one fuel stream with the four component fractions y_1-y_4 representing the fraction in the fuel gas coming from hydrogen, methane, ethane and propane, as is the case for the evaporators, is presented below:

$$\begin{aligned}(y_1\,H_2 + y_2\,CH_4 + y_3\,C_2H_6 + y_4\,C_3H_8) + \lambda z\,O_2 + \frac{79}{21}\,\lambda z\,N_2 \longrightarrow \\ m_1\,CO_2 + m_2\,H_2O + (\lambda - 1)\,z\,O_2 + \frac{79}{21}\,\lambda z\,N_2\end{aligned} \tag{4.1}$$

Where m_1 and m_2 are the stoichiometric product coefficients for water and carbon dioxide. The coefficients are calculated as presented in Equation (4.2) to (4.4), where the number of hydrogen atoms in component 1-4 are denoted a_1-a_4 and the number of carbon atoms are denoted b_1-b_4.

$$m_1 = \frac{(y_1 \cdot a_1) + (y_2 \cdot a_2) + (y_3 \cdot a_3) + (y_4 \cdot a_4)}{2} \tag{4.2}$$

For the fuel gas provided from the cracker plant, $a_1 = 2$, $a_2 = 4$, $a_3 = 6$ and $a_4 = 8$.

$$m_2 = (y_1 \cdot b_1) + (y_2 \cdot b_2) + (y_3 \cdot b_3) + (y_4 \cdot b_4) \tag{4.3}$$

For the fuel gas provided from the cracker plant, $b_1 = 0$, $b_2 = 1$, $b_3 = 2$ and $b_4 = 3$. The stoichiometric amount of air after combustion, denoted z, relates to the stoichiometric amounts of carbon dioxide, m_1, and water, m_2. They can be related via the number of hydrogen an oxygen atoms in the compounds by the following equation:

$$z = \frac{m_1 + m_2 \cdot 2}{2} \tag{4.4}$$

Which can be related to the stoichiometry via the following expression:

$$X_{O2} = \frac{(\lambda - 1)\, z \cdot \dot{n}_{\text{fuel}}}{\dot{n}_{\text{totflue}}} \tag{4.5}$$

Where $\dot{n}_{totflue}$ is defined as the total molar flow of flue gases:

$$\dot{n}_{\text{totflue}} = (m_1 + m_2 + (\lambda - 1)\, z + \frac{79}{21}\lambda z) \cdot \dot{n}_{\text{fuel}} \tag{4.6}$$

Solving Equation (4.5) combined with Equation (4.6) for λ will give the stoichiometrical value for excess air used in the combustion. The composition and volume flow for the fuel gas is known, as well as oxygen level after the evaporators and the EBK. When more than one feed stream is used, as for example in the EBK combustion where fuel gas, HP vent, LP vent, water and ammonia from the waste water are introduced to the furnace, the m_1, m_2 and z values are calculated in the same manner for each fuel stream and water becomes a separate term in the balance. The values are then multiplied by the total molar flow of that specific stream and combined to calculate the excess air ratio λ for the complete combustion process by using a modified version of Equation (4.5).

Once the stoichiometric constants m_1, m_2 and z are calculated, the molar flow of all the products in the flue gases can be determined. Using these molar flows, specifically the oxygen molar flow, and λ the following relation is used to find the total molar flow of air:

$$\dot{n}_{\text{air}} = \frac{\lambda \cdot \dot{n}_{O_2}}{0.21} \tag{4.7}$$

Using all calculated molar flows for the products after combustion the total molar flow of flue gases can be calculated. The standard volumetric flow of both inlet air and flue gas combustion products can then be found using the ideal gas law and the standard conditions T=273.15 K, P=101 325 Pa and the ideal gas constant R = 8.314 J/Kmol according to:

$$\dot{V} = \frac{\dot{n} \cdot R \cdot T}{P} \tag{4.8}$$

This means that the fractions of all components after the combustion step can be calculated using the molar flows or volumetric flows.

For January to April 2017 real time data has been retrieved once every 10 minutes for all measurement points in Table 3.1. These values have also been recalculated as hourly average values for the same months. The flue gas flow and composition has been calculated for both the EBK and the evaporators.

There are as mentioned before uncertainties in the composition and flow of vent gases as well as uncertainties concerning the other measurements since analytical

data from on-line instruments and flow meters in processes always are within some margin of error. There are also periods where start up or shut down time in the different units in the process gives values that are not within normal operation values of the incinerator. These values are in extreme cases removed from the data sets when they can be related to such start up/down time periods.

4.1.2 Post-combustion steps

4.1.2.1 Quench

The quench step described in section 3.3.3.1 contains one of the two outlets from the whole process making it a crucial part of the material balance of the process as a whole. Salt water enters above the quench and as the flue gases cool down water vapor from the hot flue gases condenses and is removed with the salt water. For this section a mass and molar balance was established using the molar flows calculated in the previous section together with real time mass flow data from point 15 and 16 in Figure 3.1. The mass balance concerning the water is achieved by assuming that the extra water in the sewage flow is the water condensed from the flue gases. Subtracting this extra molar flow of water from the flue gases a new molar flow of flue gas can be calculated. This flow and composition is then assumed to be constant through the electrostatic filter. According to data specification sheets concerning the process provided by AkzoNobel, the level of H_2O in the flue gases is expected to drop from around 40% to around 18% in the quench and separation step.

Uncertainties concerning the quench and separation step involves the amount of nitrogen in the sewage water. It is not clear how large fraction of this nitrogen that comes from dissolved ammonia. Further analyses of the sewage water to determine how much ammonia it contains would be recommended to improve the calculations.

4.1.2.2 Stack/total

For the last step of the material balance calculations the flue gases from the evaporators are added to the flue gases from the EBK after treatment. New fractions of water, carbon dioxide and oxygen were calculated and can be compared to actual data from the process.

4.1.3 Real time data overview

Interesting parameters where plotted against time in Excel to get a rough overview of possible trends and correlations that could be of interest. Fuel gas flow, heating value of the fuel gas, amount of waste water and levels of NO_x are examples of parameters that were investigated. These eventual correlations were then further investigated using the MATLAB script to plot parameters against each other to see if there are any clear trends or correlations.

4.2 Modeling

The purpose of modeling is to investigate what happens if certain parameters of the furnace are changed.

4.2.1 Chemkin setup

Since combustion processes takes place in both the evaporators and the EBK, two basic models have been derived. The model for the evaporators consists of a plug flow reactor (PFR) with two inlets, one for fuel gas and one for air. The model is designed around a base case derived from mean values of the inlet streams during a period of stable operation in January. For all evaporator model data see Table 4.1. For the EBK the model is set up as a PFR with seven inlets for air, fuel gas, HP vent, LP vent, waste water containing ammonia and waste water not containing ammonia. Since there are no analyses of the organic waste content this stream has been omitted. The base case is designed around mean values of a period of stable operation in January. See Table 4.1 for setup and inlet stream data for the EBK model.

Table 4.1: Model parameters and values for evaporators and EBK.

	Evaporators	unit	**EBK**	unit
Reactor parameters				
Length	3.0	m	7.7	m
Diameter (m)	1.5	m	3.1	m
Pressure	1 atm		1 atm	
Inlets				
Inlet 1, fuel gas	25	g/s	137.4	g/s
- CH_4	60	mol%	60	mol%
- H_2	40	mol%	40	mol%
Inlet 2, air	600	g/s	3751	g/s
Inlet 3, LP vent	-		128.22	g/s
- CH_4	-		4.8	mol%
- H_2	-		57.0	mol%
- NH_3	-		38.2	mol%
Inlet 4, HP vent	-		25	g/s
- CH_4	-		4.8	mol%
- H_2	-		57.0	mol%
- NH_3	-		38.2	mol%
Inlet 5, waste water amin	-		1.1	kg/s
- H_2O	-		97.9	mass%
- NH_3	-		2.1	mass%
Inlet 6, waste water direct	-		0.5	kg/s
- H_2O	-		100	mass%

Since the software does not support the chemical compounds propane or ethane the fuel gas composition is limited to methane and hydrogen gas.

The modelling will be used as a sensitivity study. This is done by setting up a parameter study of the temperature in Chemkin. The parameter study will assume the reactor as an isotherm reactor and run the complete reactor length of combustion calculations a specific temperature. This is then repeated over a range of temperatures. For this study the temperature interval ranged from 550-1850°C with 50°C increments. The results of the temperature parameter study then contain information about how the molar fraction of the compounds of interest change over a large spectrum of temperatures. This parameter study is then repeated for a number of other parameters where one specific parameter per test runs is changed over some interval. Important parameters for the formation of wanted and unwanted products of combustion are:

- Mixing rate (staging) of inlet streams
- Temperature
- Size of inlet streams
- Amount of excess air

Because of the relative stability of the evaporators only the modelling of the EBK will be reviewed in the sensitivity study. All inlet parameters to the EBK Chemkin model is presented in Table 4.2 and marked with * in Tables 4.3 to 4.6.

Table 4.2: Base line parameter values.

Parameter	Value	Unit
$C1_{in1fuel}$	137.4	(g/s)
$C2_{in2air}$	3715.3 (L4)	(g/s)
$C3_{in3LP}$	128.2	(g/s)
$C4_{in4HP}$	25.1	(g/s)
$C5_{in5H_2Oamin}$	1.11 (A1)	(kg/s)
$C6_{in6H_2Odirect}$	0.5 (P2)	(kg/s)
Base length of staging	150	cm

The modelling software only allows one direct inlet, all other inlets must be staged. The length of this staging affects the mixing rate of the inlet, and is therefore a parameter that can be evaluated in the model. It is however not possible to change this in the real process at the moment.

Table 4.3 to 4.6 displays the parameters run in the temperature parameter study.

Table 4.3: Air staging distance, inlet C2 and length of staging.

test name	staging length	air flow g/s
100cm	100 cm	3751.0
150cm*	150 cm	3751.0
250cm	250 cm	3751.0

Table 4.4: Direct process water parameters, inlet C6.

	PER LANCE		TOT
test name	Flow (l/h)	kg/s	kg/s
P1	1100	0.316	0.61
P2*	900	0.25	0.50
P3	700	0.19	0.39
P4	500	0.14	0.28
P5	300	0.08	0.17
P5	100	0.028	0.056

Table 4.5: Excess air parameters, inlet C2.

test name	% O2	Air flow g/s
L1	2.0	3261.4
L2	2.5	3415.9
L3	3.0	3578.9
L4*	3.5	3751.3
L5	4.0	3933.8
L6	4.5	4127.4

Table 4.6: Amine water parameters, inlet C5.

	TOT	TOT
test name	Flow (l/h)	kg/s
A1*	4000	1.11
A2	3500	0.97
A3	3000	0.83
A4	2500	0.69
A5	2000	0.56

4.3 Experimental

The following section presents the experimental evaluation setup based on modelling results.

4.3.1 Assumptions, set points, experimental setup

The parameters that have been identified as possible to change at this point are load of waste water direct from south side, load on evaporators, exit temperature of the EBK, and the amount of excess air via the set oxygen level after the EBK. The experimental test runs were performed after the maintenance stop in week 14. To evaluate the influence of the four parameters the base case parameters where maintained as close to the modeling ones as possible. The test runs where designed to evaluate the Chemkin parameter studies. Because of operational safety limits of the EBK and difficulties in regulating some parameters these models could not be followed completely, and therefore it was decided that the most reasonable objective was to evaluate the following parameters over suitable intervals:

- Flue gas temperature
- Excess air
- Process water direct
- Amine process water from evaporators

The base case values are listed below and marked with * in Tables 4.7 to 4.10.

- Temperature, 1005°C
- Excess air, 3.5 %
- Process water direct, 1800 l/h in total
- Amine water from evaporators, around 4000kg/h in total

The experiment was run in four stages. While running the intervals of one parameter the other parameters where held as constant as possible at the base case values listed above. The first parameter was direct process water flow and it was varied according to Table 4.7.

Table 4.7: Process water direct from south side.

test name	Flow (l/h)	Time/run aim (hours)	Time/run actual (hours)
P1	1100	6	6
P2*	900	6	6
P3	700	6	6
P4	500	6	6
P5	300**	6	0

**Was not run because of trouble keeping all parameters at base values.

The time interval for the parameter variations was decided based on the probable time needed for the system to adjust to the new values so that a change could be observed in the stack concentrations.

The second parameter was temperature. It was varied according to Table 4.8.

Table 4.8: Temperature parameter set up.

test name	Temperature (°C)	Time/run aim (hours)	Time/run actual (hours)
T1	1015**	6	5
T2*	1005**	6	6
T3	995***	6	1.5
**Was run at 1000 l/h per lance of direct water.	***Was discontinued because of high levels of NH_3 in the stack		

The system was then once again returned to the base case values. The third parameter excess air was varied according to Table 4.9. Since the EBK has safety systems shutting down operation at low oxygen levels (1.5%), any values lower than 3% were not pursued.

Table 4.9: Excess air parameters.

test name	O_2 after EBK (%)	Time/run aim (hours)	Time/run actual (hours)
L1	3.0	6	6
L2*	3.5	6	9
L3	4.0	6	8
L4	4.5	6	6

The last parameter to be varied was amine water from the evaporators. This parameter can not be controlled directly but only by the relative load in the evaporators. The variations that were run are presented in Table 4.10.

Table 4.10: Amine water from evaporators.

test name	Load evap. 1 (%)	Load evap. 2 (%)	Time/run aim (hours)	Time/run actual (hours)
A1*	50%	20%	6	6
A2	60%	30%	6	6
A3	40%	10%	6	6

5
Results and discussion

5.1 Validation of calculations and balances

This section presets a comparison between calculated values and actual measurements. Focus is put on the stack as this is where most measurements are located. Values for every hour during the month, and the hourly value is a calculated mean of measurements from every 10 minutes per hour, meaning the plots in this section cover 24 values per day if not stated otherwise. Calculated values for e.g. lambda and the flue gas flows related to the evaporators and the EBK can be found in Appendix A.

5.1.1 Stack/total

The flue gases are after the quench led via the electrostatic filter to the stack where they are added to the flue gases from the evaporators, leading to the total balance of the system being closed.

The following section presents the total outlet streams from the process by adding up the flue gases from the evaporators with the flue gases from the electrostatic filter, comparing it to the analyses that are made in the stack.

5.1.1.1 Volume flows

Volume flow of flue gases in January is presented in Figure 5.1.

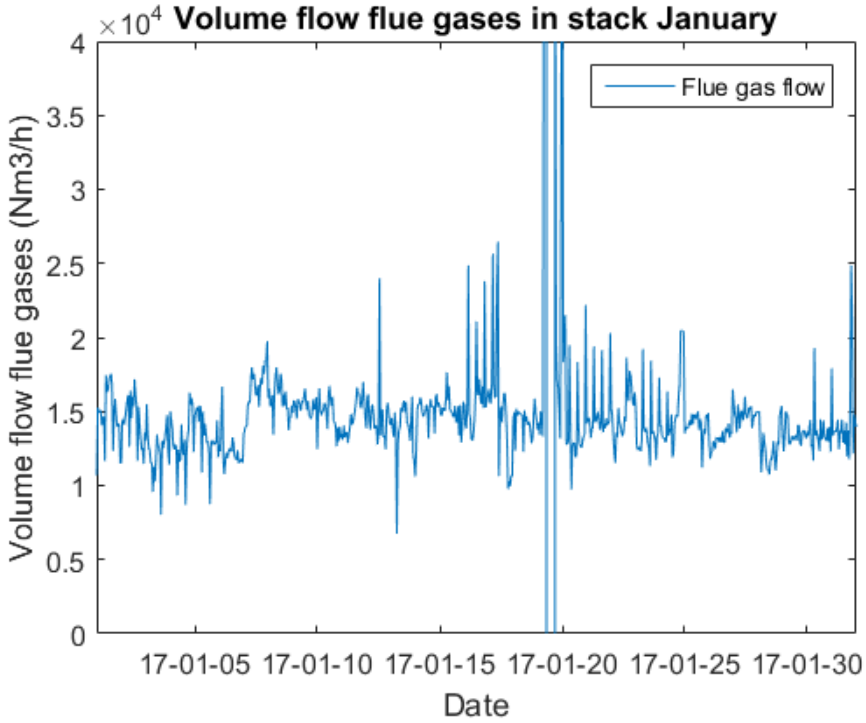


Figure 5.1: Volume flow of flue gases in the stack January 2017.

Documentation from AkzoNobel states that the flue gas flow after the quench is 15 000 Nm^3/h and combining that with the 3 000 Nm^3/h from the evaporators would land the stack flow at 18 000 Nm^3/h wet gas. An external report on the emissions from the WINC states that the measured flow in the stack was 15 700±2400 Nm^3/h and 16 400±2500 Nm^3/h dry gas on two separate days respectively. The resulting flow in Figure 5.1 is then slightly low, but considering the WINC was not operating at the higher load it is designed for but a lower one at the time of the calculations the result is still realistic.

5.1.1.2 Gas fractions

Figure 5.2 compares the calculated oxygen levels after combining evaporator flue gases with the flue gases from the EBK with the values measured in the stack.

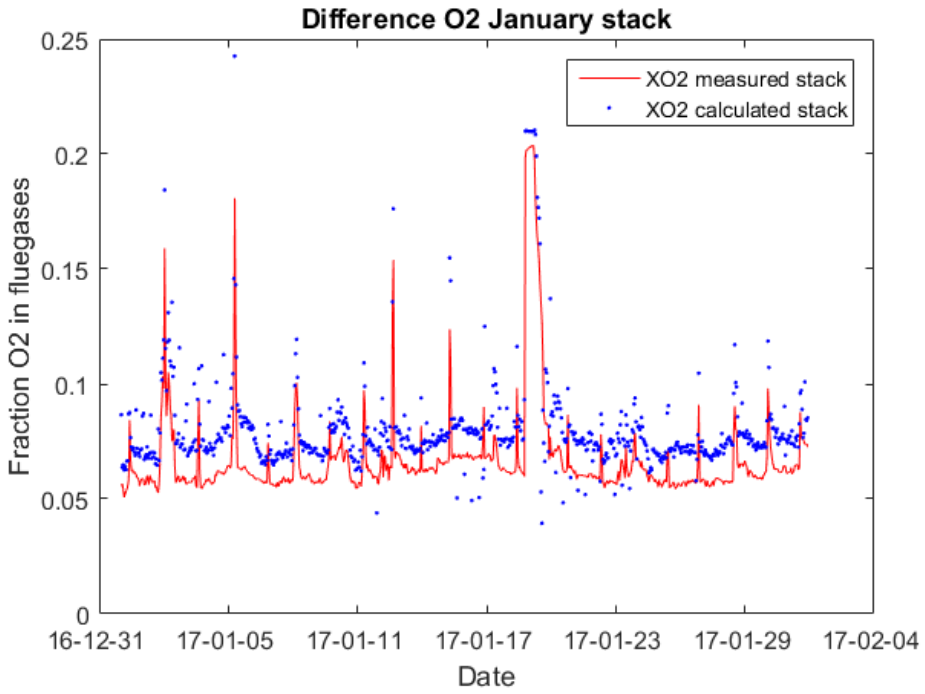


Figure 5.2: O_2 fraction from balance calculations compared to measured O_2 fraction in the stack January 2017.

The calculated values are slightly higher than the measured values, and this is probably due to uncertainties in measurements as well as inlet streams. It is though clear the the calculated values follow the measurement well over the month.
Figure 5.3 displays the same relations but for the water fraction in the stack.

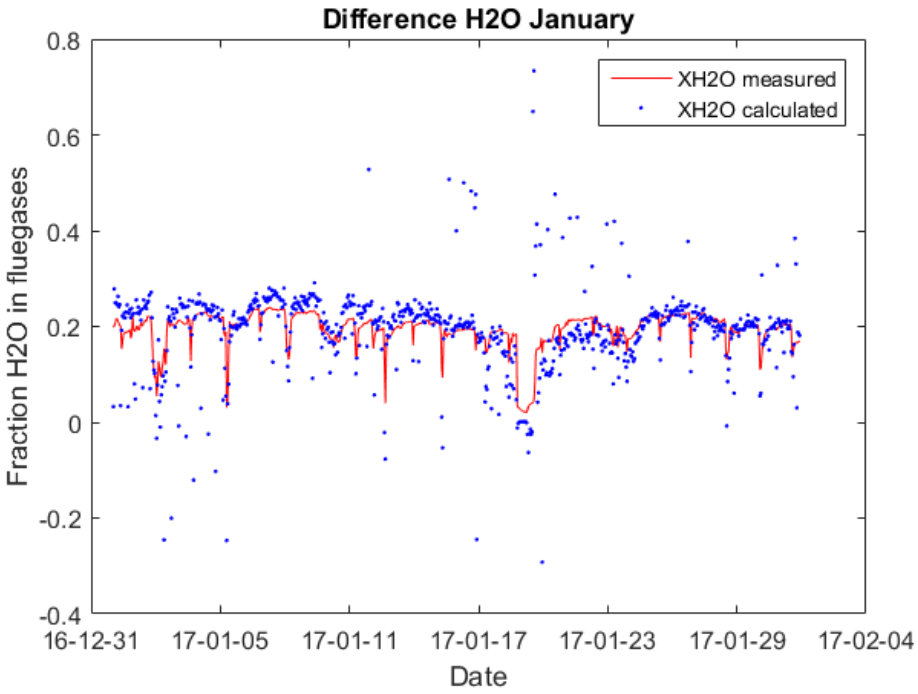


Figure 5.3: Water fraction from balance calculations compared to measured water fraction in the stack January 2017.

For the water fraction the values are slightly higher than the measured values, again as above likely due to uncertainties in the inlet flow measurements. There are also a larger number of outliers or extra large and low values. It is for example impossible to have a negative water fraction in the flue gases. This is probably because of the above described flushing of the electrostatic filter, leading to extreme values from the quench calculations resulting in these extreme peaks and dips. However, the largest part of the calculated values follows the measurements well over the month.

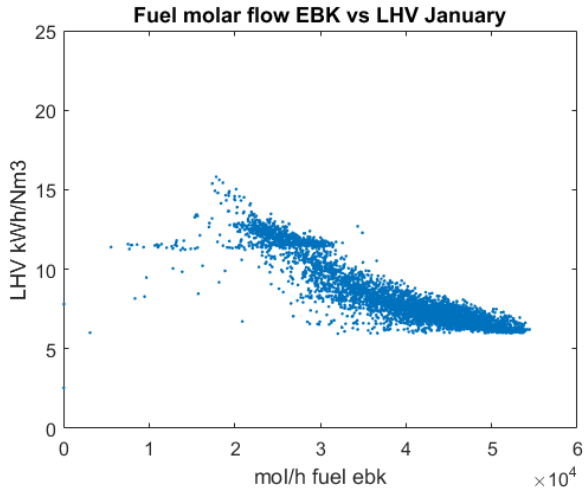
The biggest uncertainty in the process data is the flow and composition of the HP and LP gases. There is only one analysis of the composition which can be assumed varies at least weekly, and the flows used for the calculations are mean values from the last 10 days of February, since this is the only available time with functioning instruments for these variables. But the maximum error is around 5% and generally around 1-2% from the measured value.

5.2 Correlations

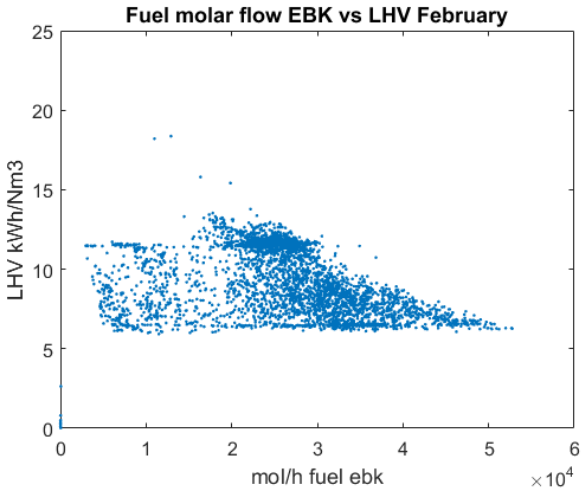
Interesting parameters where plotted in MATLAB and trends were investigated. Considering the radical chemistry theory described in section 2.3.3 the most interesting parameters to investigate are NO, NH_3, oxygen fraction, temperature and water content. It is also interesting to see how the calculations correlate with real time data for fuel gas flow based on the heating value regulation. The plots are made using the full data set of one mean value for every hour during January and

February 2017. Some outliers have been removed in these plots, specifically for the days of 19 - 20th of January when the EBK was shut down. Negative values for concentrations measured in the stack have been set to zero. It is also of importance to know that evaporator 2 was shut down from the 20th of January and all of February, which means that the operation of the process is not optimal in relation to it's design parameters during this time. The whole WINC process was shut down for maintenance during week 14 in April, generating start up and shut down periods. The shut down was initiated in the end och March meaning this month was also not run continuously.

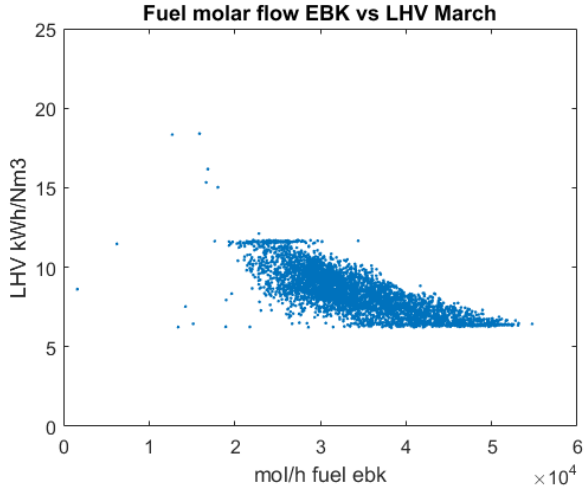
In Figure 5.4 a trend can be seen, most clear for January, that indicates a higher molar flow of fuel gas when the heating value is low. This is to be expected since it is desired for the temperature and performance of the furnace to be constant. January and March have very clear trends while February and April are more diffuse for the lower fuel flows, which is explained by the amount of start up and shut down time during these months.



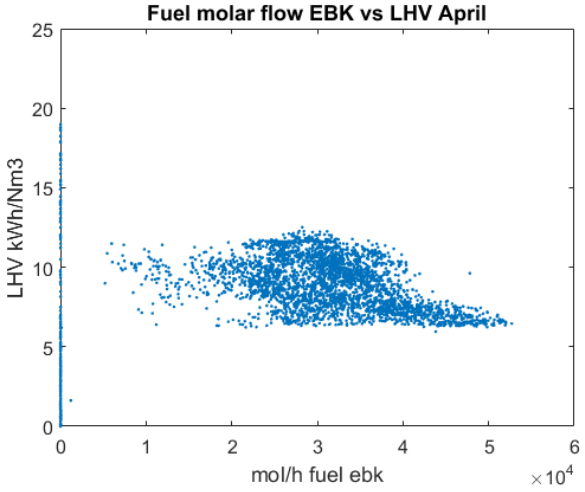
(a) January 2017.



(b) February 2017.



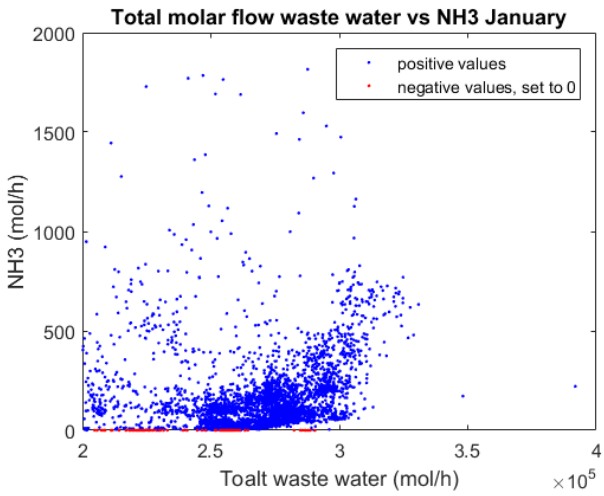
(c) March 2017.



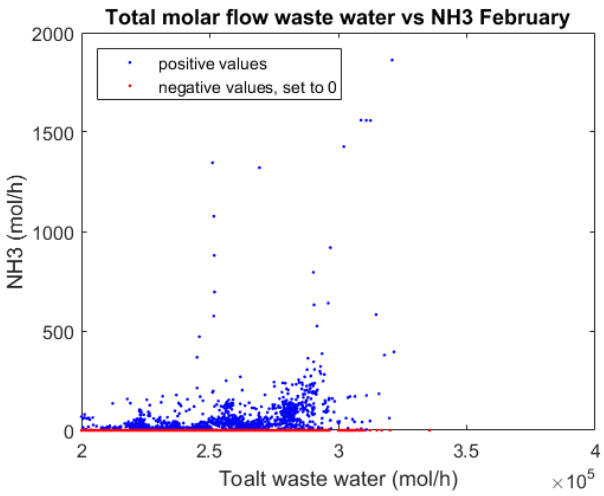
(d) April 2017.

Figure 5.4: Lower heating value plotted against the molar flow of fuel for the EBK in January to April 2017.

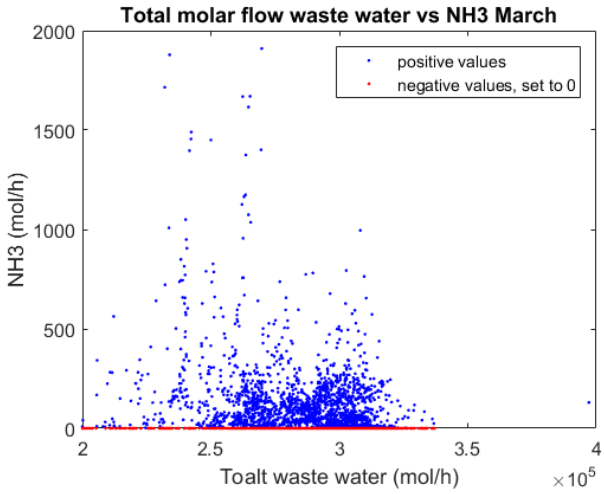
Figure 5.5 displays the relation between the molar flow of NH_3 in the stack based on flue gas calculations in section 5.1.1 and the total molar flow of waste water to the EBK.



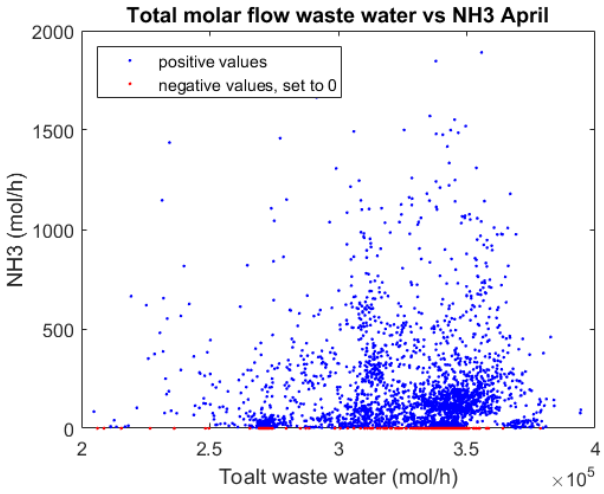
(a) January 2017.



(b) February 2017.



(c) March 2017.

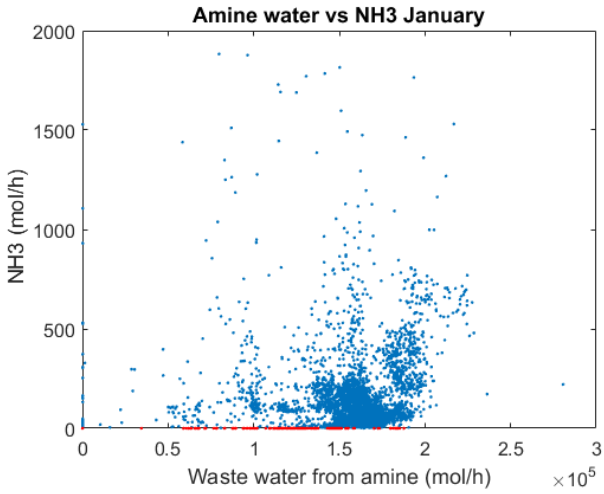


(d) April 2017.

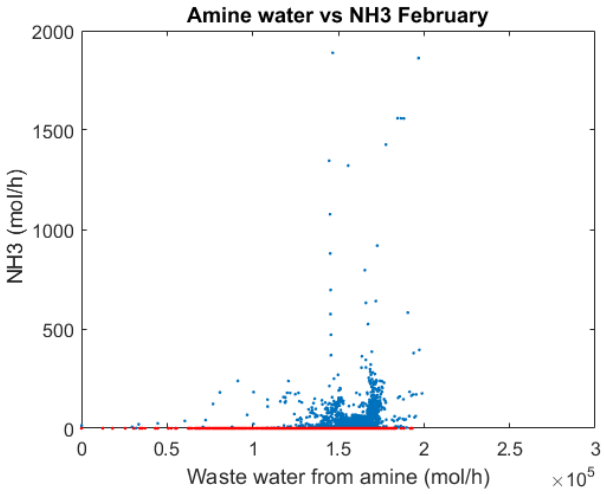
Figure 5.5: Molar flow of NH_3 plotted against total molar flow of waste water in January to April 2017.

There is a clear difference between the months but a weak trend towards an increase in NH_3 in the stack when the amount of waste water increases can be seen, especially for January. The trend even weaker in March, which could be explained by the shut down of the EBK.

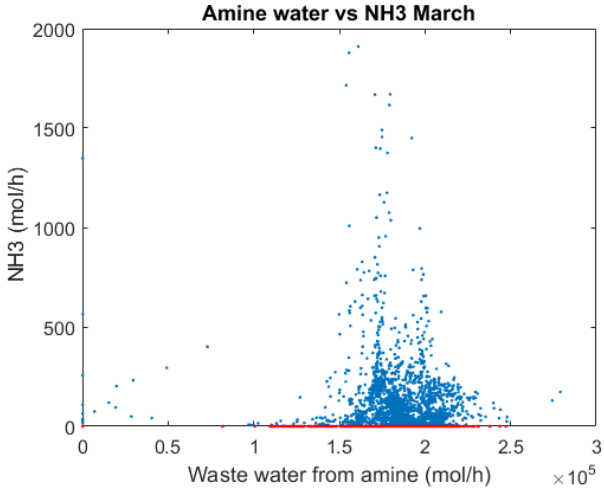
In Figure 5.6 the amount of NH_3 is plotted against the molar flow of water from the evaporators, containing NH_3.



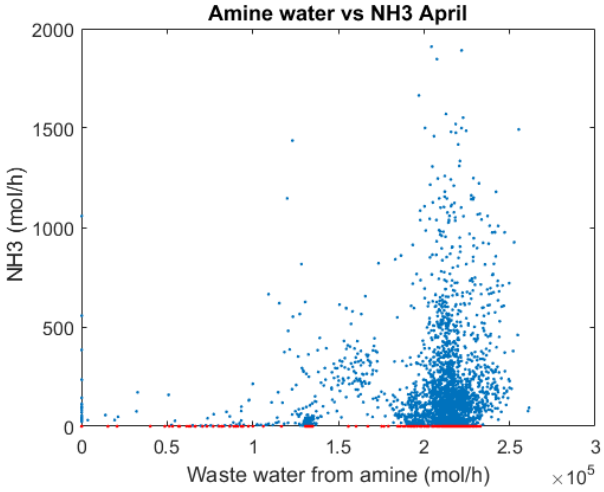
(a) January 2017.



(b) February 2017.



(c) March 2017.

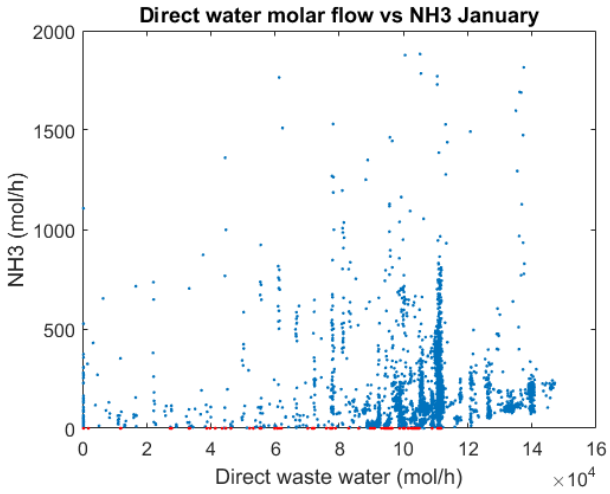


(d) April 2017.

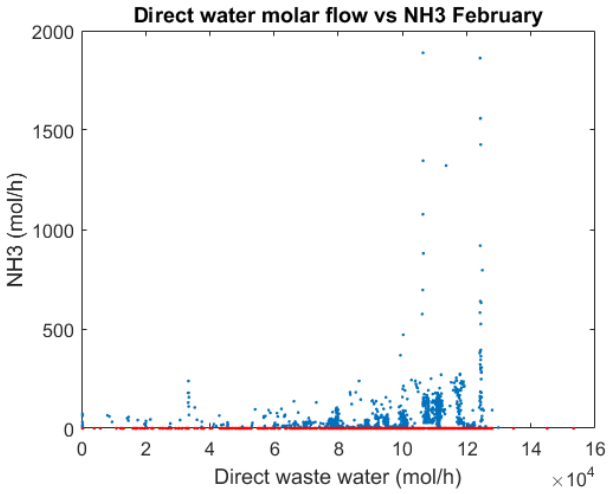
Figure 5.6: Molar flow of NH_3 plotted against molar flow of amine waste water in January to April 2017.

By looking at Figure 5.6, a very slight trend can be observed between amine water and the amount of NH_3 emitted. It is however not as clear as could be excpected. This is an important observation as the amine water contributes is the main source of NH_3 (although significant amounts are also coming from the HP vent gas).

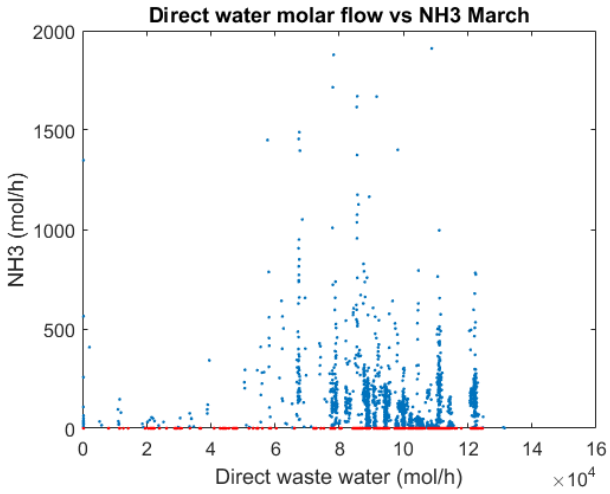
In Figure 5.7 direct water molar flow is plotted against ammonia molar flow in stack.



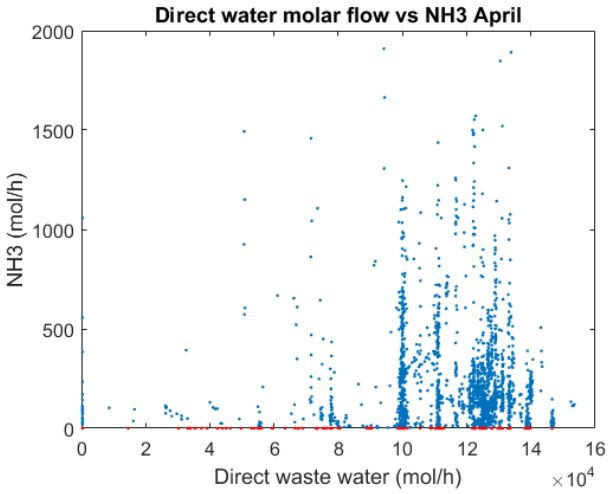
(a) January 2017.



(b) February 2017.



(c) March 2017.



(d) April 2017.

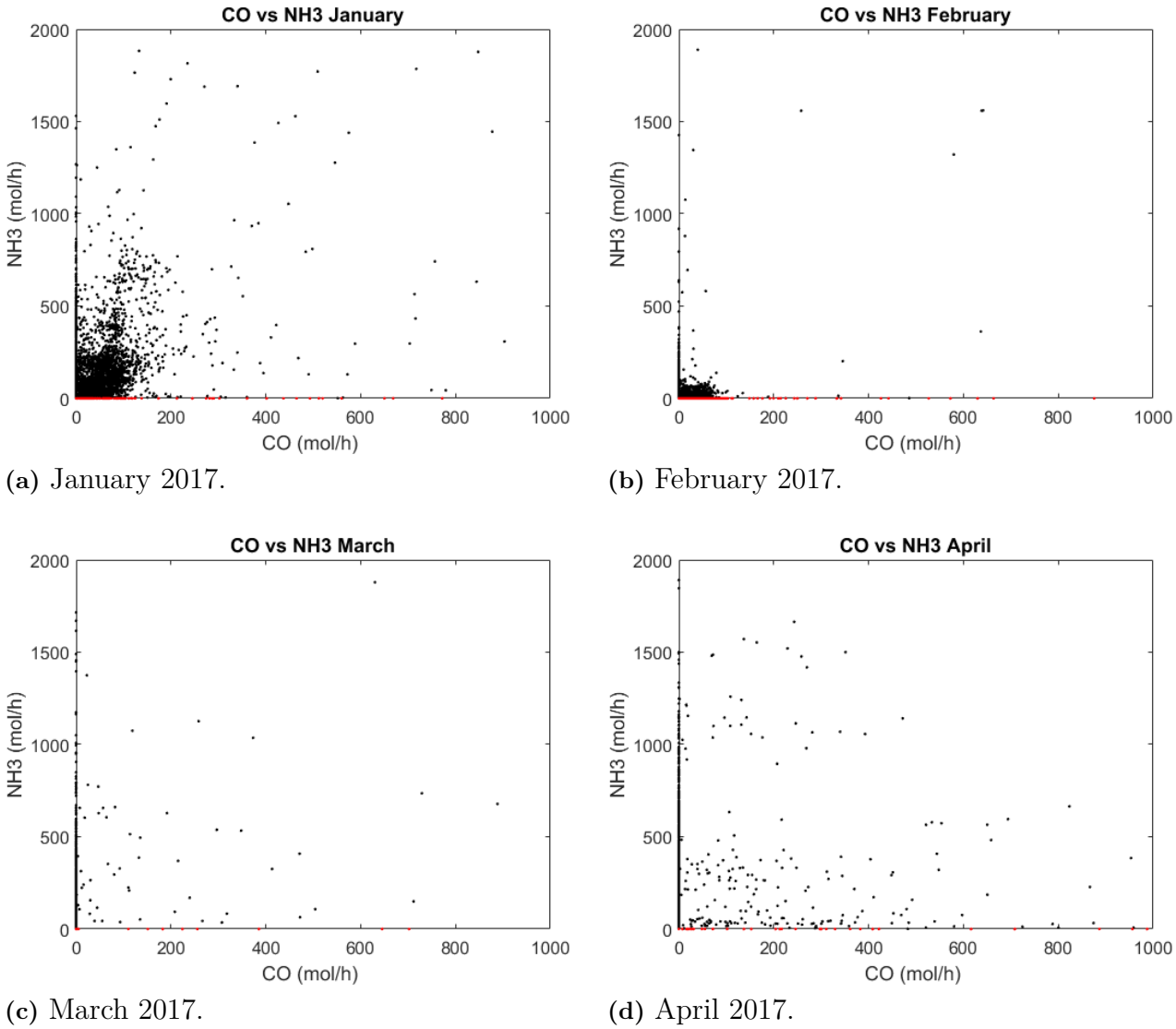
Figure 5.7: Molar flow of NH_3 plotted against molar flow of direct waste water in January to April 2017.

In Figure 5.7 there is always some ammonia in the stack at high flows in January, flows over 120 kmol/h generates ammonia. The same correlation can be seen for January and February but February has less ammonia and more negative values, probably due to down time. March and April has an even weaker correlation, especially March.

Typical "stripes" in the values are because the flow of direct water is more easily regulated on flow meaning it is more constant over time than the water from the evaporators. The results indicate that the direct water is more important for the amount of ammonia that is emitted. One explanation for this is that the amine water is already in large parts evaporated, meaning it does not affect the temperature in the furnace as much as the direct water, affecting the combustion. This is inter-

esting since the amine water contains most of the ammonia that enters the furnace and would therefore be expected to have a large effect on the ammonia emissions.

In Figure 5.8 the molar flow of NH_3 is plotted against the molar flow of CO. One trend that could be expected is that the flow of NH_3 increases with an increasing flow of CO, which would be explained by incomplete combustion. There is a vague such trend for January. However, a very large part of the data points for in NH_3 February are at 0 due to the script settings that sets negative values to zero (red dots), which could be and explanation to the difficulties in finding a trend during that month. March and April has a lot less CO over the month making it even harder to say anything certain about this trend.



(a) January 2017.

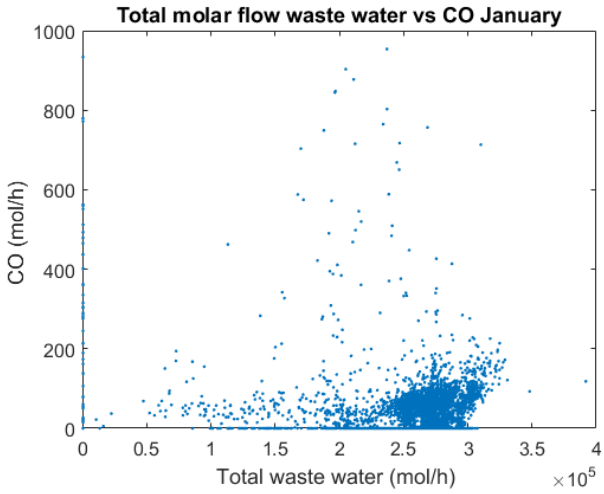
(b) February 2017.

(c) March 2017.

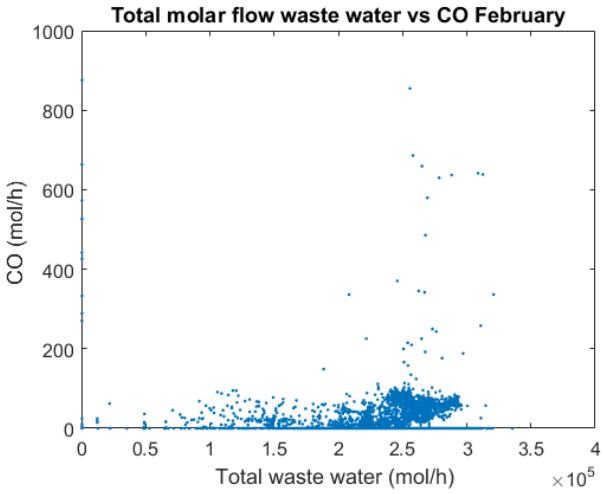
(d) April 2017.

Figure 5.8: Molar flow of NH_3 plotted against molar flow of CO in January to April 2017.

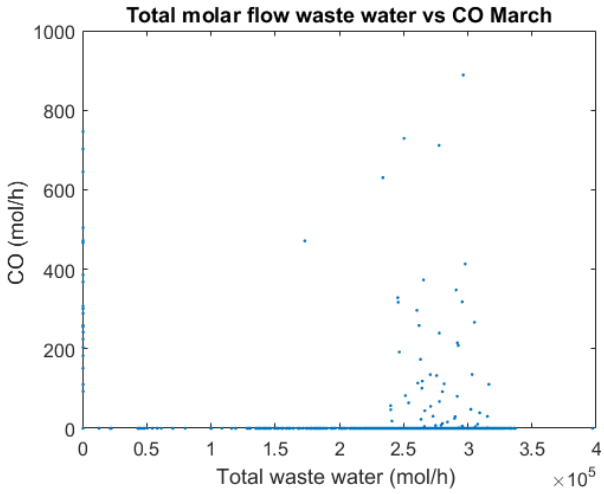
In Figure 5.9 CO is plotted against total molar flow of waste water.



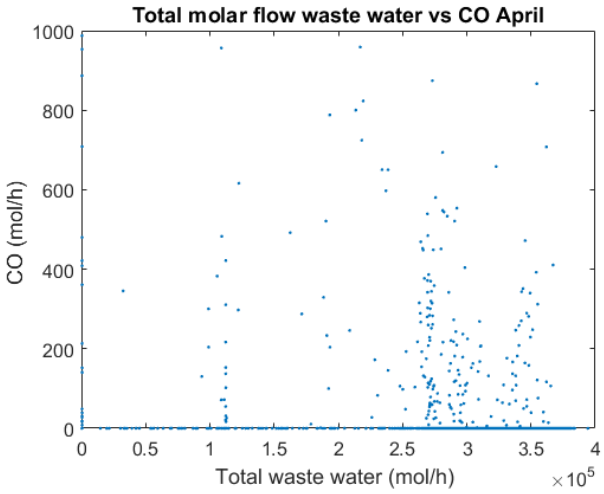
(a) January 2017.



(b) February 2017.



(c) March 2017.

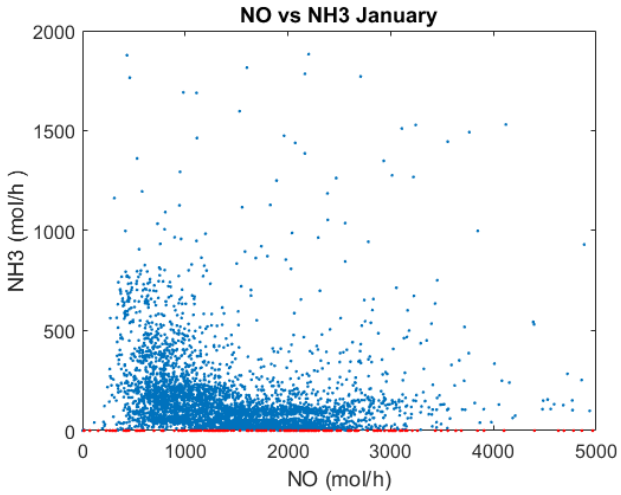


(d) April 2017.

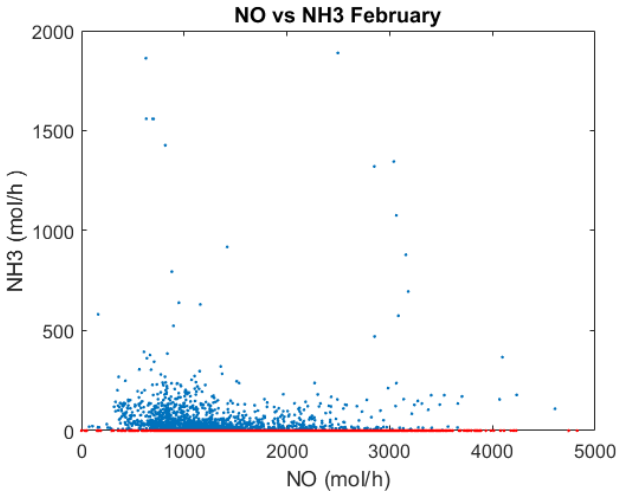
Figure 5.9: Molar flow of CO plotted against total molar flow of waste water in January to April 2017.

At higher flows of waste water there could be an indication of higher flows of CO, but as for NH_3 there are a lot of zero points for CO in February and also a lower molar flow of water. For March and April there is even less CO but there is still a weak trend towards increasing amount of CO with increasing amount of water.

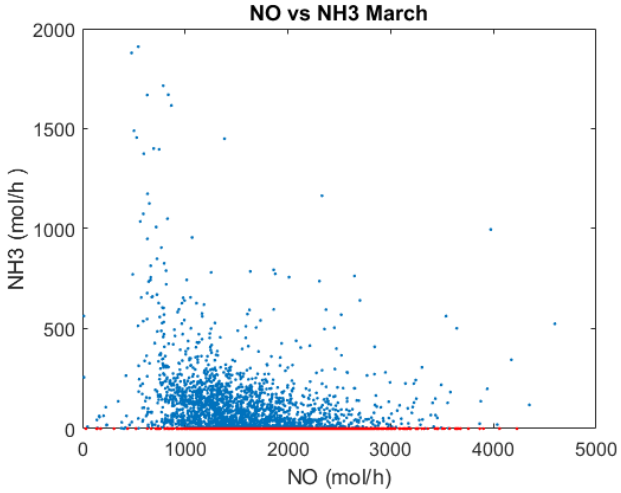
Figure 5.10 displays the molar flow of NH_3 against the molar flow of NO. There is an indication that there is not often a lot of both ammonia and NO, it is one or the other. Here as well it is illustrated that a lot of data points in February is zero for NH_3. The trend is visible for all four months and in accordance with the NO reduction with ammonia theory described in section 2.3.



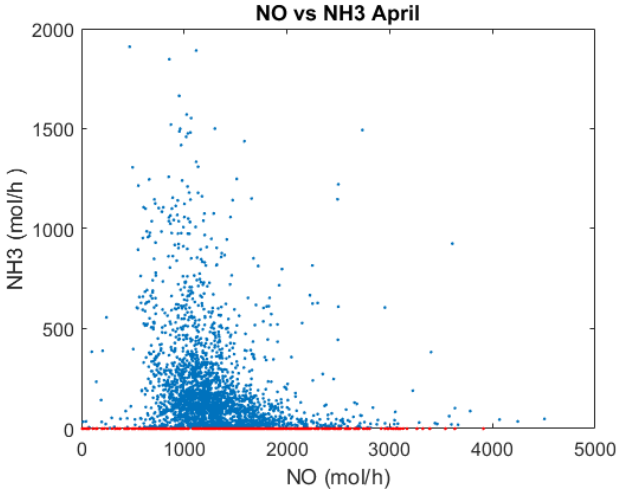
(a) January 2017.



(b) February 2017.



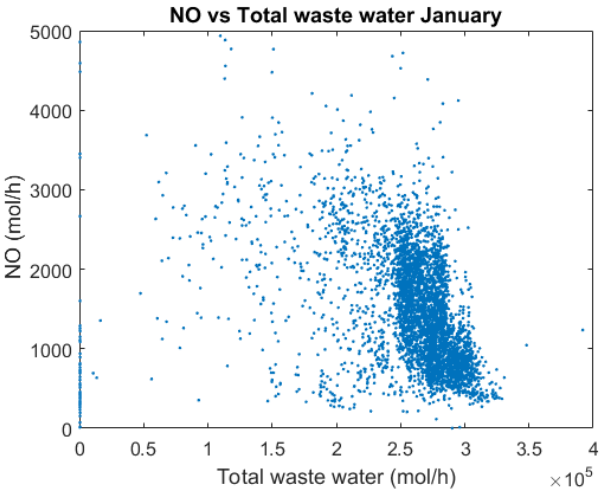
(c) March 2017.



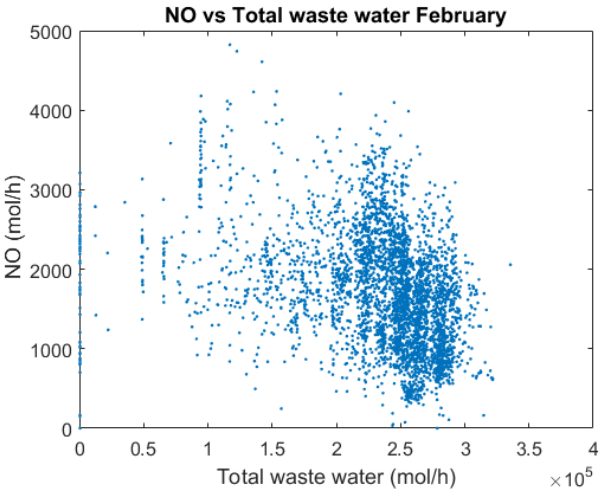
(d) April 2017.

Figure 5.10: Molar flow of NH_3 plotted against molar flow of NO in January to April 2017.

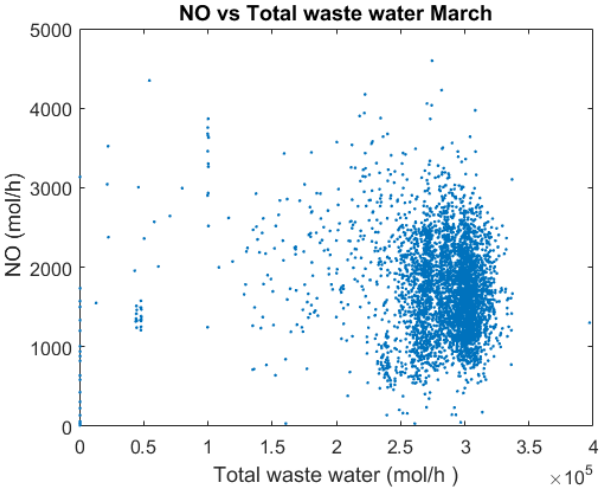
Figure 5.11 displays the molar flow of NO plotted against total molar flow of waste water. There is an indication of a lower molar flow of NO when the total flow of waste water increases. This can be explained by the fact that there are significant amounts of unconverted ammonia at these high water flows, although the numbers don't add up exactly. Lower temperatures and an increase in OH radicals due to the higher water flows may also affect the NO formation chemistry.



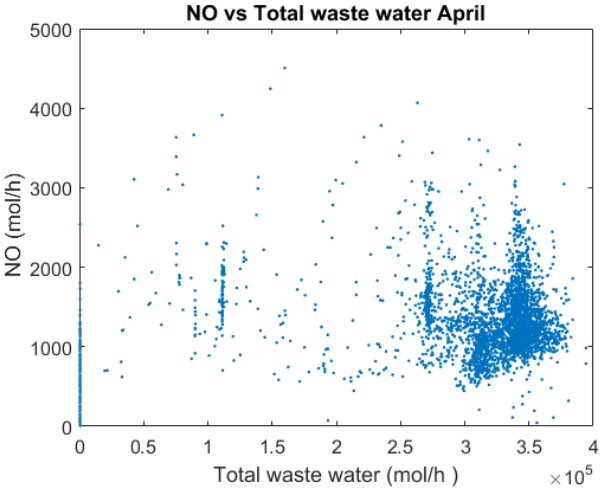
(a) January 2017.



(b) February 2017.



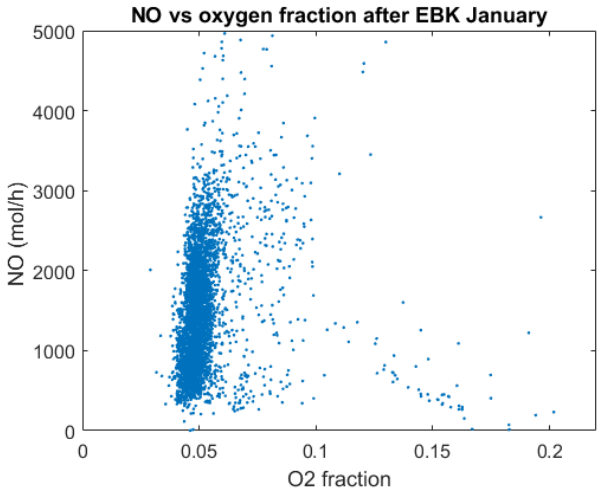
(c) March 2017.



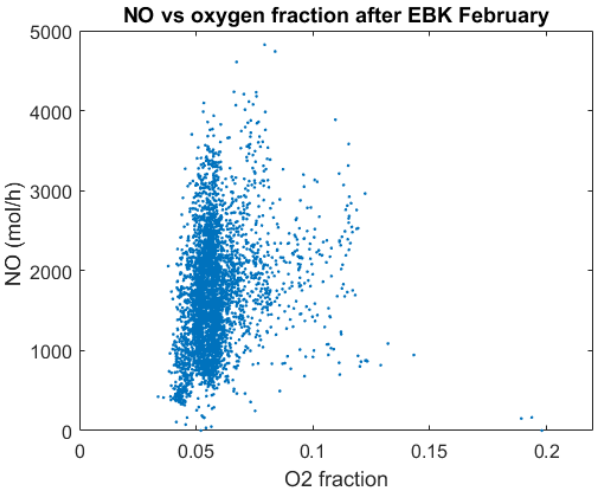
(d) April 2017.

Figure 5.11: Molar flow of NO plotted against total molar flow of waste water in January to April 2017.

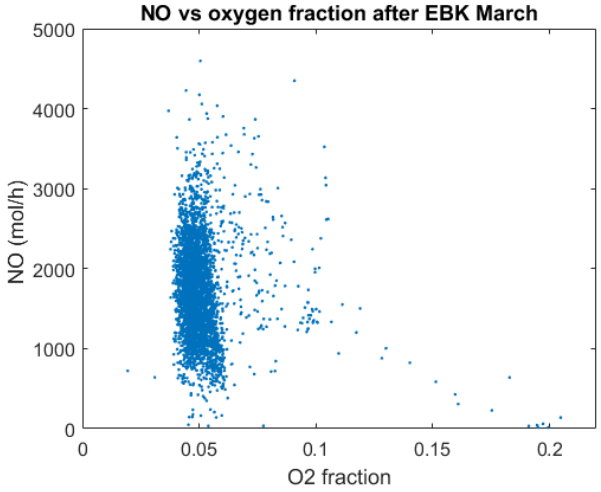
Figure 5.12 shows a trend in the relation between NO and the level of oxygen after the EBK for the moths of January, February and April. The lower the level of oxygen the lower the molar flow of NO. This is consistent with NO_x reduction chemistry. March does show an almost reversed relation which is strange but could have to do with the shut down of the WINC.



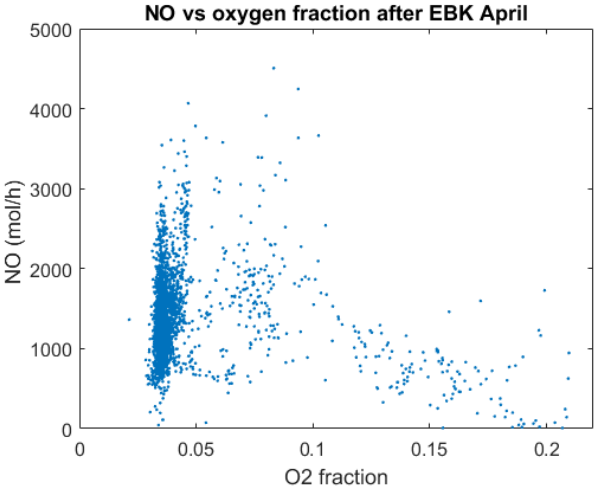
(a) January 2017.



(b) February 2017.



(c) March 2017.



(d) April 2017.

Figure 5.12: Molar flow of NO plotted against the oxygen level after the EBK in January to April 2017.

5.3 Chemkin results

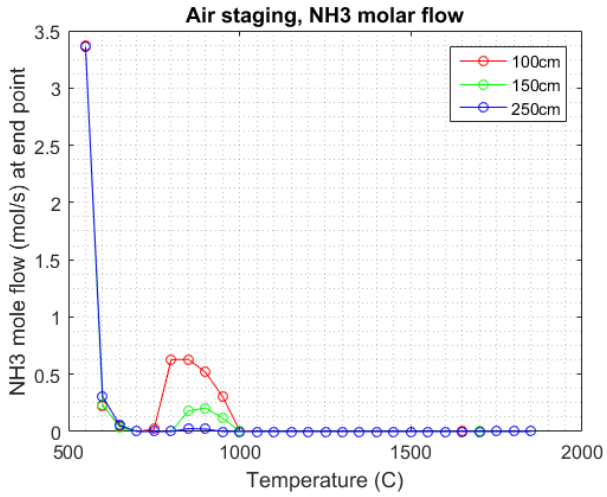
The following section will present the results of the parameter study. The results are presented based on the parameter that is investigated. The plots are over temperature and every value in the plots represent the end point value of the component that is investigated at that specific temperature.

5.3.1 NH_3

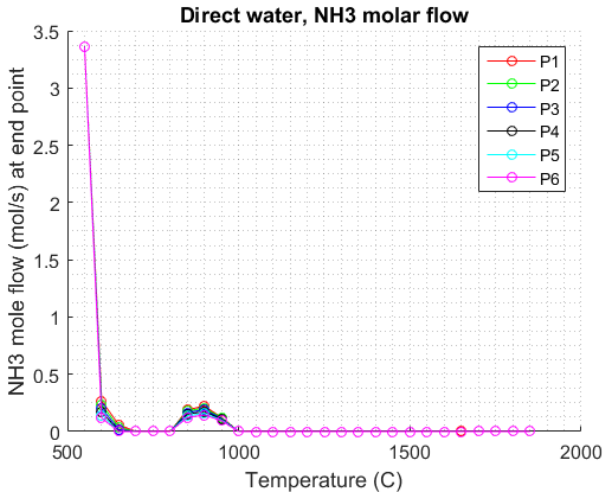
The effect of the model test run parameters are displayed in Figure 5.13.

In Figure 5.13 (a) to (d) it is clear that the temperature has the over all great-

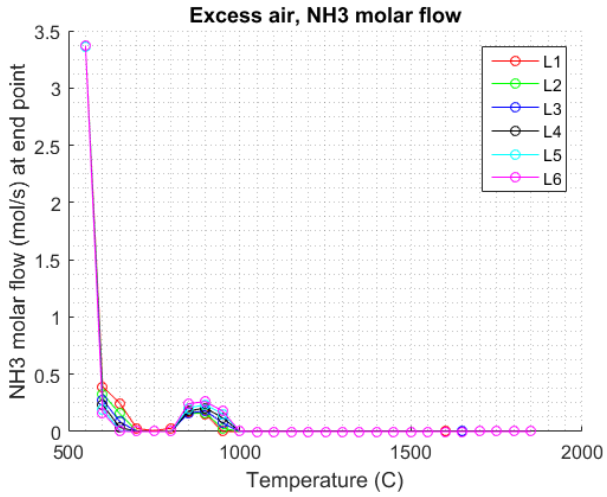
est effect on the molar flow at the end point. Over 1000°C there is no ammonia at the end point and before 500°C there is no significant combustion taking place. Between 600-700°C the ammonia is not completely consumed, probably since the reaction producing the necessary $^{\bullet}OH$ and $O^{\bullet}$ radicals (Equation (2.15)) is not fast enough at these temperatures.



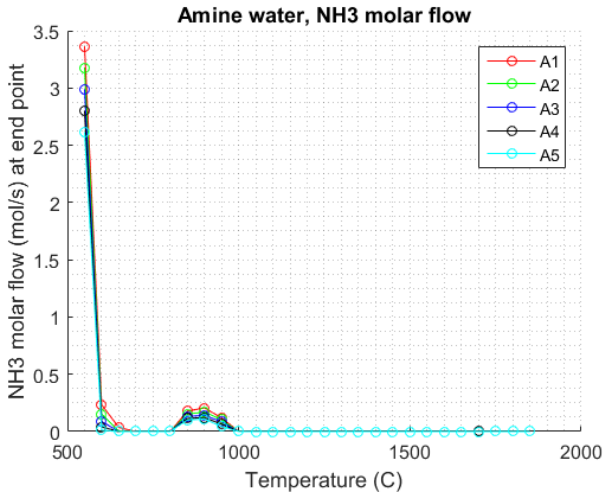
(a) NH_3 at end point, air staging.



(b) NH_3 at end point, direct water.



(c) NH_3 at end point, excess air.



(d) NH_3 at end point, amine water.

Figure 5.13: NH3 molar flow at end point over the given temperature interval for all four test parameters.

In the temperature range 700-800°C all ammonia is consumed since there are more radicals available. Over 800°C the NO reduction with ammonia works well and a lot of the ammonia is consumed by this. However since there are a lot of other compounds involved in this combustion process, e.g. hydrogen, methane and ethane that also react with ammonia and NH_2, these competing reactions lead to an excess ammonia at the end point.

Over 1000°C the formation of radicals is very fast, especially the formation of $^{\bullet}OH$ and $O^{\bullet}$ that are the precursors for the NH_3 to NH_2 reactions (Equation (2.9)-(2.10)). This means all ammonia is consumed and the formed NH_2 does not react with NO directly, leading to a lowered NO reduction ability. The residence time for the reactions is also shorter at higher temperatures.

In Figure 5.13 (a) the length of the staging clearly makes a difference in the amount of ammonia at the end point, especially in the range between 750°C to 1000°C. The staging affects the mixing velocity, and the shorter the staging the more ammonia, meaning it could be beneficial to mix the air in slower to achieve a lower ammonia slip. The probable explanation for this is that the radicals that are important for the reduction of NO with NH_3 are available over a longer time period when the mixing is slower.

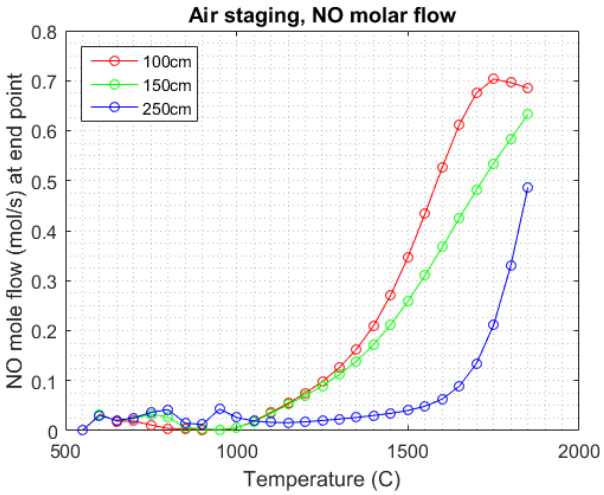
In Figure 5.13 (b) the same behavior is observed with respect to temperature but the amount of waste water from the surfactant side seem to have a lower effect than the air staging. The water also contributes with $^{\bullet}OH$ that could speed up the formation of NH_2, but also the formation of ammonia in the competing reactions which could explain why there is more ammonia at the higher water flows.

Figure 5.13 (c) shows that low oxygen levels at low temperatures gives a higher ammonia slip, but in the range 800-1000° the reverse is true. In the low temperature region the formation of $^{\bullet}OH$ and $O^{\bullet}$ radicals (Equation (2.15)) is slow but higher air flows then contribute with more O_2 that can react instead, explaining why the higher air flows gives a lower ammonia slip in the low temperature area. The higher temperatures increases the reduction of NO with ammonia, leading to lower amounts of ammonia in this range when it is instead converted to NH_2 and then reacted with NO, which also works better when there is less oxygen. The excess air has a slightly larger influence than the direct water flow on the amount of ammonia at the end point.

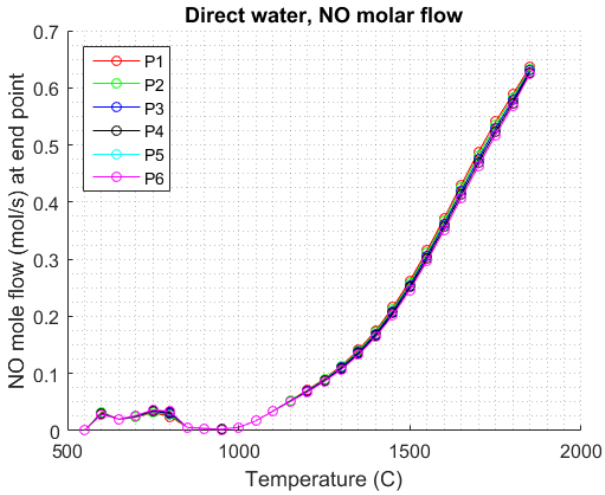
In Figure 5.13 (d) similar results as the direct water flow can be observed, slightly higher ammonia slip in the range 800-1000°C for larger water flows. This water contains ammonia which is visible at the staring point at 550°C. When there is less ammonia at the starting point there is less remaining ammonia also at lower temperatures. In the range between 800-1000°C it is clear that higher flows of amine water gives more ammonia at the end point.

5.3.2 NO

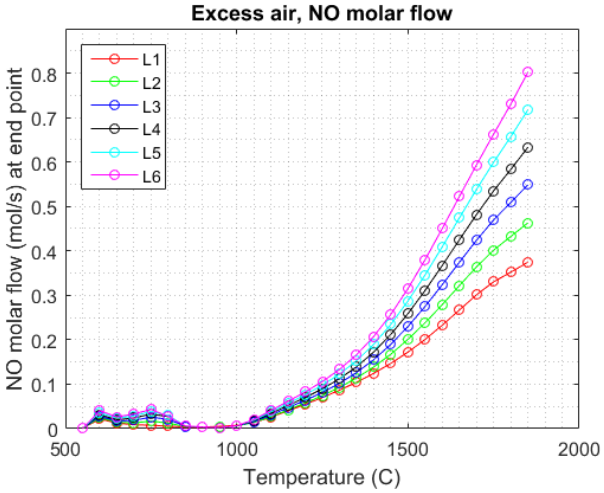
The effects of the different parameters were evaluated in the same way for NO, the results are presented in Figure 5.14.



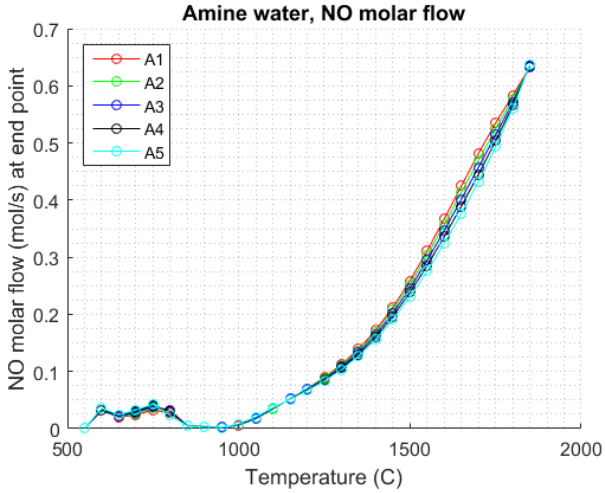
(a) NO at end point, air staging.



(b) NO at end point, direct water.



(c) NO at end point, excess air.



(d) NO at end point, amine water.

Figure 5.14: NO molar flow at end point over the given temperature interval for all four test parameters.

All sub-figures in Figure 5.14 shows the same general behavior where NO is formed at low temperatures and then completely consumed in the temperature range 850-1000°C. After 1000°C the amount of NO increases significantly and almost linearly with increasing temperature. As explained in the previous section the reduction of NO works best in the temperature interval 800-1000°C which explains the absence of NO in these regions, while after 1000°C the reduction is almost non-existing while the formation of thermal NO is significant over 1500°C, leading to the high levels of NO observed here.

In Figure 5.14 (a) it is clear that the staging has a large effect on the amount of NO. In the range 500-1000°C the longer mixing step gives more NO but the relationship is reversed over 1000°C. This is probably due to the formation of radicals and their availability over time, it is more beneficial with slower mixing at high temperatures

where there are less radicals available that are inclined to react with NO, but they are available for longer. Under 1000°C the radicals are more inclined to react with NO, but there are more competing reactions at these temperatures leading to a higher level of NO when the mixing is slow here.

Figure 5.14 (b) shows the same behavior as (a) but the water seems to have a lot less effect than staging, and could be deemed insignificant.

In figure 5.14 (c) the temperature once again is a big factor but here the relationship is the same both over and under 1000°C, the less air the less NO. This is most evident at very high temperatures, due to the thermal formation of NO at these temperatures.

Figure 5.14 (d) has similar behaviour to the direct water effect and the air staging but it is also here very little difference between the flow levels. .

5.3.3 N_2O

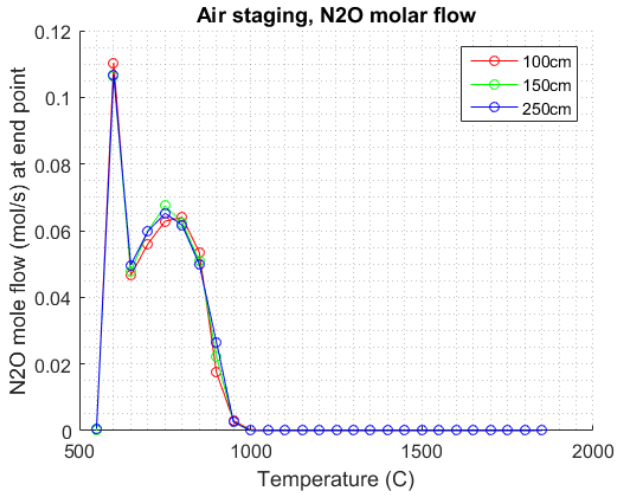
The influence of the parameters where also evaluated for N_2O, results are presented in Figure 5.15. All sub-figures show the same behaviour, there is a large peak of N_2O forming at 600°C which then goes down. From 650-1000°C there is an increase in the N_2O formation again before it is completely disappeared after 1000°C. The peak is probably explained by the large amount of ammonia available at that time, which is converted to NH_2 which then reacts with NO_2 forming N_2O at this temperature. This is a very short span though since when the temperature increases there are a lot more competing reactions. The next span where there are a lot of N_2O is when there is little NO, indicating that the reduction of NO may result in N_2O at his range. The scale of the molar flow is however one tenth of the flow of NO which is in turn one tenth of the NH_3 flows scale.

In Figure 5.15 (a) temperature has great influence, there is no N_2O after 1000°C. It does however not seem as if the staging distance affects the flow that much, especially not at the 600°C peak.

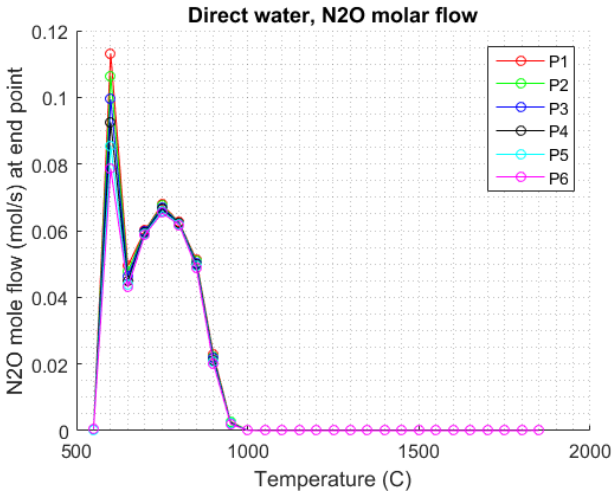
Figure 5.15 (b) shows the same behavior as Figure 5.15 (a) and little effect of direct water amount, except at the 600°C peak where more water gives more N_2O. This could be because of there are more $^{\bullet}OH$ radicals available with more water.

In Figure 5.15 (c) however there is a large influence of the amount of excess air in the temperature range 600-1000°C, the lower amount of excess air the lower the amount of N_2O. This is probably due to that the N_2O formation is very dependent on the availability of O_2, the less oxygen the less N_2O.

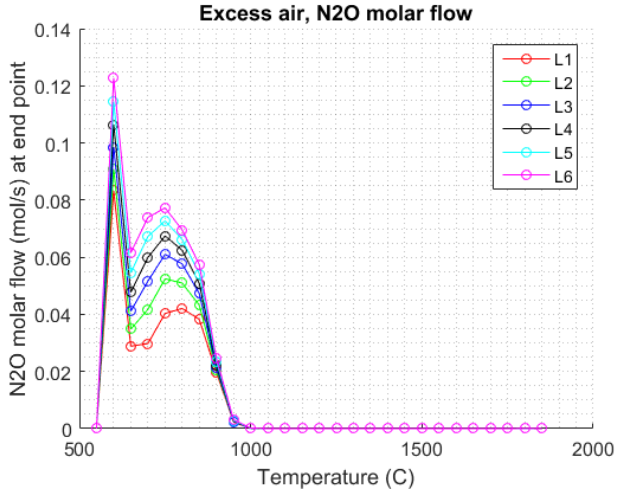
Figure 5.15 (d) shows the same behavior as the direct water graph, but with slightly larger differences in the 700-1000°C range. This could be because the ammonia contributes with more available radicals, meaning the more ammonia the more N_2O.



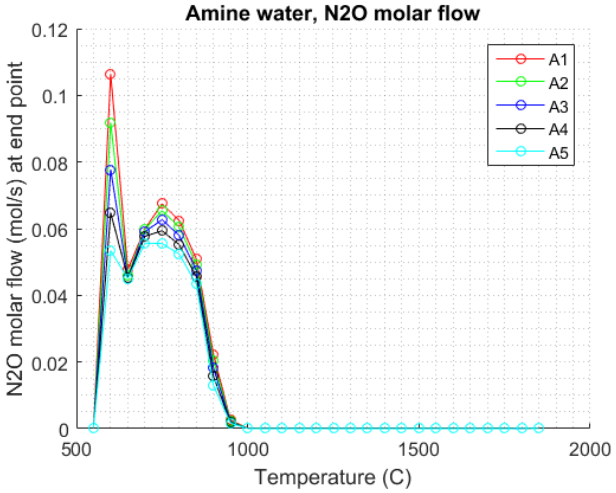
(a) N_2O at end point, air staging.



(b) N_2O at end point, direct water.



(c) N_2O at end point, excess air.



(d) N_2O at end point, amine water.

Figure 5.15: N_2O molar flow at end point over the given temperature interval for all four test parameters.

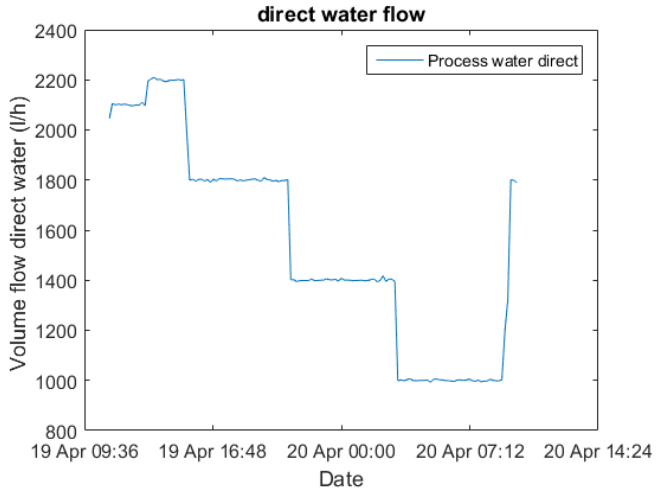
Over all conclusion from the sensitivity study is that temperature, mixing velocity and amount of excess air seem to have the largest influence on the slip of the nitrogen compounds, except for N_2O where the staging does not seem to matter as much.

5.4 Experimental

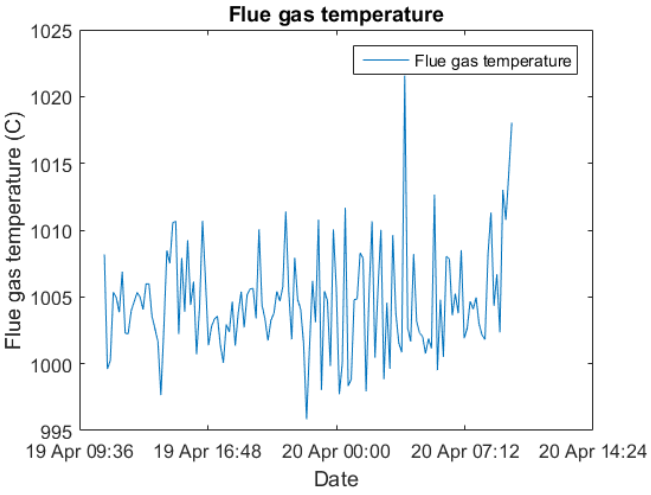
Experiments where run through the time period of April 19th to April 25th. The methods are described in section 4.2. The results are presented in the following section.

5.4.1 Direct water (P)

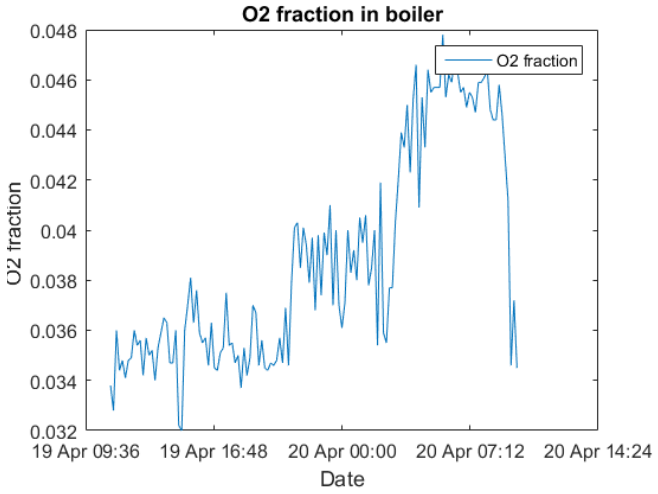
The test period for direct waste water from surfactants south side of the plant was run starting at 11:00 on the 19th of April until 9:00 on the 20th of April. The resulting values for the four test parameters over this testing period are presented in Figure 5.16.



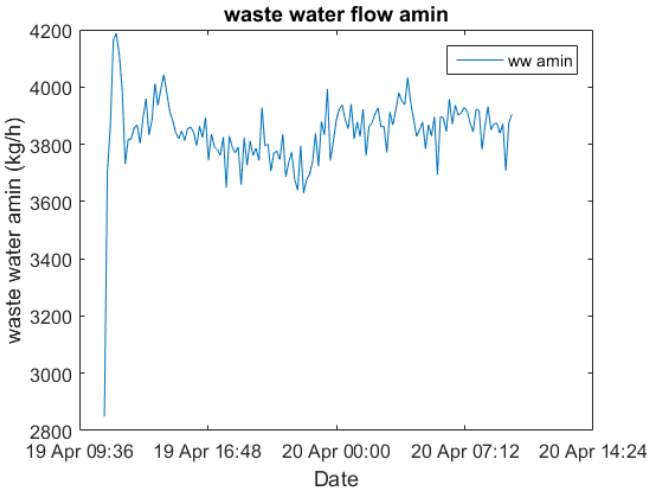
(a) Direct water flow during test period.



(b) Flue gas temperature during test period.



(c) O_2 fraction during test period.



(d) Amine waste water flow during test period.

Figure 5.16: All test parameters during the direct water testing period.

In Figure 5.16 (a) it is easy to verify the four levels of water flow that were run over

this period. The temperature set for this run was 1005°C, but as Figure 5.16 (b) shows it fluctuates quite a lot around this value. The oxygen level set value was 3.5%, but as Figure 5.16 (c) shows the level is not constant. When the amount of direct waste water is lowered the oxygen level rises. This is probably due to the regulatory system of the EBK burner. When the water flow drops the temperature rises, leading to a lowered need for fuel to keep the set temperature, illustrated by a lowered heat input in the furnace, see Figure 5.17. This lowered heat from the fuel regulates the vents controlling the air flow to the EBK, probably reaching the minimum power of the air fan, leading to an increasing oxygen level since the fan can not lower the flow below this limit.

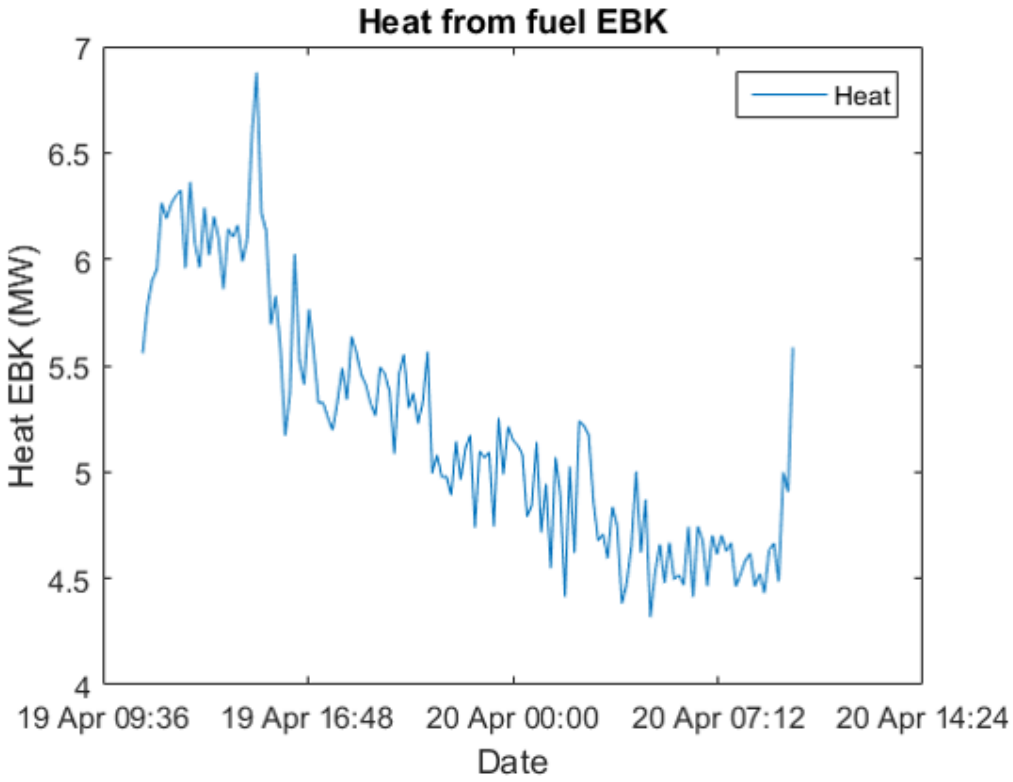
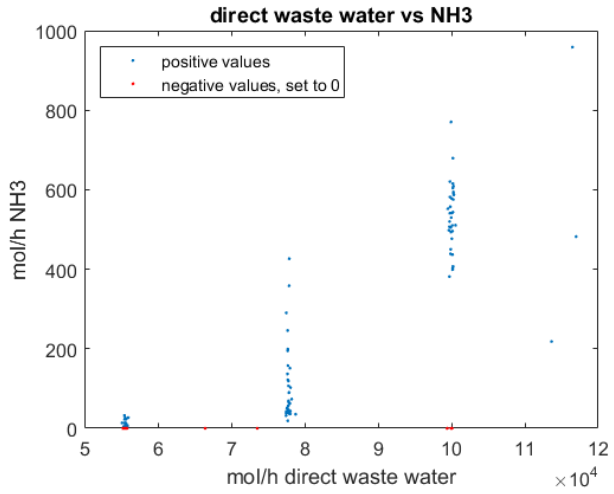


Figure 5.17: Total heat from fuel in the EBK during direct water test run.

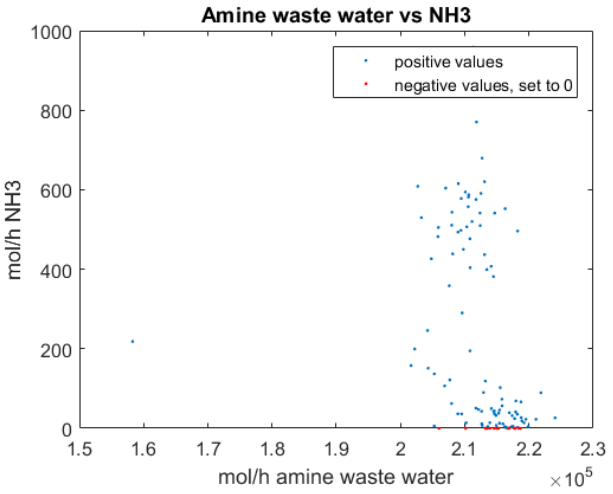
Further lowering of the effect would cause more excess of oxygen after the combustion since it is not possible to match the fuel flow. Temperature is still able to remain close to the set value but the last test value was not run since the oxygen level was not constant. This regulation means that the effects of this test run when looking at components after the combustion can not be conclusively attributed to the lowering of the direct water flow, the increased oxygen level is also a factor. The amine water flow is as can be seen in Figure 5.16 (d) fairly stable at 3800-3900 kg/h.

5.4.1.1 Ammonia slip and NO reduction, (P)

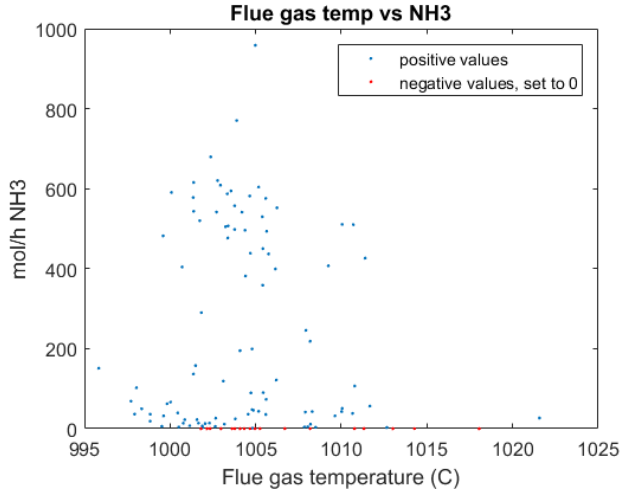
This section investigates the influence of the direct water on the ammonia slip, see Figure 5.18.



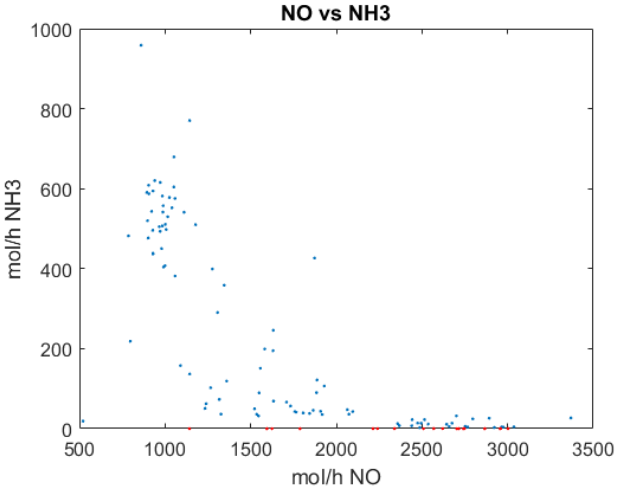
(a) Direct water flow against NH_3.



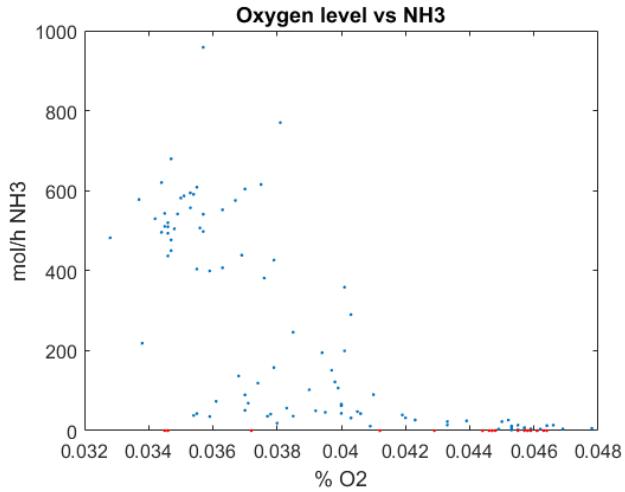
(b) Amine water flow against NH_3.



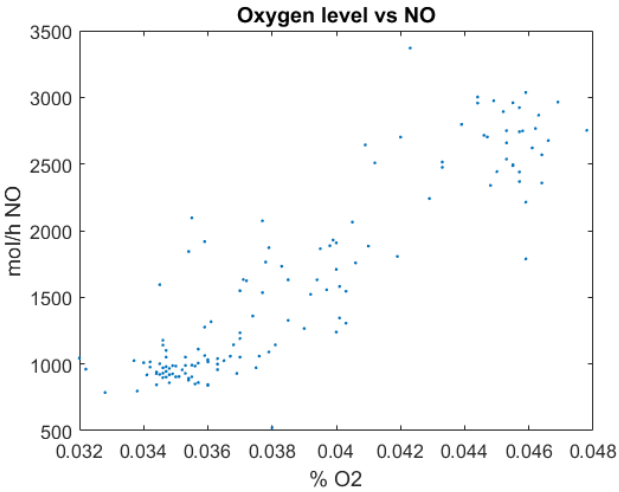
(c) Flue gas temperature against NH_3.



(d) NO against NH_3.



(e) O_2 fraction against NH_3.



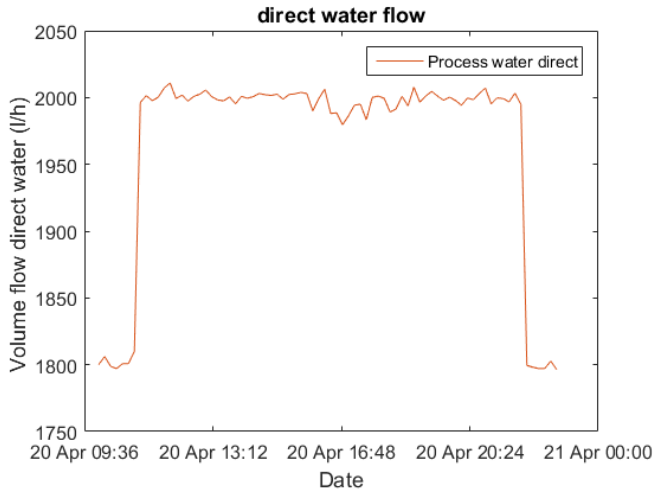
(f) O_2 fraction against NO.

Figure 5.18: The test parameters plotted against NO and NH_3 to investigate their influence on the ammonia slip and NO reduction during the direct water test run.

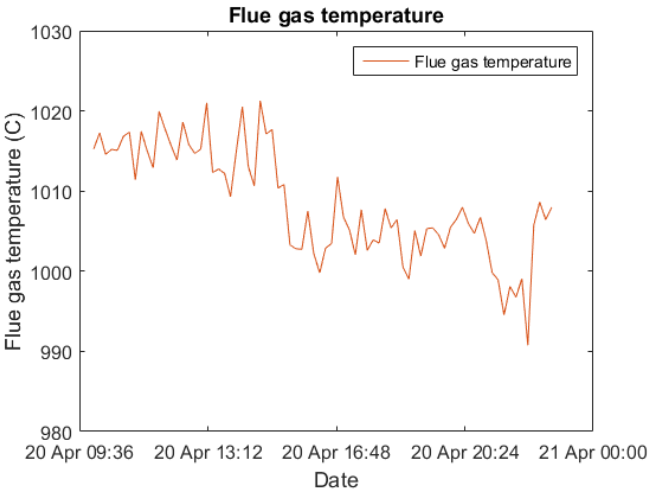
Figure 5.18 (a) and (b) shows that there is a clear trend in increasing ammonia slip when the direct water low is lowered, which could also be observed in Figure 5.7. This can be related both to the assumed lowered temperature and the lowered amount of radicals initiating the NO reduction with NH_2 described in Equation (2.9) and (2.10). Figure 5.18 (d) to (f) then shows the relation between the oxygen level and the nitrogen compounds, Figure 5.18 (d) specifically showing the very clear connection between NO and ammonia. Figure 5.18 (c) does not show any clear trends regarding temperature.

5.4.2 Temperature (T)

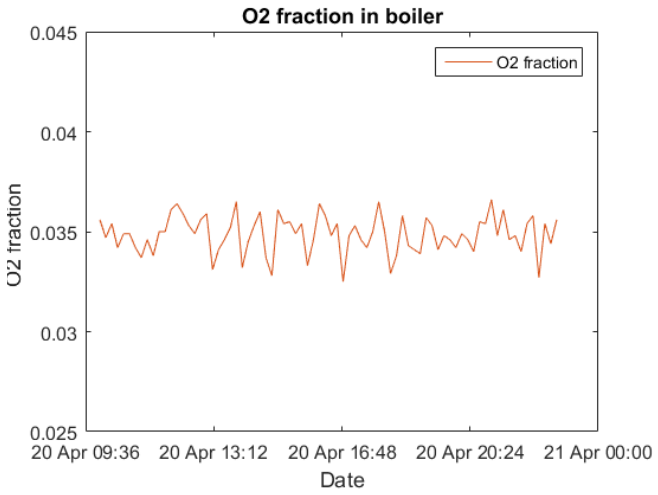
The temperature testing period was run between 10:00 and 22:30 on the 20th of April. Because of increasing ammonia slip the lowest temperature level was not run. See Figure 5.19 for the resulting parameter values during this test.



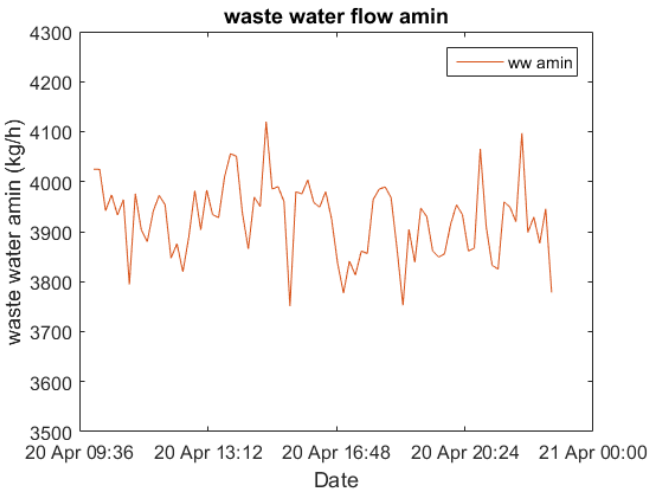
(a) Direct water flow during test period.



(b) Flue gas temperature during test period.



(c) O_2 fraction during test period.



(d) Amine waste water flow during test period.

Figure 5.19: All test parameters during the temperature testing period.

In Figure 5.19 (a)-(d) it is clear that all parameters except temperature are kept constant during the test period. Direct water flow (Figure 5.19 (a)) is at 2000 l/h instead of the decided 1800 l/h since the operators found that the process was stable at this higher value. Preferably this value would have been kept at the previous level for comparison. The temperature was varied from 1015°C down to 995°C, but as can be seen in Figure 5.19 (b) it still fluctuates a lot around these values, making it more difficult to decipher the effects of the temperature change. The last run at 995°C was also discontinued after around one hour since the ammonia slip was deemed too high after that.

Figure 5.20 shows the effect in the EBK during the test run. It follows the raise and drop in temperature well which is to be expected since a lower temperature lowers the fuel gas flow.

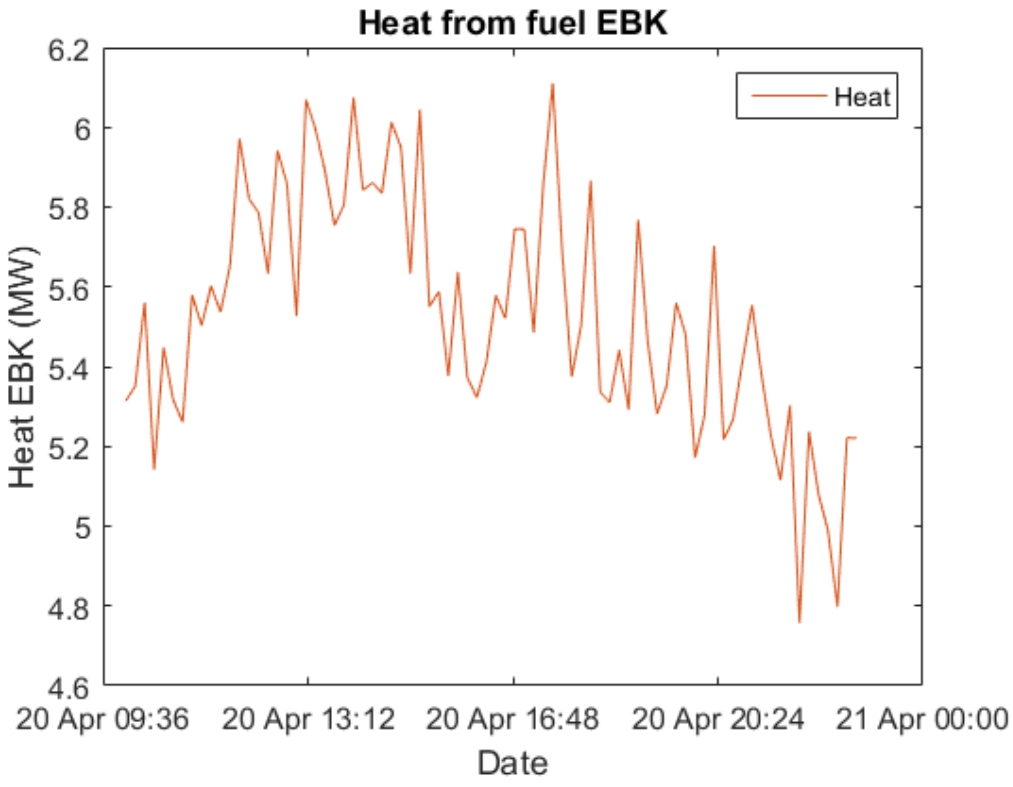
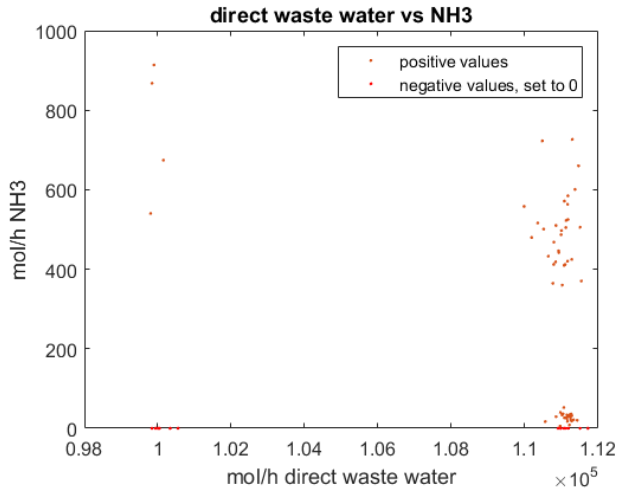


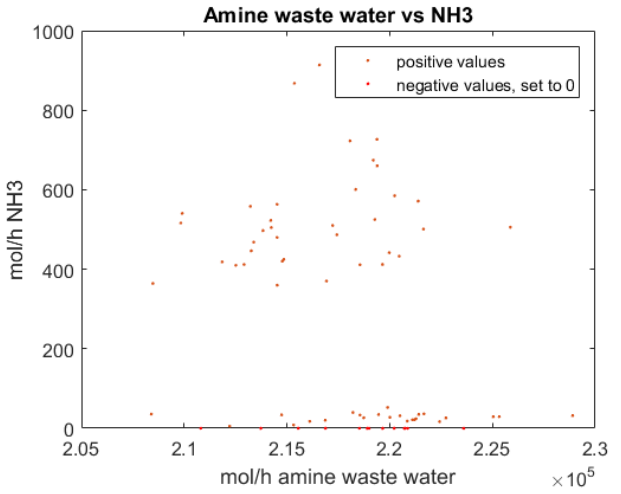
Figure 5.20: Total heat from fuel in the EBK during the temperature test run.

5.4.2.1 Ammonia slip and NO reduction, (T)

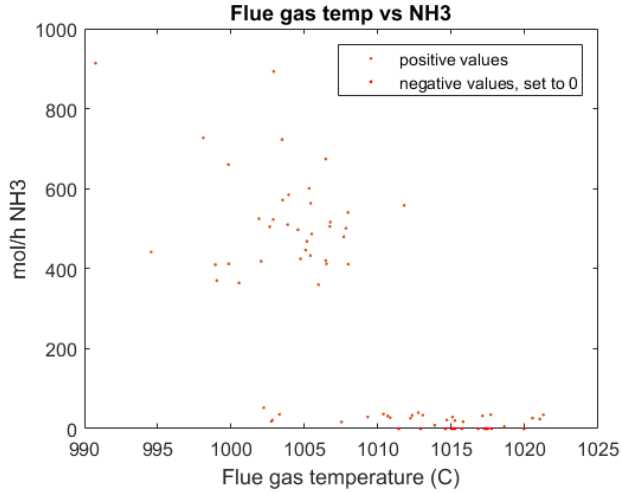
Figure 5.21 displays the influence of the test run on the ammonia slip and NO reduction.



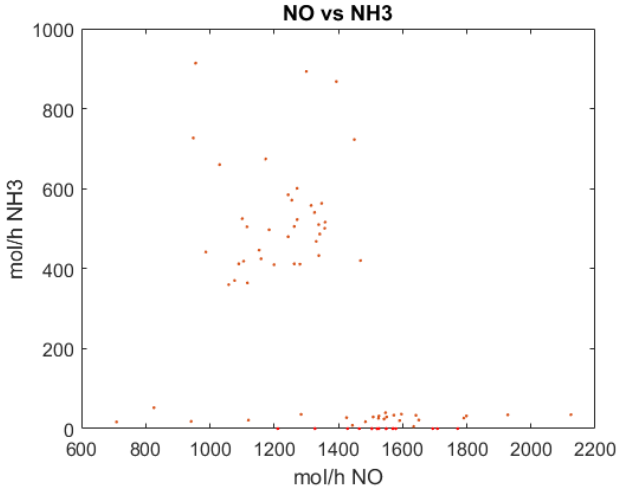
(a) Direct water flow against NH_3.



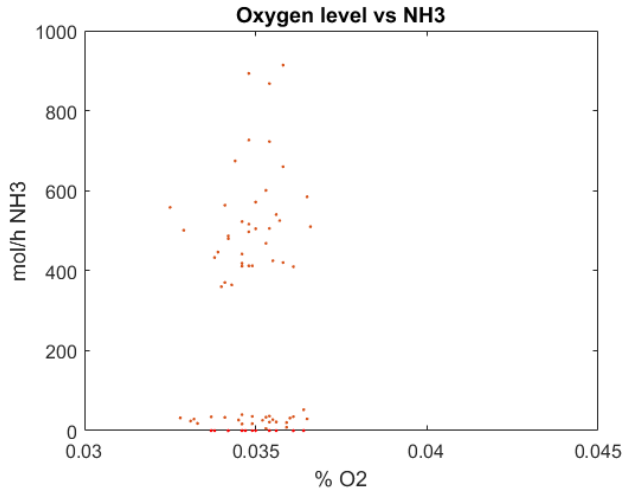
(b) Amine water flow against NH_3.



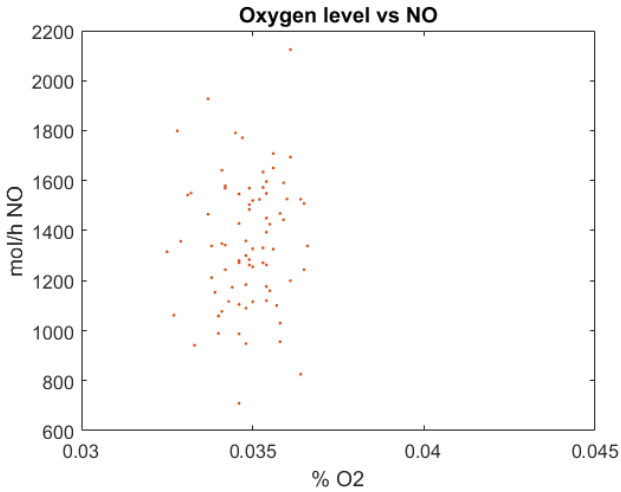
(c) Flue gas temperature against NH_3.



(d) NO against NH_3.



(e) O_2 fraction against NH_3.



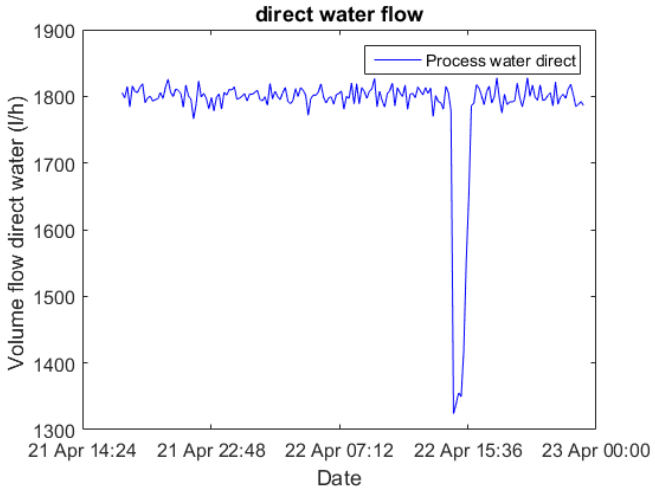
(f) O_2 fraction against NO.

Figure 5.21: The test parameters plotted against NO and NH_3 to investigate their influence on the ammonia slip and NO reduction during the temperature test run.

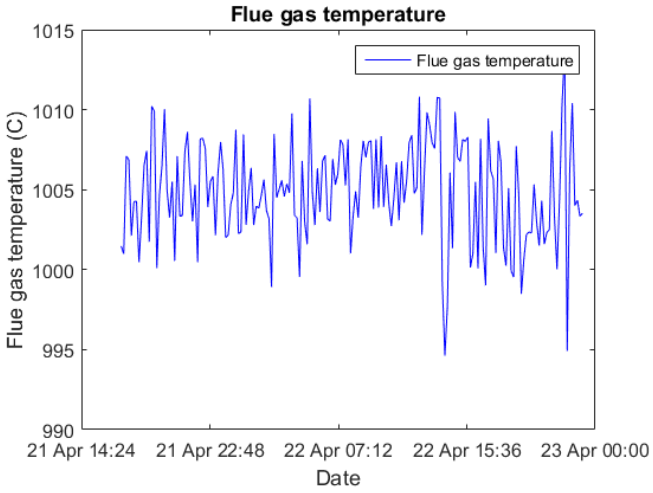
There are no clear trends in Figure 5.21, but Figure 5.21 (c) shows the tendency that the higher temperature gives a lower ammonia slip, giving the expected reversed relation between ammonia and NO.

5.4.3 Excess air (L)

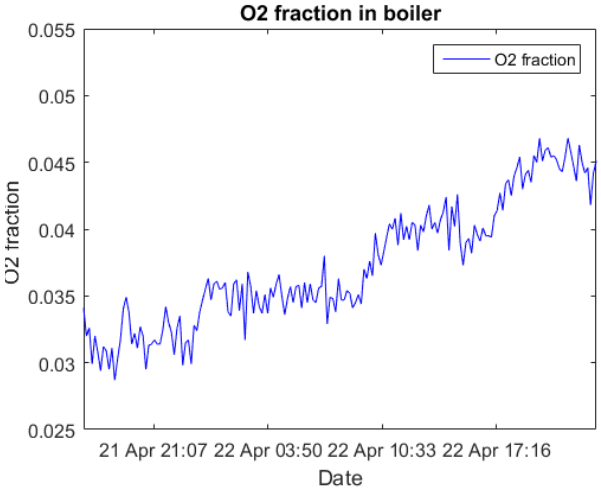
The excess air tests where run from 17:00 on April 21st to 23:15 on April 22nd. The resulting parameter values during this time period are presented in Figure 5.22.



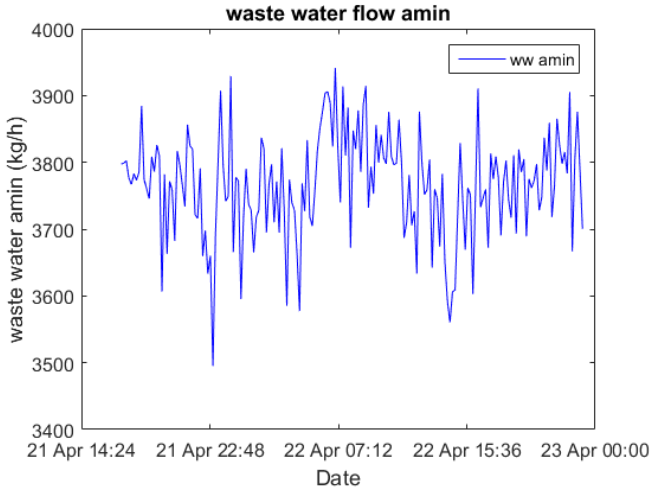
(a) Direct water flow during test period.



(b) Flue gas temperature during test period.



(c) O_2 fraction during test period.



(d) Amine waste water flow during test period.

Figure 5.22: All test parameters during the excess air testing period.

The parameters are kept constant within their fluctuations, but as can be seen in Figure 5.22 (a), there is a large dip in the direct process water volume flow. Unfortunately the operators notes were lost from this test run, but it is probable that the large dip is due to the de-sooting process being run. This process requires lower water flows for short periods of time. This is also observable in the total heat

from the fuel in the EBK, see Figure 5.23 where the heat dips down below 3 MW at around 15:00. Other than that it is hard to see any trend in the heat from fuel. The excess oxygen test runs were apart from that run according to schedule, observable in Figure 5.22 (c).

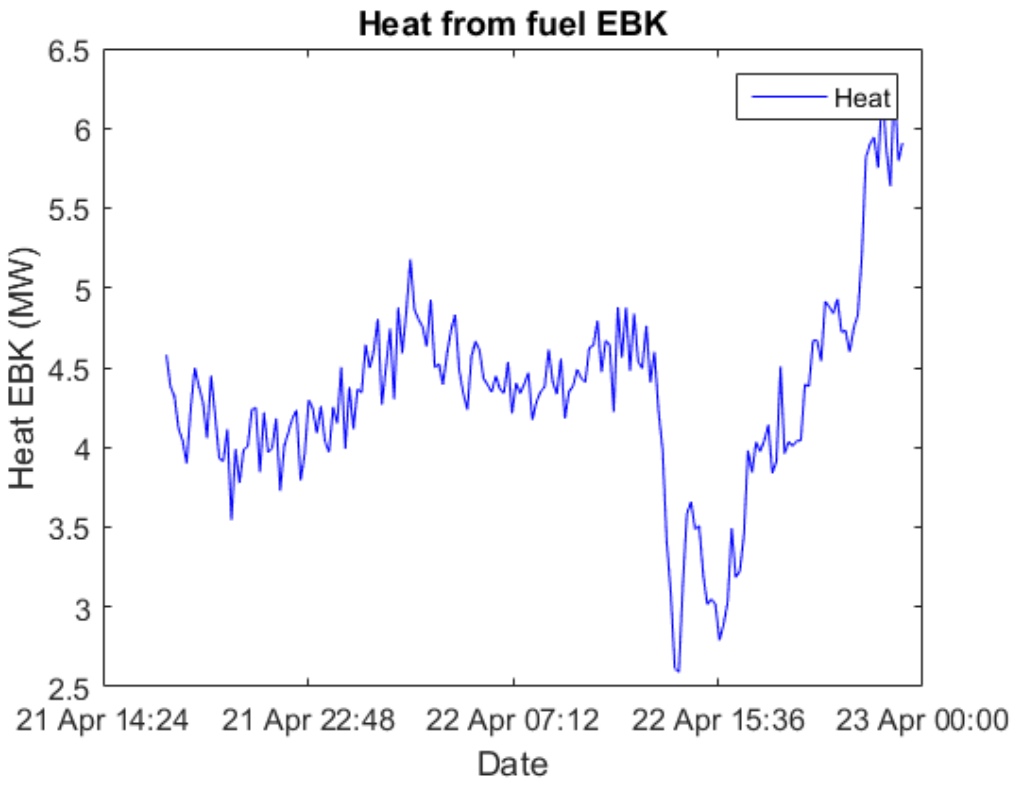
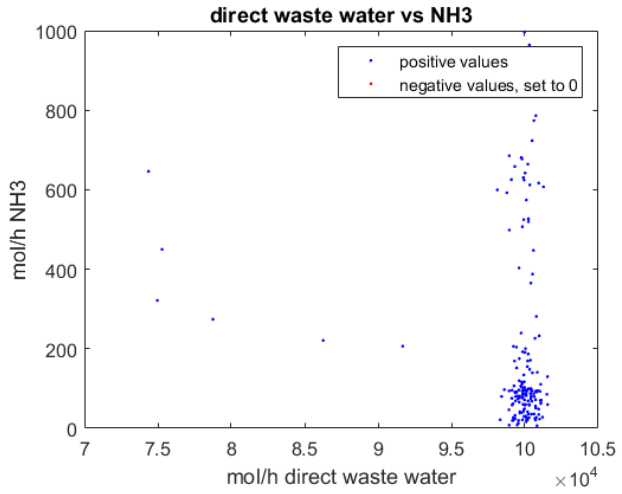


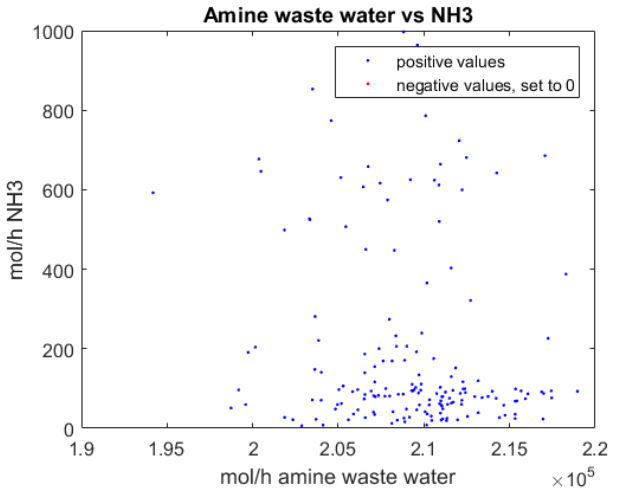
Figure 5.23: Total heat from fuel in the EBK during the excess air test run.

5.4.3.1 Ammonia slip and NO reduction, (L)

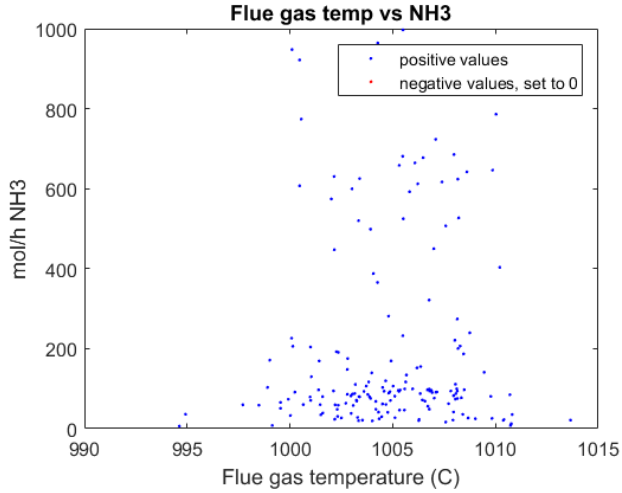
The influence of the parameters are presented in Figure 5.24. The excess air causes an increase in oxygen level after the EBK that gives a clear trend in the before mentioned relation between NO and ammonia, the more ammonia the less NO and reversed. This relation can therefore probably be confirmed as very dependent on the amount of oxygen available. It is also probable that the selectivity towards NO increases with increasing amount of oxygen available, which is consistent with the modeling results in Figure 5.14 (c).



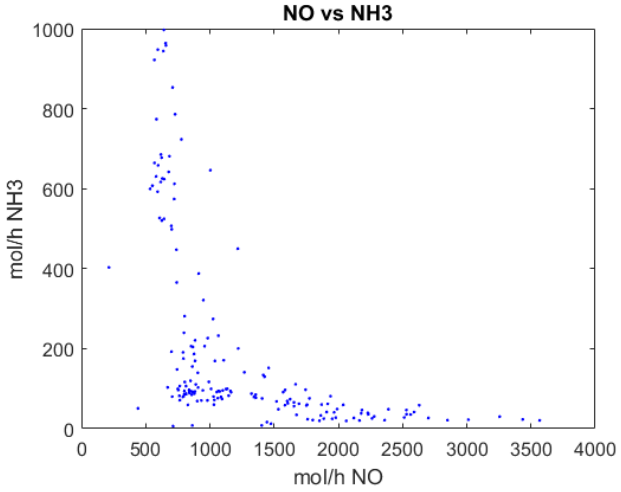
(a) Direct water flow against NH_3.



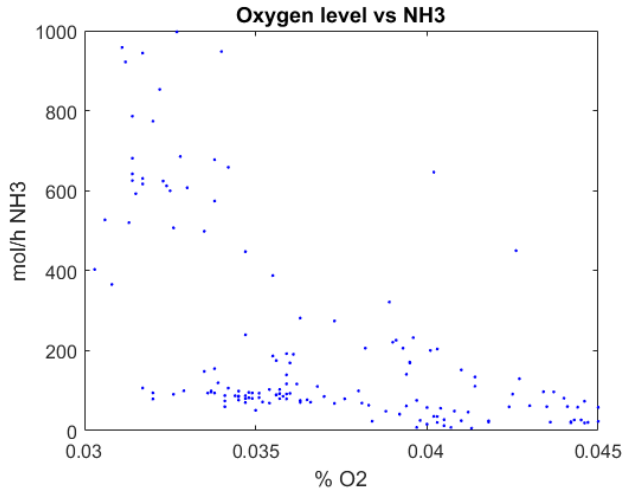
(b) Amine water flow against NH_3.



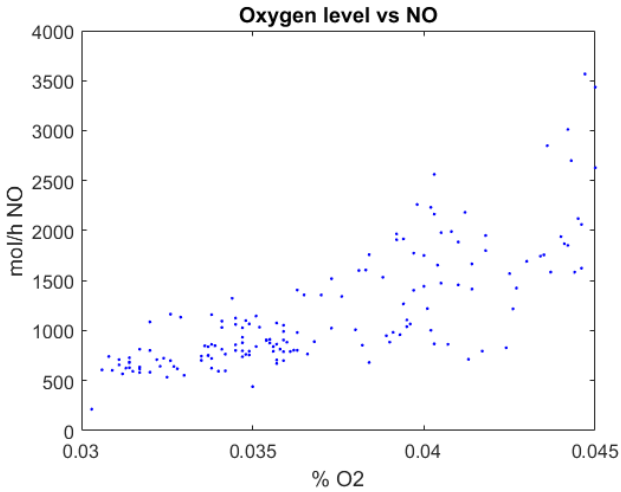
(c) Flue gas temperature against NH_3.



(d) NO against NH_3.



(e) O_2 fraction against NH_3.

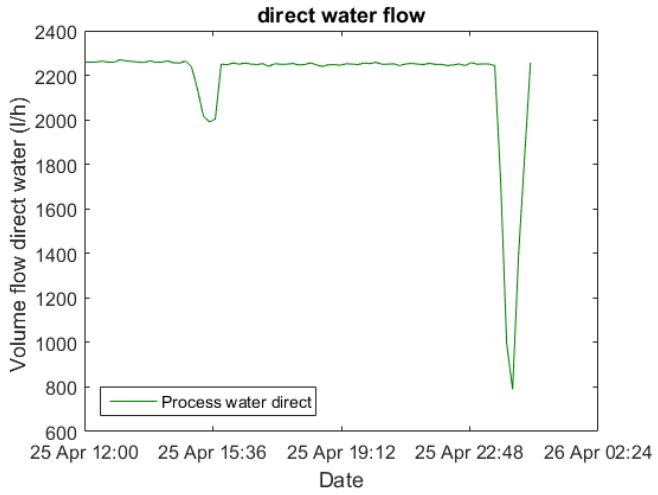


(f) O_2 fraction against NO.

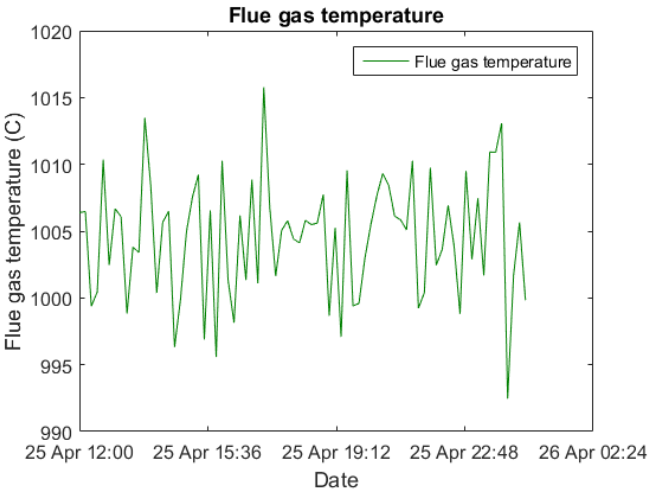
Figure 5.24: The test parameters plotted against NO and NH_3 to investigate their influence on the ammonia slip and NO reduction during the excess air test period.

5.4.4 Amine water from evaporators, (A)

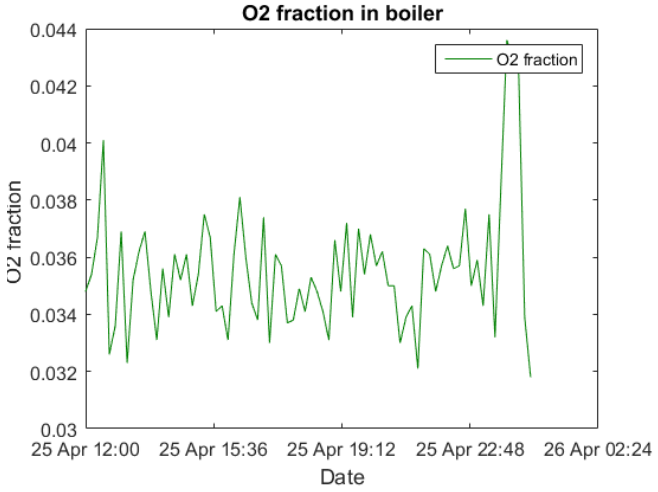
The last test set, varying the amine process water according to Table 4.10 was run from 12:00 on the 25th of April to 00:30 on the 26th of April. The resulting parameter values during the test period are presented in Figure 5.25.



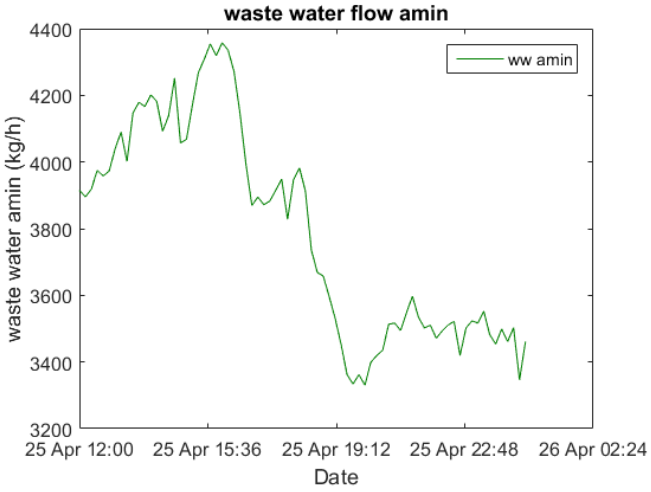
(a) Direct water flow during test period.



(b) Flue gas temperature during test period.



(c) O_2 fraction during test period.



(d) Amine waste water flow during test period.

Figure 5.25: All test parameters during the amine water testing period.

The parameters are kept at their set levels except for the direct water flow, Figure 5.25 (a). There is a small dip around 15:00 and a large dip at around 23:00. The smaller one is un identified but for the larger one it is noted that the de-sooting process was run. This probably affected the over all heat from fuel at that time as can be seen in Figure 5.26. Besides that the heat does not follow the lowered level of the amine waste water flow. This could be since the amine water flow plotted in Figure 5.25 (d) is equal to the total amount of water measured before the evaporators. Since a large fraction of the water is already evaporated when it enters the EBK the fluctuations in this water flow might not affect the temperature in the

furnace as much as changes in the un-evaporated direct water flow.

The eheat from fuel in the EBK over the test period is presented in Figure 5.26. There is a possible correlation between a lower total heat when the amine water flow is reduced, but it is not as clear as for when the direct water flow was reduced.

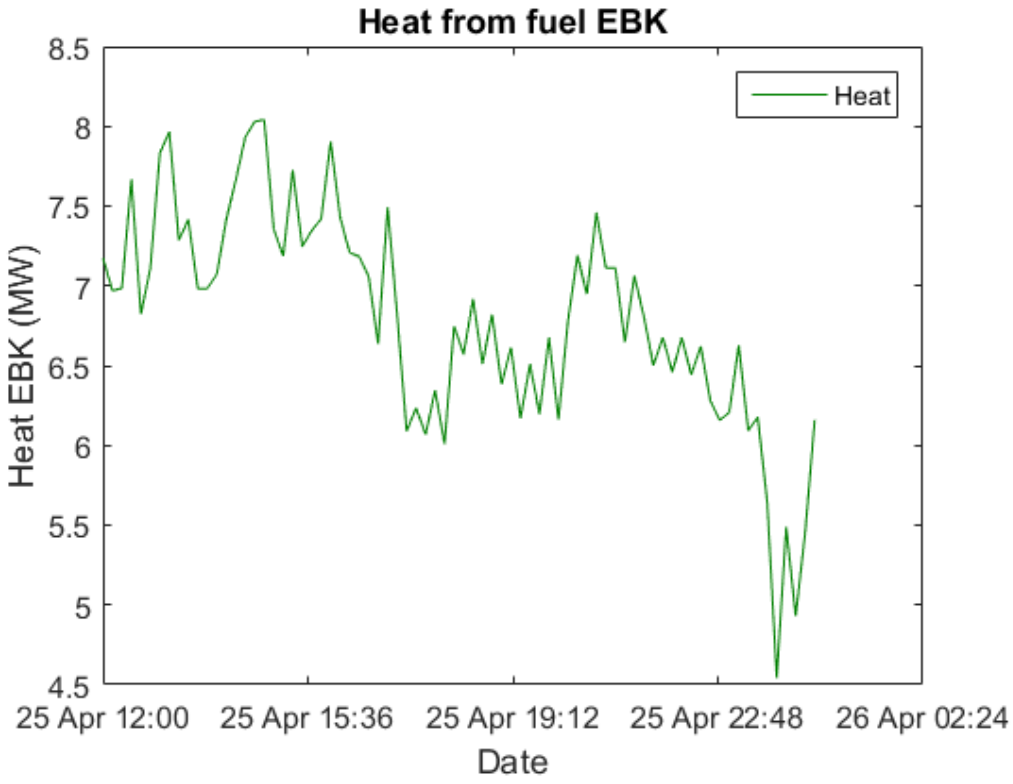
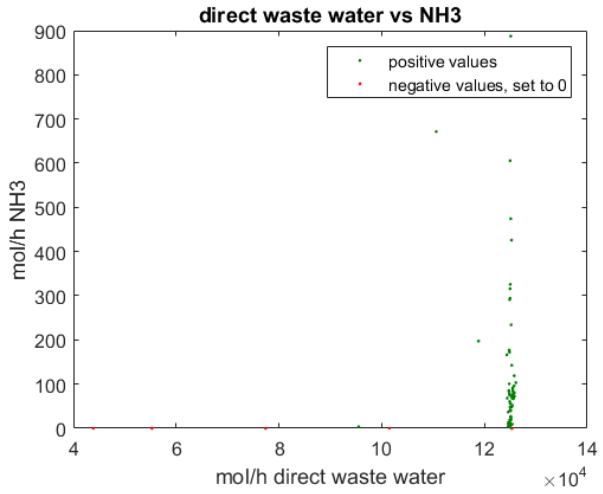


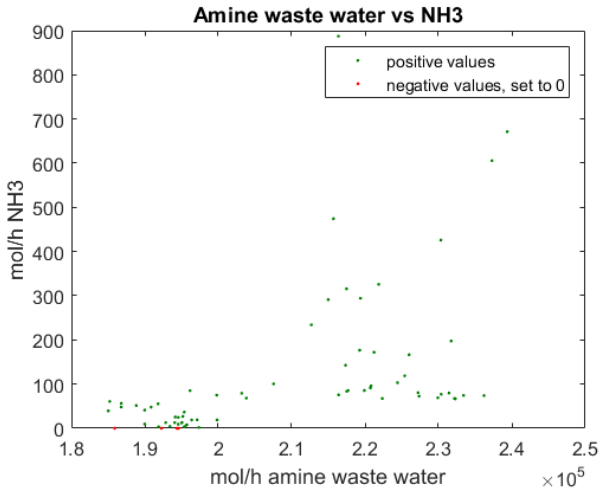
Figure 5.26: Total heat from fuel in the EBK during the amine water test run.

5.4.4.1 Ammonia slip and NO reduction (A)

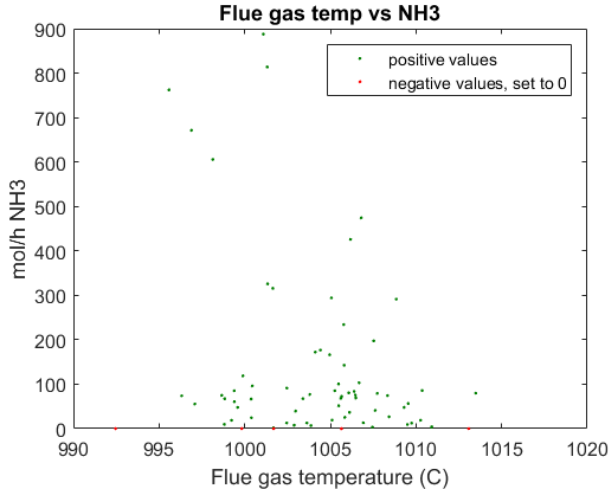
The influence of the parameters on the ammonia slip and NO reduction during the amine water test run is presented in Figure 5.27.



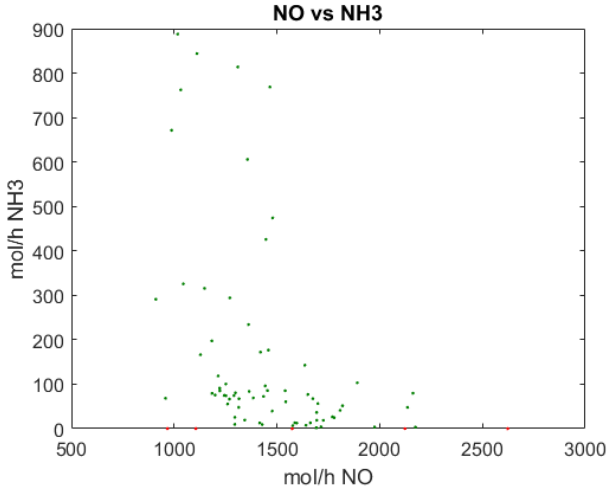
(a) Direct water flow against NH_3.



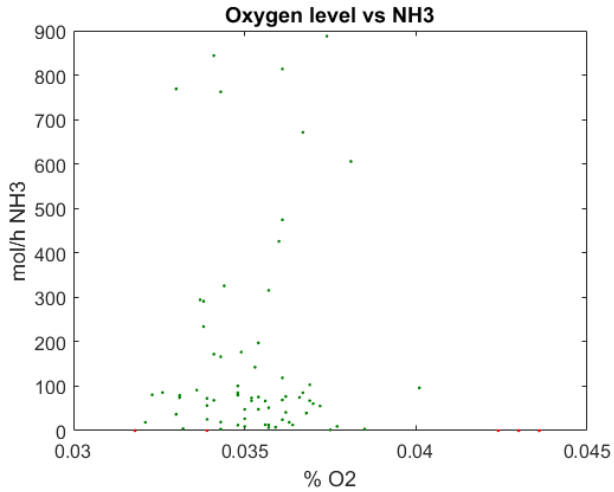
(b) Amine water flow against NH_3.



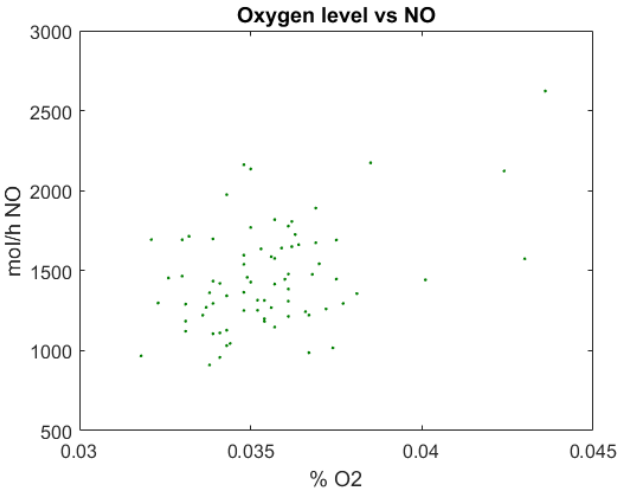
(c) Flue gas temperature against NH_3.



(d) NO against NH_3.



(e) O_2 fraction against NH_3.



(f) O_2 fraction against NO.

Figure 5.27: The test parameters plotted against NO and NH_3 to investigate their influence on the ammonia slip and NO reduction during the amine water test period.

There is a trend in Figure 5.27 (b) indicating that the amount of ammonia in the flue gases increases with the amine water flow increase which is consistent with the modeling results in Figure 5.13 (d). The oxygen level also seems to have a large influence on the combustion conditions, but mostly for the amount of NO, see Figure 5.27 (f). The reversed relation between NO and ammonia is still clear in Figure 5.27 (d).

All in all the results from the test runs confirm the trends in the modeling, namely that high temperature and high oxygen levels ensures low amounts of ammonia in the stack, while low temperatures and low oxygen levels gives less NO formation.

6
Conclusion

This thesis has evaluated the performance of waste water incineration through a case study at AkzoNobel in Stenungsund. The evaluation focused om the destruction of ammonia and the formation of NO_x emissions. The evaluation consisted of elemental balances over important unit steps, a sensitivity study by modeling important parameters and a set of experimental test runs to evaluate the parameters in the real waste water incineration process. The conclusions are that the most important parameters for the operation of the waste water incineration concerning the NO_x emissions and ammonia slip level are temperature, amount of water fed to the furnace and stoichiometric amount of oxygen fed to the furnace. In particular, achieving an adequate residence time and temperature above 1000°C is crucial for NH_3 destruction. High temperatures and high oxygen levels yields a low ammonia slip but increases the NO formation. This is in accordance with the literature since the NO formation is highly dependent on the presence of radicals, which in turn depends on heavily on temperature and available oxygen.

The experimental runs showed that the total amount of water affects the ammonia emissions more than just the amine water. This is believed to be due to large amounts of water (both liquid and vapour) disturb the flame and the NH_3 destruction potential, mainly by lowering the temperature. The large amount of water is unusual in combustion processes and the relatively low temperature of the direct water makes it an important parameter for the incineration process control.

The modeling study confirms that the amount of water is has an effect but also indicates that temperature is an important factor. Modeling shows that to eliminate the ammonia slip and also the emission of N_2O, temperatures over 1000°C is required. This was however not possible to evaluate in the real process. The best reduction of NO is below 1000°C which leads to a quite narrow temperature window where both good NO reduction and a low ammonia slip are achieved.

For future evaluation it would be recommended to further analyze the water leaving in the separation step and also the other waste stream compositions. This could give an even better understanding of the waste water incineration process and more exact results. Another observation is that the relative difficulties in keeping certain parameters stable, e.g. temperature, excess air and amine water, indicates that the margin of error in the process is small. It often operates near the critical temperature of 1000°C. If possible, an increase in the combustion temperature could reduce the risk of un-reacted ammonia in the stack, making the operation a bit more robust.

Bibliography

Bowman, C. T. (1992). Control of combustion-generated nitrogen oxide emissions: Technology driven by regulation. *Symposium (International) on Combustion*, 24(1):859–878.

European Commission - Environment (2017). *The industrial emissions directive*. `http://ec.europa.eu/environment/industry/stationary/ied/legislation.htm`. Accessed:2017-1-20.

European Environment Agency (2010). *Nitrogen oxides (NOx) emissions European Environment Agency*. `http://www.eea.europa.eu/data-and-maps/indicators/eea-32-nitrogen-oxides-nox-emissions-1`. Accessed: 2017-01-19.

European Environment Agency (2017). `https://www.eea.europa.eu/data-and-maps/indicators/emissions-of-primary-particles-and-5`. Accessed: 2017-05-20.

Fan, W., Zhu, T., Sun, Y., and Lv, D. (2014). Effects of gas compositions on NOx reduction by selective non-catalytic reduction with ammonia in a simulated cement precalciner atmosphere. *Chemosphere*, vol 113:182–187.

Glarborg, P., Jensen, A., and Johnsson, J. (2003). Fuel nitrogen conversion in solid fuel fired systems. *Progress In Energy And Combustion Science*, 29(2):89–113.

Glarborg, P., Miller, J. A., and Kee, R. J. (1986). Kinetic modeling and sensitivity analysis of nitrogen oxide formation in well-stirred reactors. *Combustion and Flame*, 65(2):177–202.

Kampa, M. and Castanas, E. (2008). Human health effects of air pollution. *Environmental Pollution*, 151(2):362–367.

Keck, O., Meier, W., Stricker, W., and Aigner, M. (2002). Establishment of a Confined Swirling Natural Gas/Air Flame as a Standard Flame: Temperature and Species Distributions from Laser Raman Measurements. *Combustion Science and Technology*, 174(8):117–151.

Lodder, P. and Lefers, J. (1985). Effect of natural gas, C_2H_6 and CO on the homogeneous gas phase reduction of NO_x by NH_3. *The Chemical Engineering Journal*, 30(3):161–167.

Miller, J. A. and Bowman, C. T. (1989). Mechanism and modeling of nitrogen

chemistry in combustion. *Progress in Energy and Combustion Science*, 15(4):287–338.

Moskaleva, L. and Lin, M. (2000). The spin-conserved reaction CH+N_2 -> H + NCN: A major pathway to prompt no studied by quantum/statistical theory calculations and kinetic modeling of rate constant. *Proceedings of the Combustion Institute*, 28(2):2393–2401.

Naturvårdsverket (2017). `http://www.riksdagen.se/sv/dokument-lagar/dokument/svensk-forfattningssamling/forordning-2013253-om-forbranning-av-avfall_sfs-2013-253`. Accessed: 2017-01-31.

Parliament, T. E. and the Council of the European Union (2017). Directive (EU) 2015/2193. `http://eur-lex.europa.eu/legal-content/EN/TXT/PDF/?uri=CELEX:32015L2193&from=EN`. Accessed: 2017-1-20.

Raask, E. (1985). *Mineral impurities in coal combustion*. Hemisphere Pub. Corp., 1 edition. Washington.

Thomas, K. (1997). The release of nitrogen oxides during char combustion. *Fuel*, 76(6):457–473.

Thunman, H. (2016). *Combustion Engineering*. Chalmers University of Technology, 1 edition. Course compendium.

Toray Engineering Co, Ltd. (2017). Principle of Measurement of Zirconia Oxygen Analyzers. `www.toray-eng.com/measuring/tec/zirconia.html`. Accessed: 2017-05-11.

Van der Lans, R., Glarborg, P., and Dam-Johansen, K. (1997). Influence of process parameters on nitrogen oxide formation in pulverized coal burners. *Progress In Energy And Combustion Science*, 23(4):349–377.

Zandaryaa, S. and Buekens, A. (2009). Control of sulfur oxides. *Pollotion control technologies*, vol II. Eolss Publishers CO. Ltd., Oxford UK.

Zeldovich, Y., Frank-Kamenetskii, D., and Sadovnikov, P. (1947). *Oxidation of nitrogen in combustion*. Publishing House of the Acad of Sciences of USSR.

A

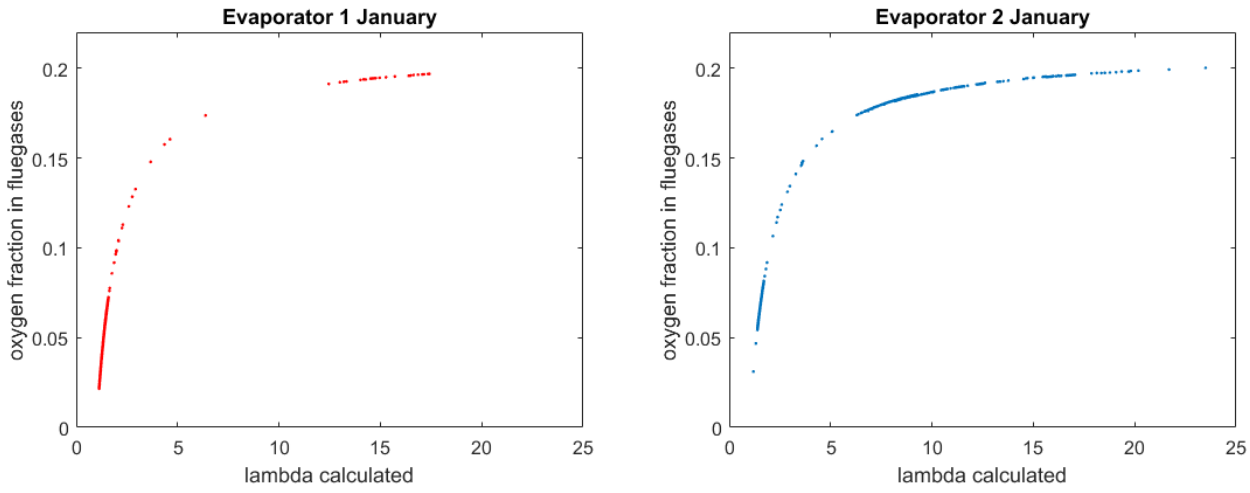
Appendix 1

A.1 Calculation results and operationg conditions

A.1.1 January 2017

A.1.1.1 Evaporators

The results for the stoichiometric calculations concerning the evaporators are presented in Figure A.1 to A.2.



(a) January 2017 evaporator 1.

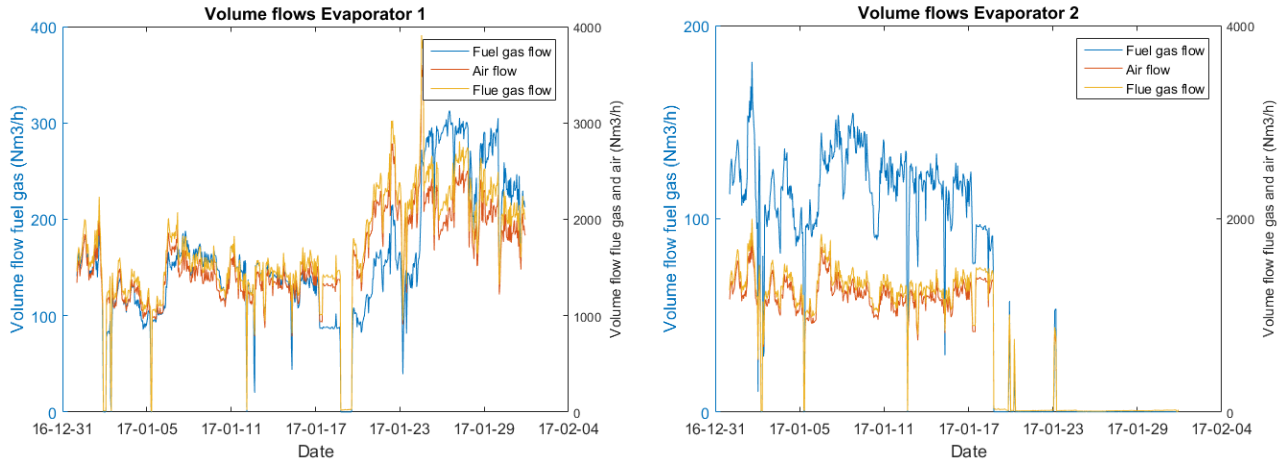
(b) January 2017 evaporator 2.

Figure A.1: The calculated value for lambda plotted against the measured oxygen fraction after the evaporators in January 2017.

As can be observed in Figure A.1 the oxygen level varies between around 2 and 20% for evaporator 1 (a) and 4.5 and 20% for evaporator 2 (b). The very high levels at 18-21% can be explained by evaporator down time, meaning that when the evaporators are not in use at for example start up periods the oxygen meters register close to atmospheric levels of oxygen. These high levels are more frequent for evaporator 2, explained by mechanical trouble with leaking flue gas tubes that caused it to be shut down during all of February. It is therefore not running on the same high capacity as evaporator 1 leading to the generally higher oxygen levels after combustion as well. The value for lambda varies between around 1.15 and 14,

the latter falling under the same explanation as for the high oxygen levels, when the evaporators are not in use the calculated lambda will be very large. A lambda at 1 would mean that the amount of air that is used is exactly the theoretical amount needed for the combustion to be complete.

In Figure A.2 above the measured fuel gas volume flow is presented as well as calculated volume flows of air and flue gases after evaporator 1 and 2.



(a) January 2017 evaporator 1. **(b)** January 2017 evaporator 2.

Figure A.2: Fuel gas, flue gas and air flows for evaporator 1 and 2 in January 2017.

In documentation from AkzoNobel concerning the evaporators it is stated that the design flow of flue gases from both evaporators is determined to 3000 Nm^3/h, which means that the result above of 1100 to 1500 is reasonable. The higher values starting at January 21st are due to the fact that evaporator 2 was closed down for maintenance work, leading to evaporator 1 being run on a higher load which is also visible when looking at the volume flow of fuel gas during the same period.

A.1.1.2 EBK

The same calculations as for the evaporators where also performed for the EBK, adding feed streams HP and LP vent and waste water. The results for lambda and measured oxygen level after the EBK are presented in the section below.

The calculated value for lambda is plotted against the measured oxygen level in the steam boiler, meaning it is dependent only of the combustion process in the EBK, see Figure A.3. The oxygen level ranges from 3.5 to around 20% and the high levels are also here explained by process down time. Extreme outliers have been removed from the graph.

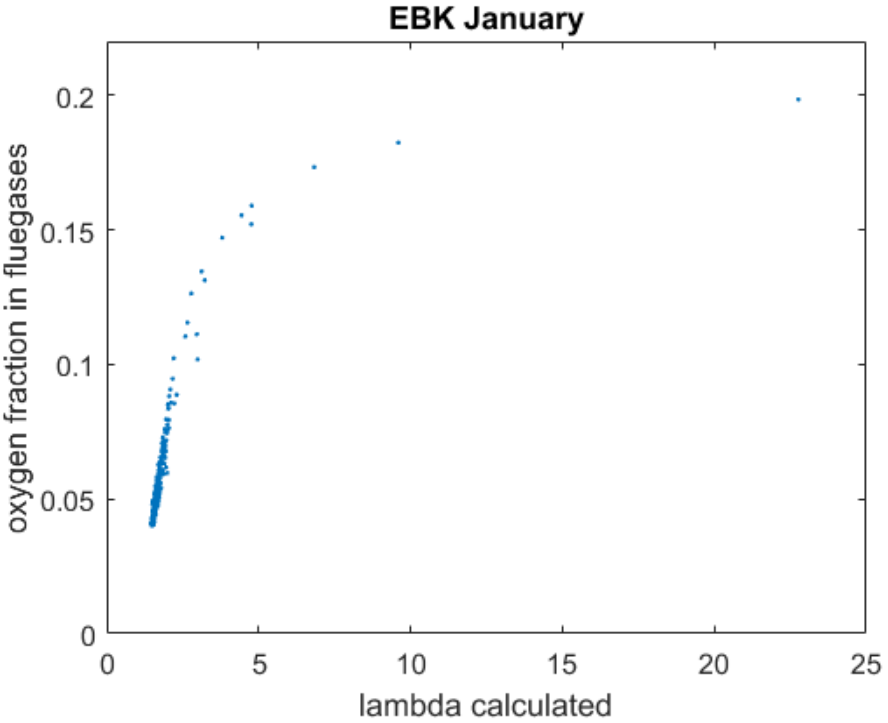


Figure A.3: Lambda for the EBK plotted against oxygen levels in the steam boiler for January 2017.

As can be observed in Figure A.3 there is a very clear increasing trend correlating oxygen levels and lambda which is to be expected since the calculations for lambda are performed using the oxygen levels. It can however also be observed that the correlation is less linear and well defined for the EBK as for the evaporators. This is explained by the complexity of the calculations, the EBK has seven inlet streams; air, fuel gas, waste water from amine, waste water from surfactants, HP vent, LP vent and organic waste, all of them varying in composition to some degree. Compared to only air and fuel gas for the evaporators since the waste water is not taking part in the combustion.

It is also observed that the values for lambda is higher for the EBK than for the evaporators. The control system regulating the air flow to the EBK was at the time not functioning satisfactory and the desired level of 3.5% was not met.
Volume flows EBK The volume flows of fuel gas, air and flue gases for the EBK during January is presented in Figure A.4.

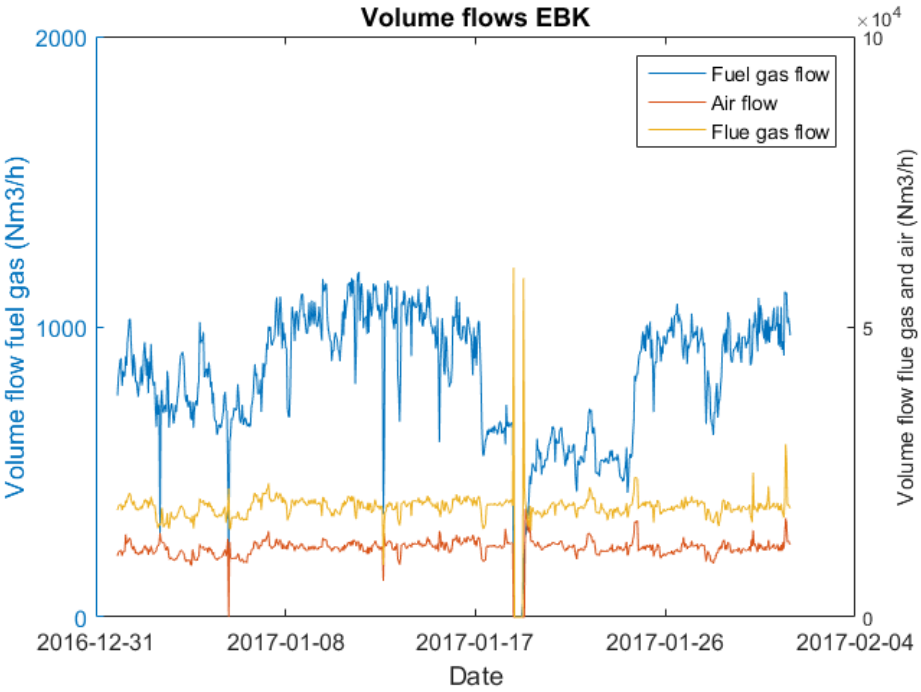


Figure A.4: Volume flows of fuel gas, air and flue gas for the EBK during January 2017.

There is a period of down time at the 19th of January. The variations in fuel gas flow is explained partly by the variations in heating value of the gas depending on the composition, varying daily.

A.1.2 February 2017

The following section presents all results from the February calculations and operation conditions.

Figure A.5 presents the fuel gas composition and lower heating value during February.

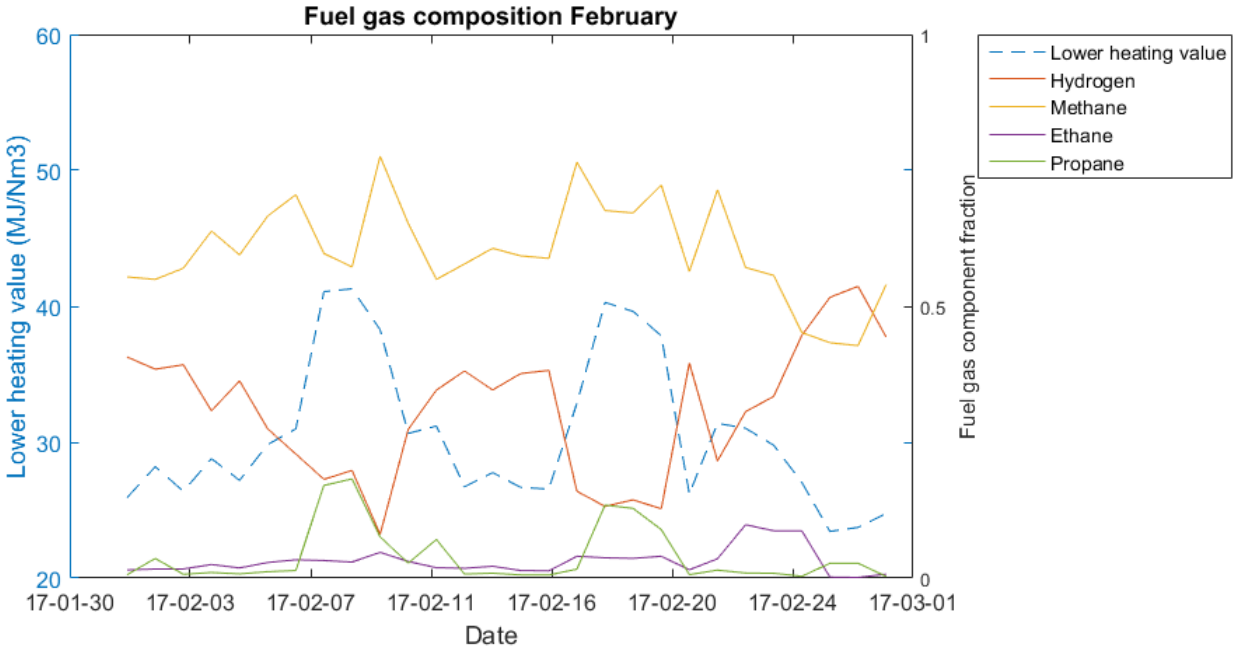


Figure A.5: Fuel gas composition in February 2017.

Figure A.6 presents the calculated values for lambda in the EBK during February. In Figure A.12 the calculated volume flows for the EBK are presented.

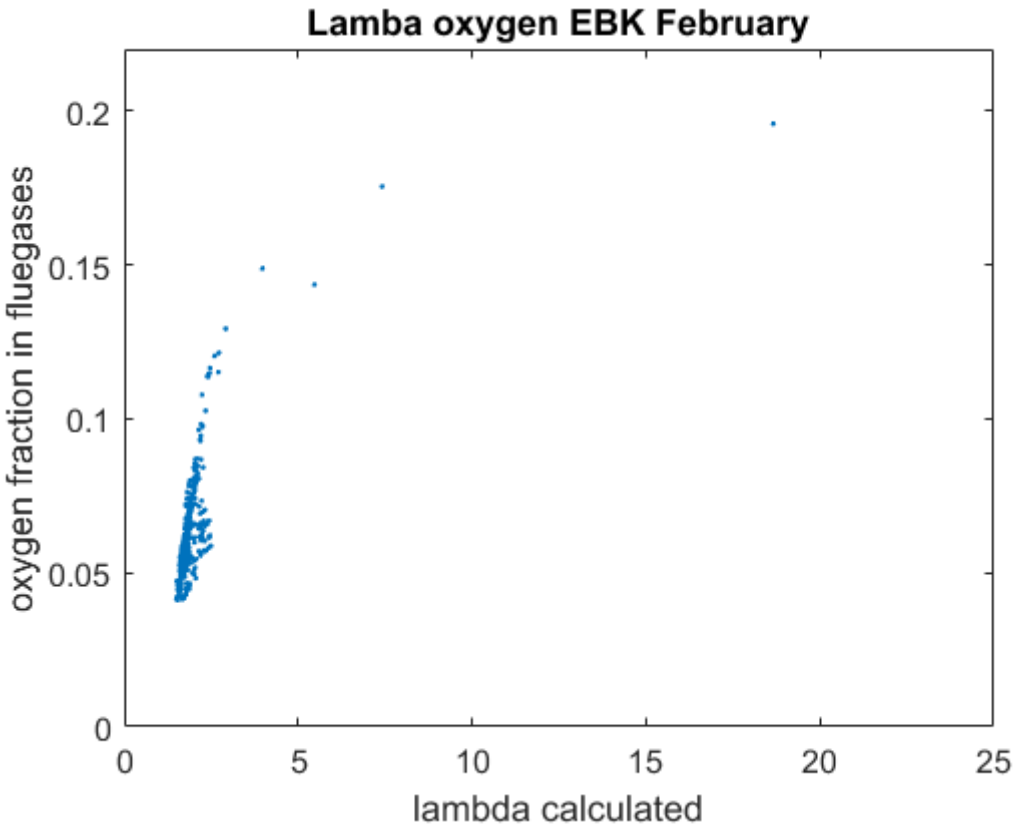


Figure A.6: Lambda EBK February 2017.

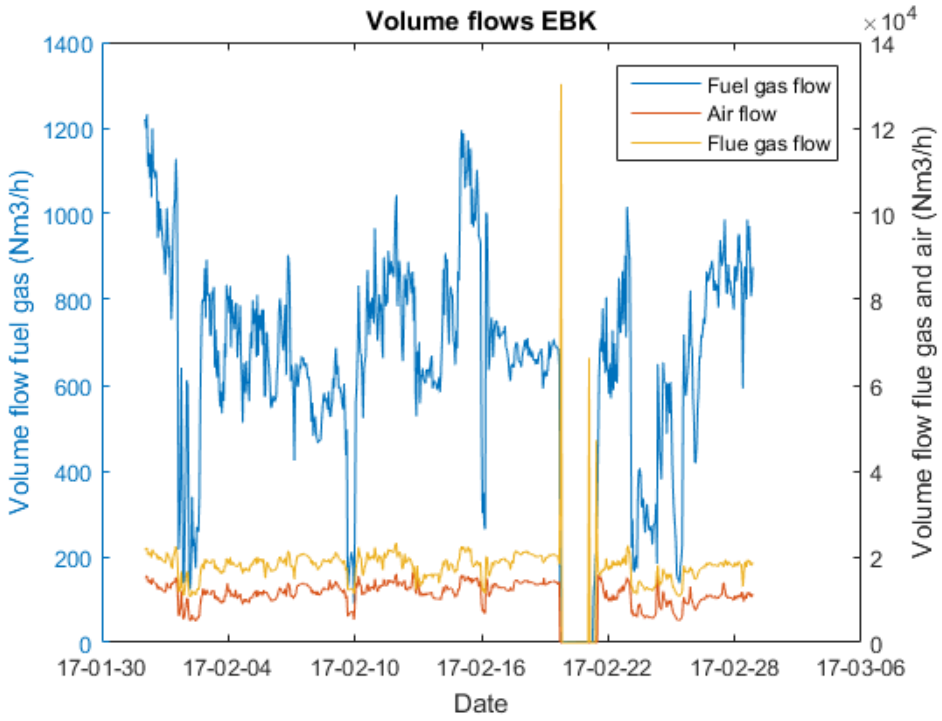
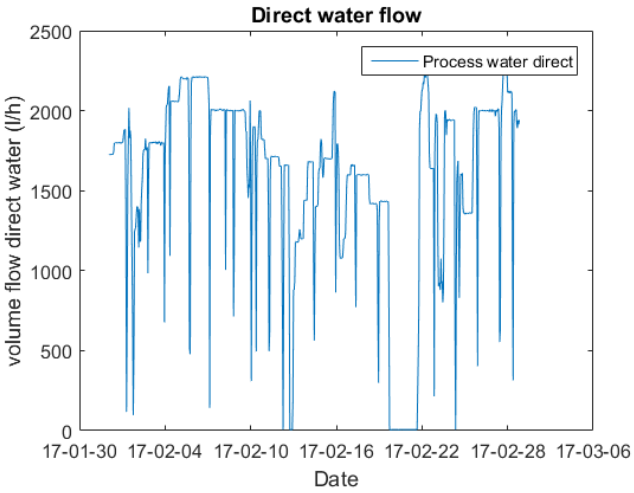
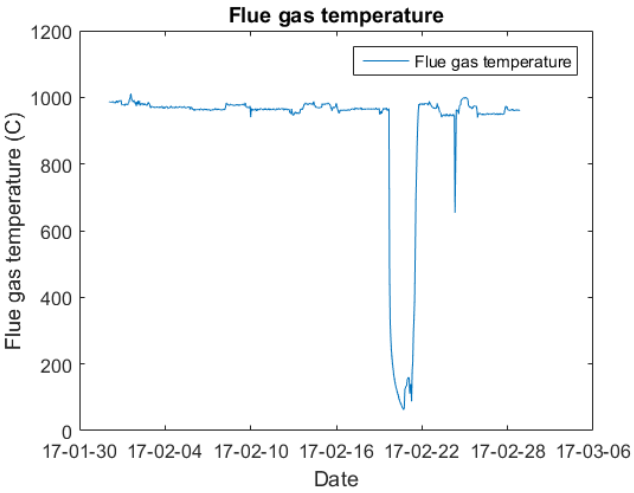


Figure A.7: Volume flows EBK February 2017.

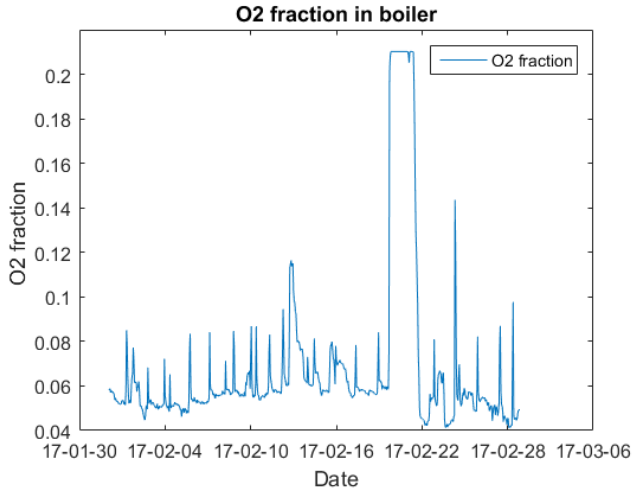
Figure A.8 (a) to (d) the operating conditions during February for the investigated parameters are presented.



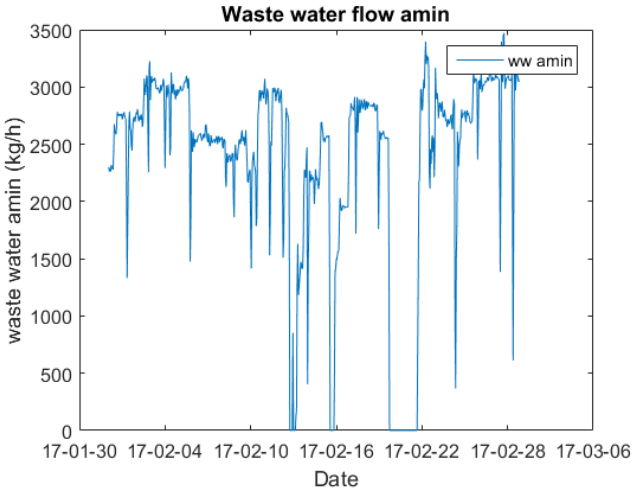
(a) Direct water flow during February.



(b) Flue gas temperature during February.



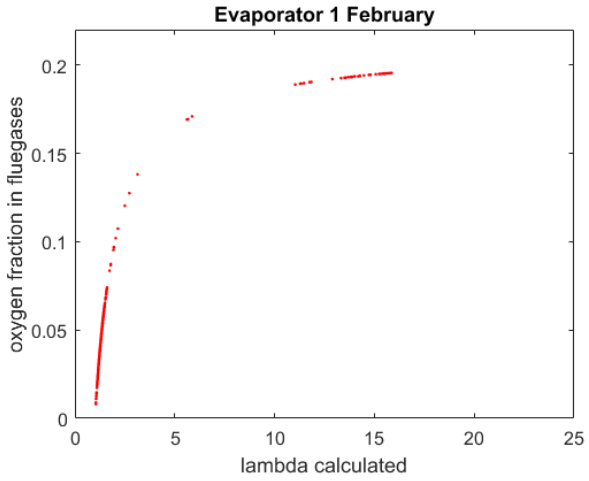
(c) O_2 fraction during February.



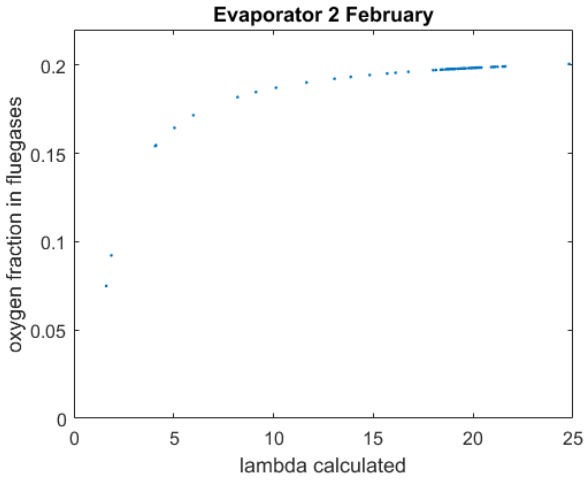
(d) Amine waste water flow during February.

Figure A.8: Test parameters during February.

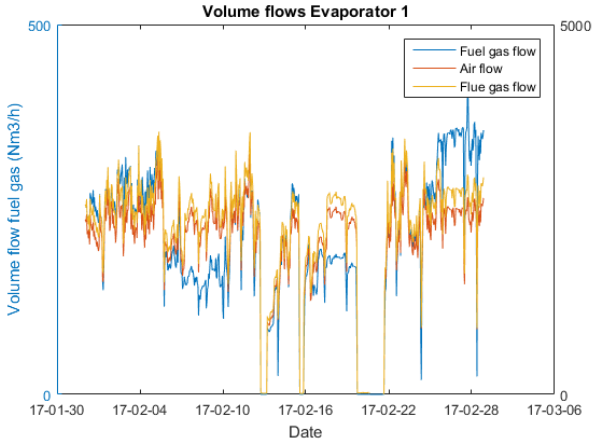
In Figure A.9 the results for the evaporators and the water and oxygen fractions for February are presented.



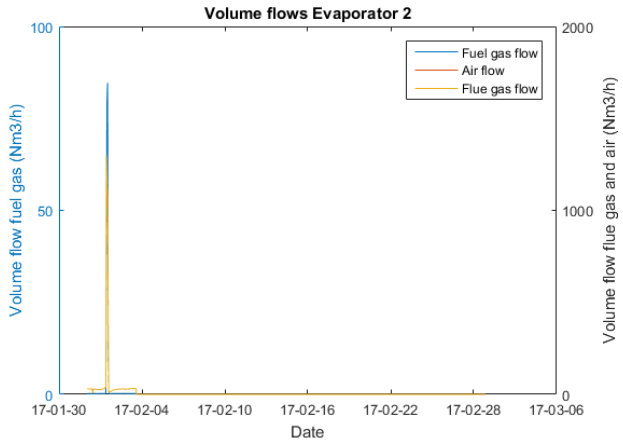
(a) Calculated lambda in evaporator 1.



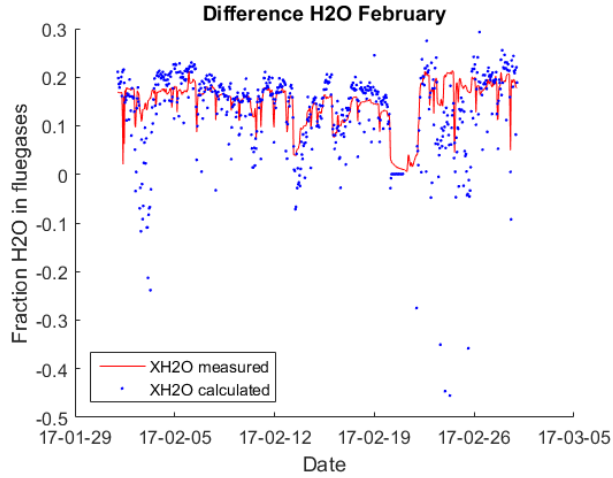
(b) Calculated lambda in evaporator 2.



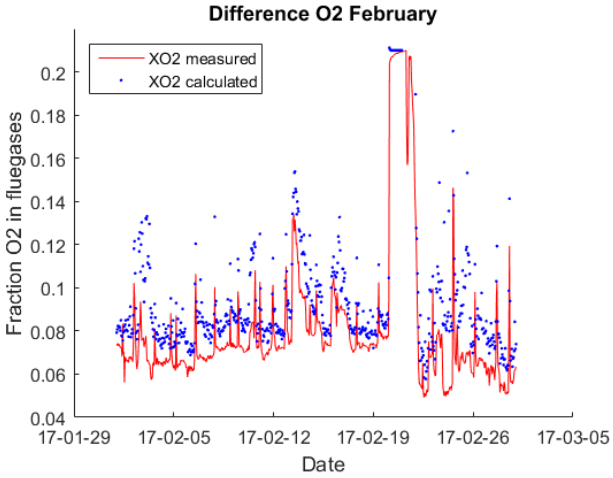
(c) Volume flows for evaporator 1 in February.



(d) Volume flows for evaporator 2 in February.



(e) Calculated H_2O fraction in fluegases against measured fraction.



(f) Calculated O_2 fraction in fluegases against measured fraction.

Figure A.9: Calculation results from February.

A.1.3 March 2017

The following section presents all results from the March calculations and operation conditions.

Figure A.10 presents the fuel gas composition and lower heating value during March.

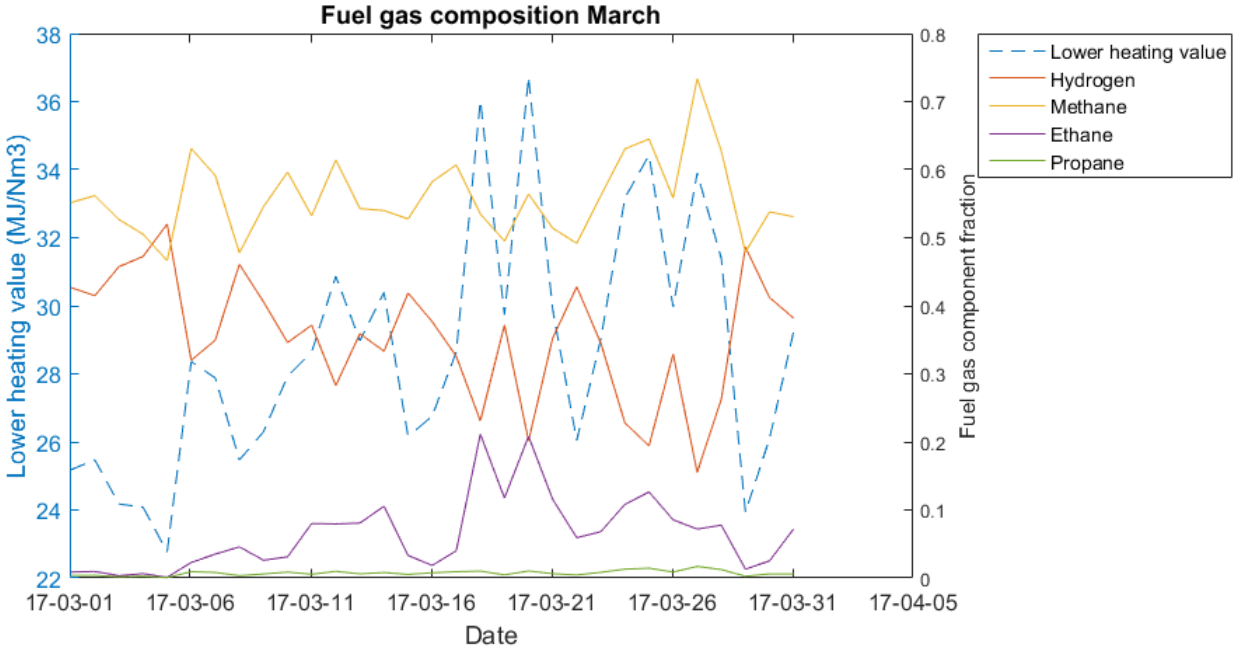


Figure A.10: Fuel gas composition in March 2017.

Figure A.11 presents the calculated values for lambda in the EBK during March. In Figure A.12 the calculated volume flows for the EBK are presented.

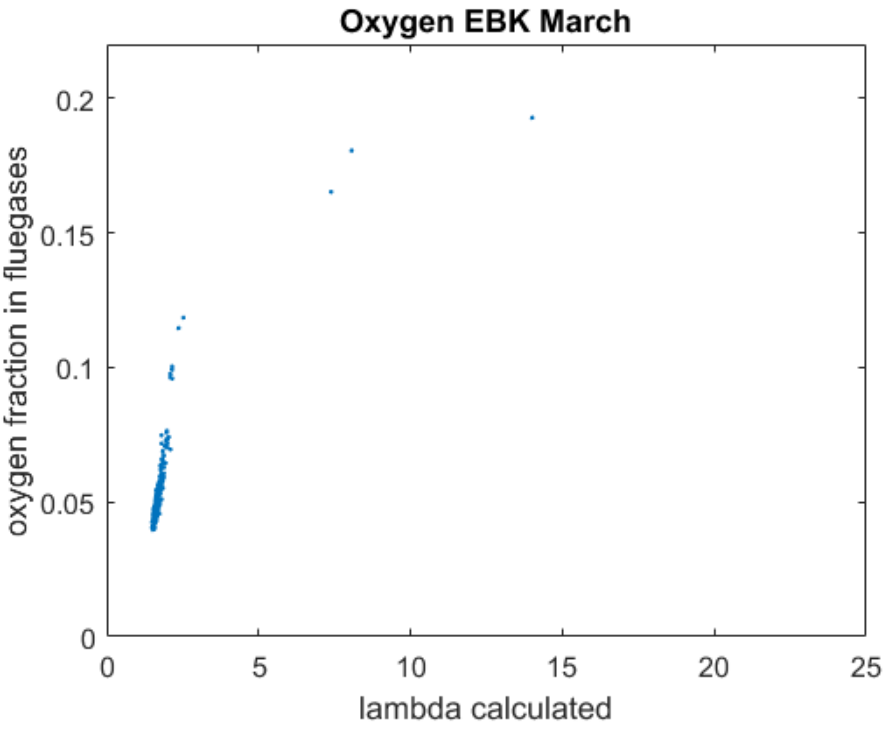


Figure A.11: Lambda EBK March 2017.

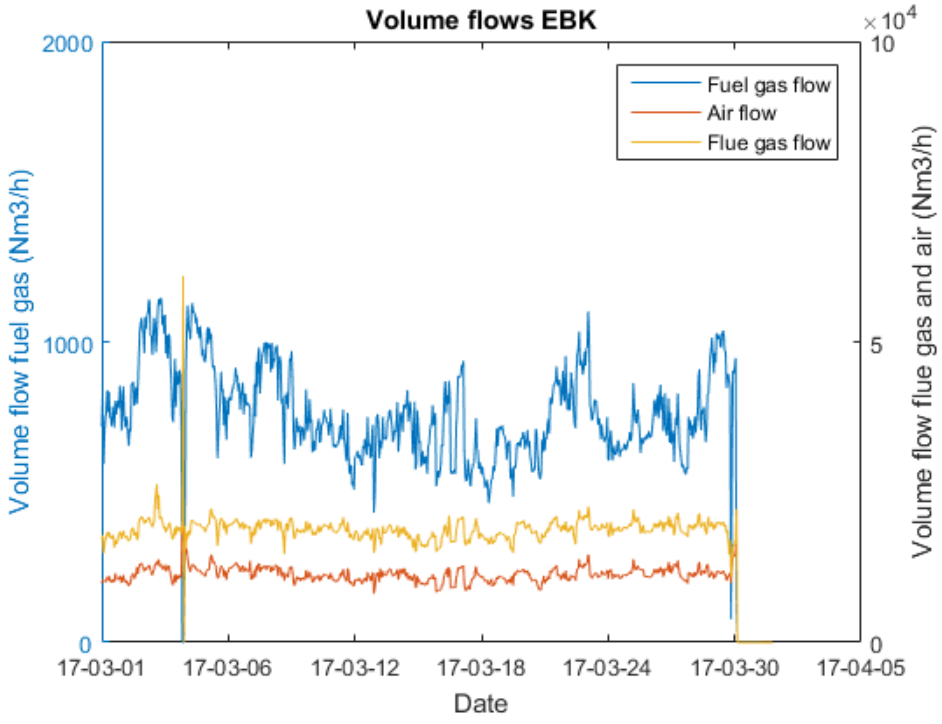
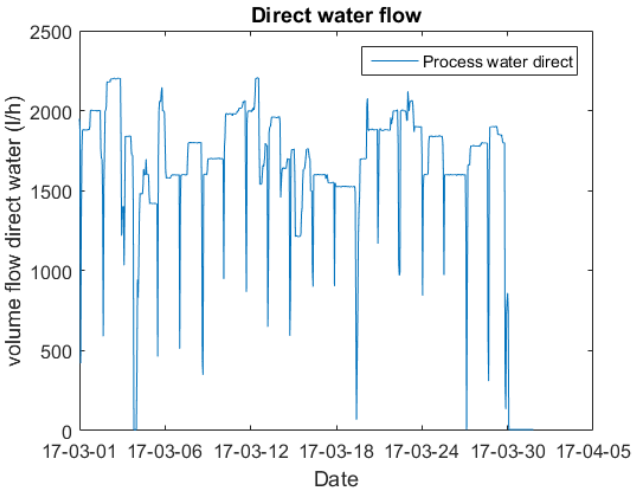
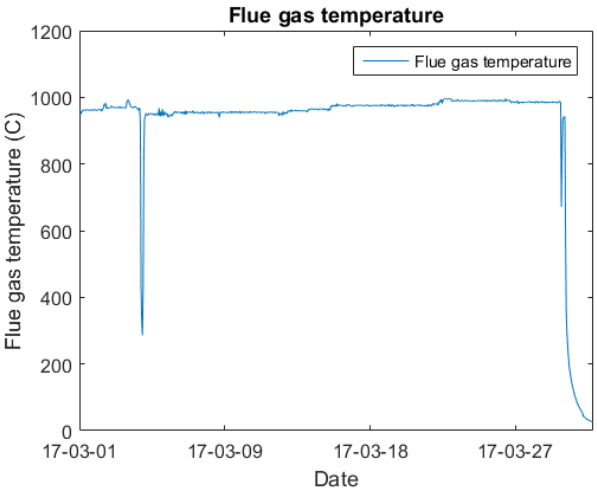


Figure A.12: Volume flows EBK March 2017.

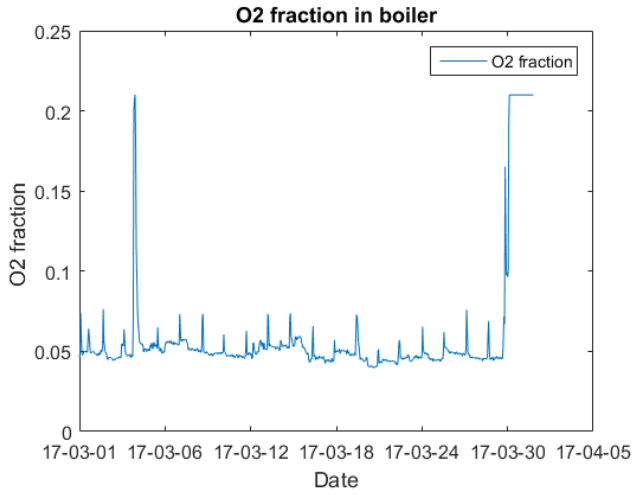
Figure A.13 (a) to (d) the operating conditions during March for the investigated parameters are presented.



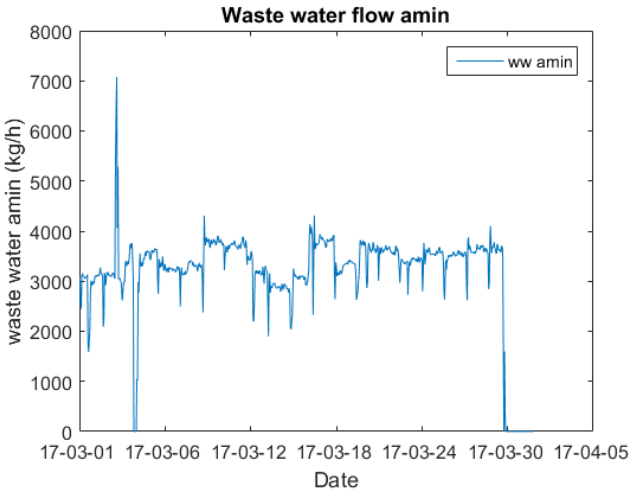
(a) Direct water flow during March.



(b) Flue gas temperature during March.



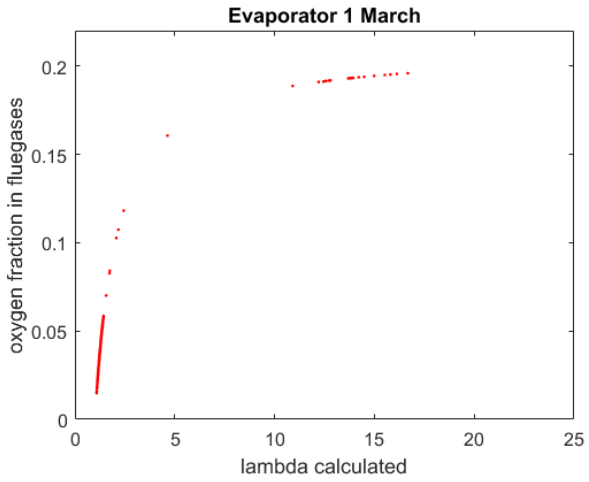
(c) O_2 fraction during March.



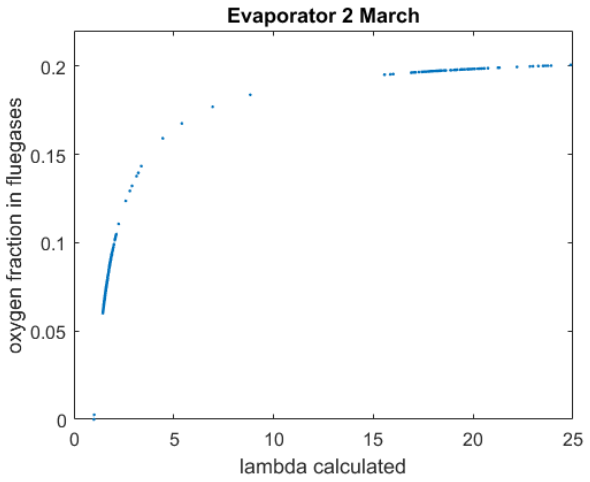
(d) Amine waste water flow during March.

Figure A.13: Test parameters during March.

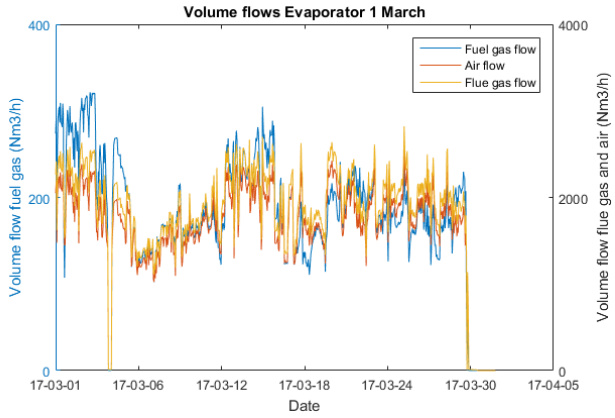
In Figure A.14 the results for the evaporators and the water and oxygen fractions for March are presented.



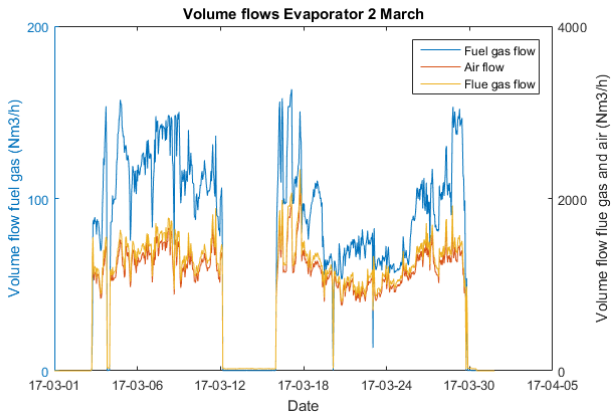
(a) Calculated lambda in evaporator 1.



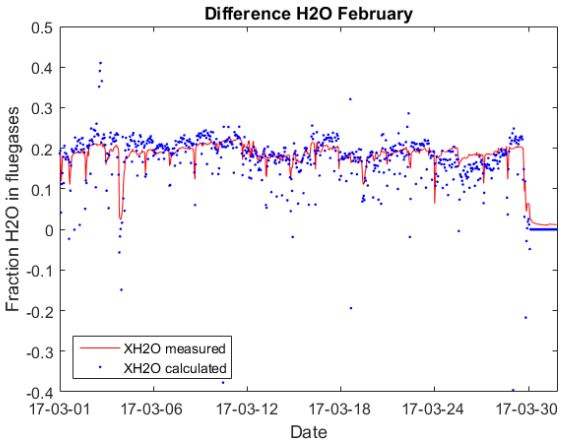
(b) Calculated lambda in evaporator 2.



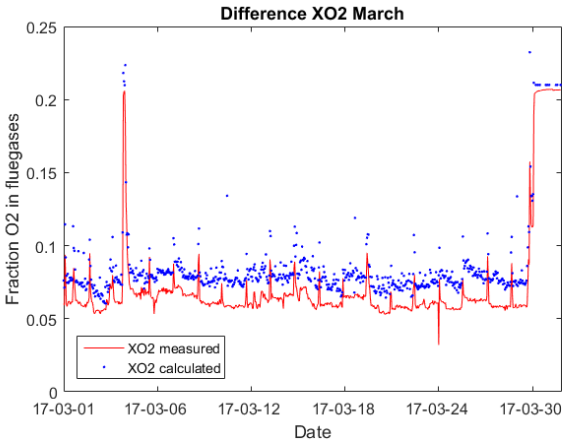
(c) Volume flows for evaporator 1 in March.



(d) Volume flows for evaporator 2 in March.



(e) Calculated H_2O fraction in flue gases against measured fraction.



(f) Calculated O_2 fraction in flue gases against measured fraction.

Figure A.14: Calculation results from March.

A.1.4 April 2017

The following section presents all results from the April calculations and operation conditions.

Figure A.15 presents the fuel gas composition and lower heating value during April.

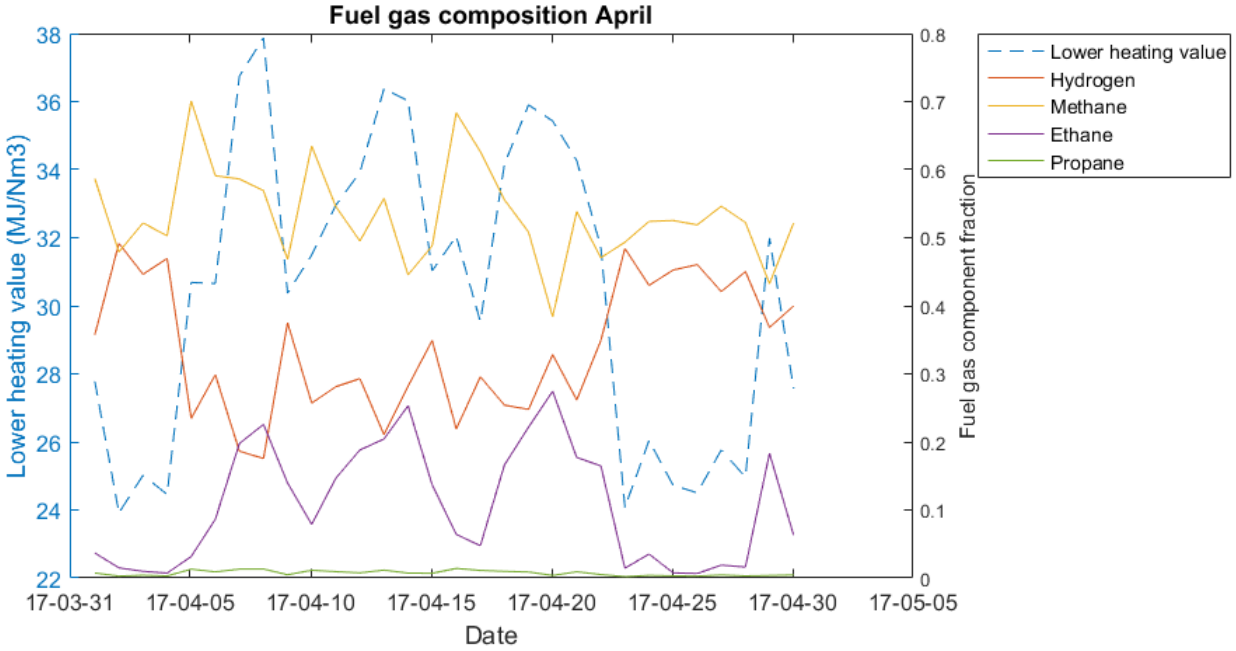


Figure A.15: Fuel gas composition in April 2017.

Figure A.16 presents the calculated values for lambda in the EBK during April. In Figure A.17 the calculated volume flows for the EBK are presented.

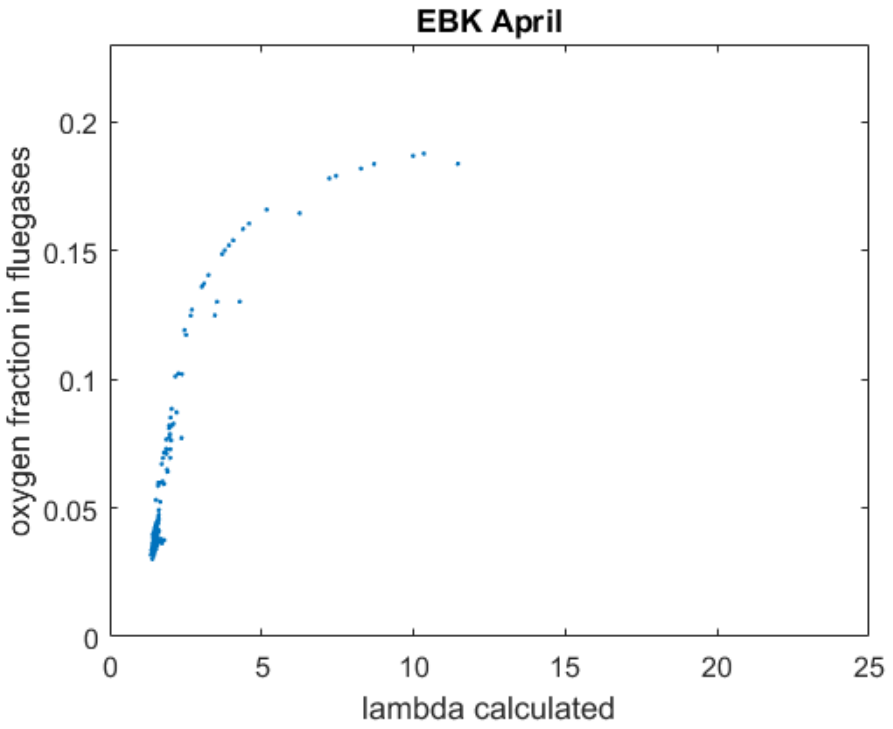


Figure A.16: Lambda EBK April 2017.

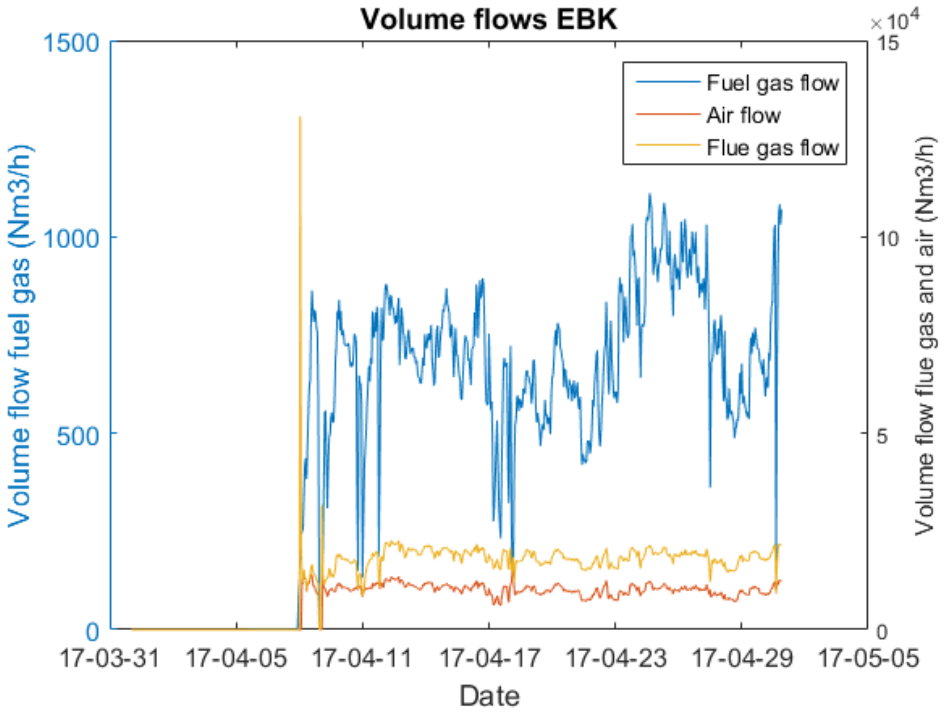
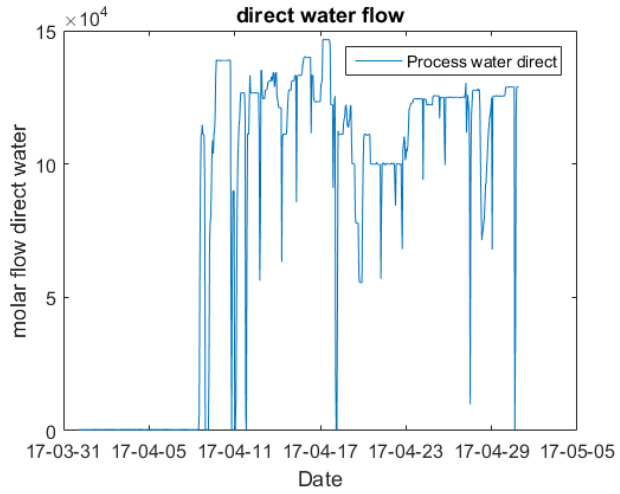
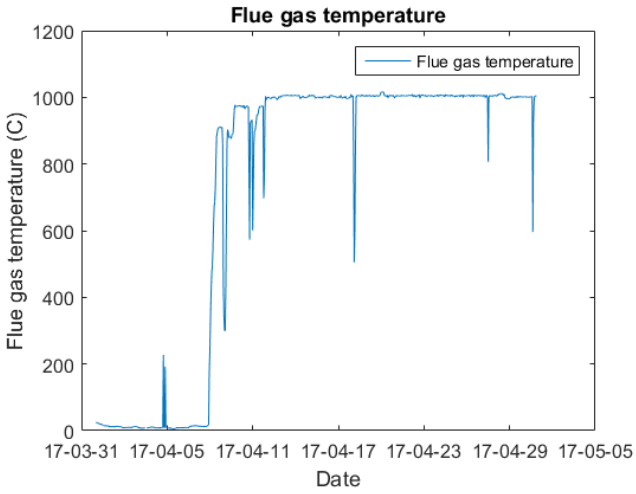


Figure A.17: Volume flows EBK April 2017.

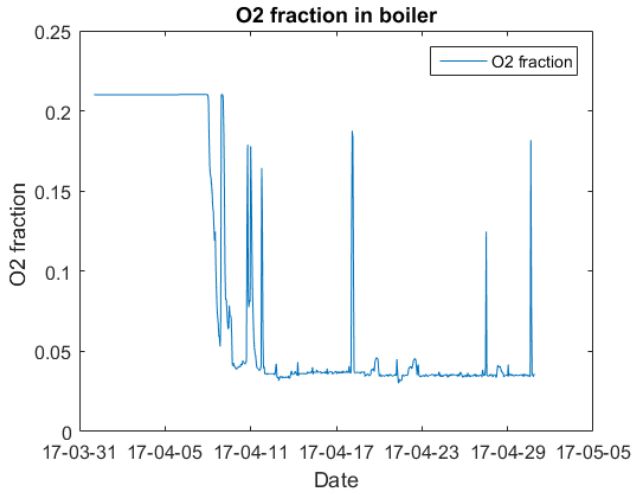
Figure A.18 (a) to (d) the operating conditions during April for the investigated parameters are presented.



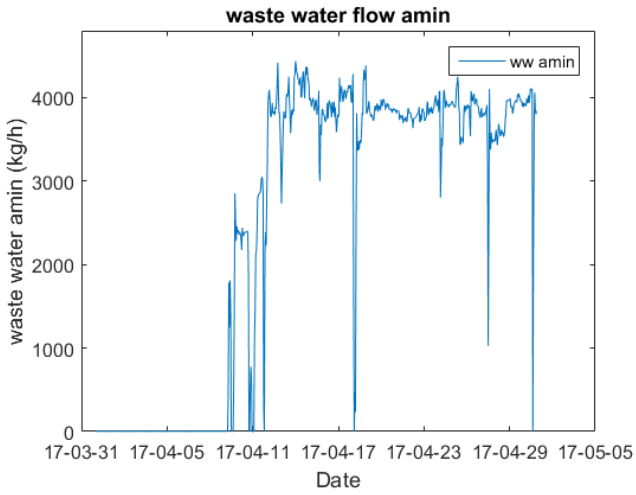
(a) Direct water flow during April.



(b) Flue gas temperature during April.



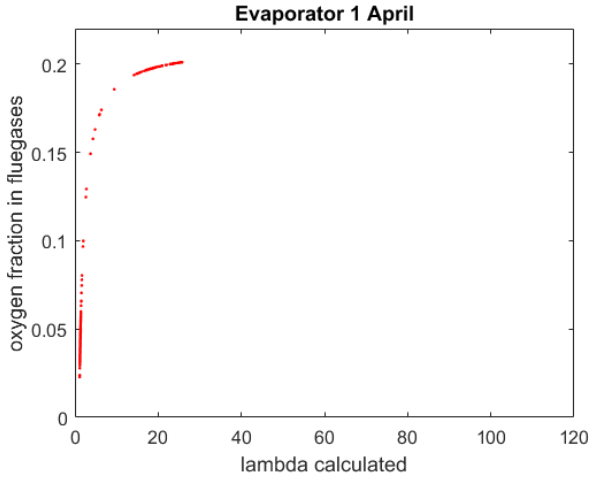
(c) O_2 fraction during April.



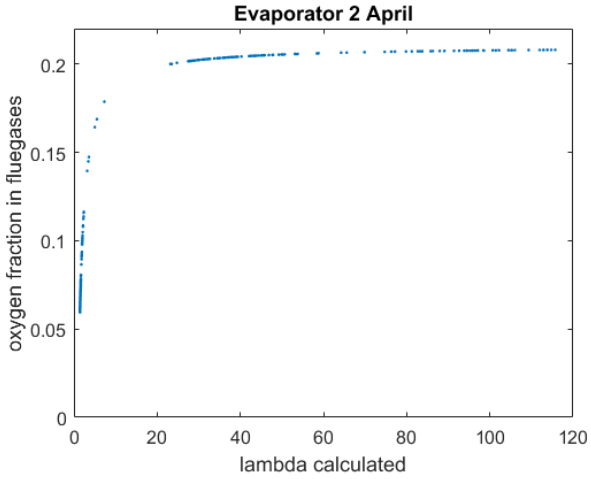
(d) Amine waste water flow during April.

Figure A.18: Test parameters during April.

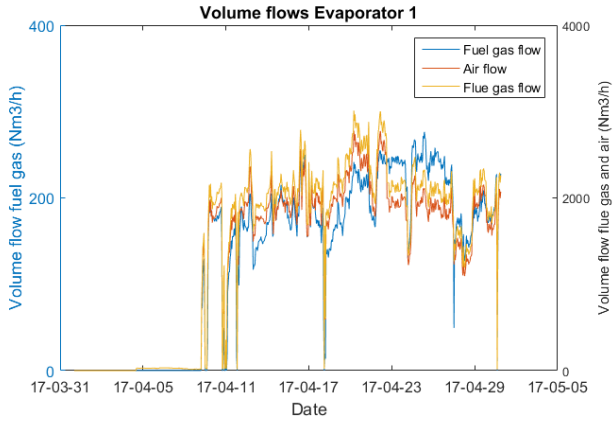
In Figure A.19 the results for the evaporators and the water and oxygen fractions for April are presented.



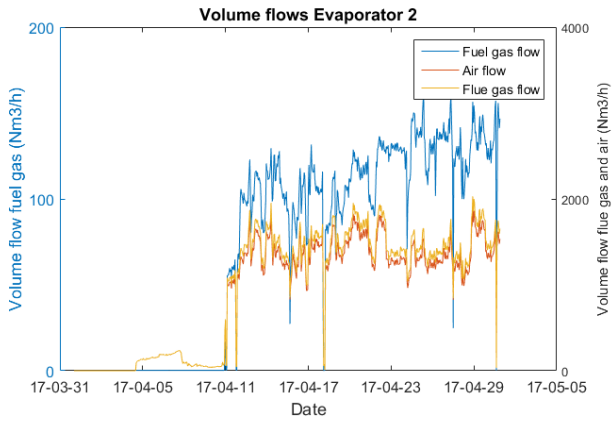
(a) Calculated lambda in evaporator 1.



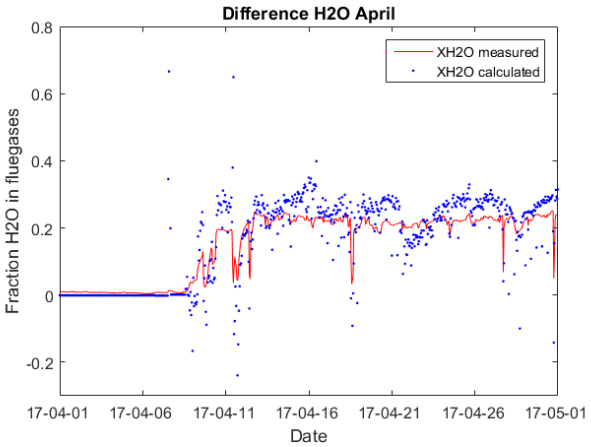
(b) Calculated lambda in evaporator 2.



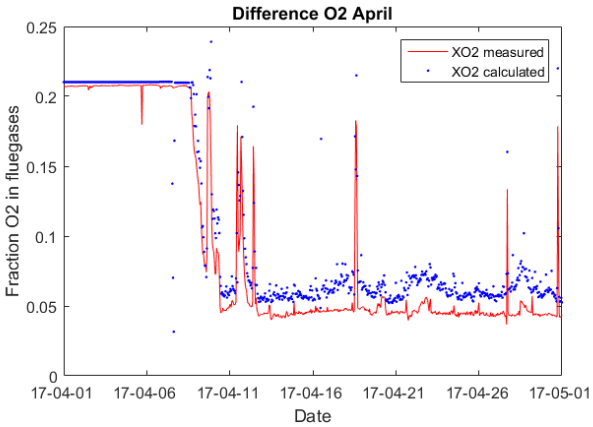
(c) Volume flows for evaporator 1 in April.



(d) Volume flows for evaporator 2 in April.



(e) Calculated H_2O fraction in flue gases against measured fraction.



(f) Calculated O_2 fraction in flue gases against measured fraction.

Figure A.19: Calculation results from April.